Consensus Control of Multi-Agent Systems Under Constraints

by

Yuan Sun

Thesis submitted for the degree of

Doctor of Philosophy

in

School of Electrical and Electronic Engineering
Faculty of Sciences, Engineering and Technology
The University of Adelaide, Australia

July 2022

Supervisors:

Prof. Peng Shi, School of Electrical & Electronic Engineering

Prof. Cheng-Chew Lim, School of Electrical & Electronic Engineering

THE UNIVERSITY of ADELAIDE

Contents

Abstract

Multi-agent systems (MAS), as they are more effective to perform complex tasks in real-world applications, have been extensively studied in the past ten years. The consensus control problem has emerged as the foundation of MAS, as its theoretical framework is widely applied to achieve cooperative behaviour within a networked system. A distributed consensus control algorithm aims to synchronize all states of agents to a common state by exchanging information with its neighbouring agents in a distributed manner. Whilst the distributed consensus control algorithms have been promising, how to achieve consensus subject to various constraints has not been fully investigated, especially for a class of nonlinear MAS.

The primary aim of this thesis is to analyse and design novel consensus control schemes for both linear and nonlinear MAS in the presence of communication, state and input constraints. For the consensus control problem of linear MAS under communication constraints, event-triggered control and integral sliding mode control methods are applied to synthesize a leaderless consensus controller for linear discrete-time MAS. The adaptive backstepping technique is also integrated with the event-triggered control method to derive an effective leaderless consensus control algorithm for nonlinear continuous-time MAS. Furthermore, a novel state transformation function is employed to solve constant and time-varying state constraint problems, so that the adaptive backstepping technique is feasible to formulate a leader-follower consensus control scheme for nonlinear MAS. Moreover, a new quadratic programming (QP) based safe consensus controller is developed to achieve consensus while ensuring safety by considering input constraints for linear MAS.

The main contributions of the thesis are threefold. First, the distributed consensus is achieved under communication constraints for linear and nonlinear MAS, respectively. Second, in the presence of state constraints, the proposed leader-follower consensus control protocol guarantees the desired tracking performance for nonlinear MAS. Third, a safe consensus is guaranteed with input constraints embedded in the QP problem for linear MAS. Numerical and practical systems are simulated to verify the proposed control algorithms that reach consensus while considering various constraints.

Statement of Originality

I certify that this work contains no material which has been accepted for the award of any other degree or diploma in my name, in any university or other tertiary institution and, to the best of my knowledge and belief, contains no material previously published or written by another person, except where due reference has been made in the text. In addition, I certify that no part of this work will, in the future, be used in a submission in my name, for any other degree or diploma in any university or other tertiary institution without the prior approval of the University of Adelaide and where applicable, any partner institution responsible for the joint award of this degree.

I give permission for the digital version of my thesis to be made available on the web, via the University's digital research repository, the Library Search and also through web search engines, unless permission has been granted by the University to restrict access for a period of time.

I acknowledge the support I have received for my research through the provision of an Australian Government Research Training Program Scholarship.

Signed: ..... **Yuan Sun** ..... Date: ..... **21 July 2022** .....

Acknowledgements

First and foremost, I would like to express my sincere gratitude to my supervisors Prof. Peng Shi and Prof. Cheng-Chew Lim. Their patience, guidance, encouragement, motivation and immense knowledge have helped me in all the time of academic research and writing of this thesis. I could not have imagined having better supervisors and mentors for my PhD journey.

I am extremely grateful to my principal supervisor Prof. Peng Shi for giving me the opportunity of commencing PhD study, providing financial support for living expenses, offering funds for practical experiments, and training me to grow as a research scientist. Support and guidance during the PhD program from you will benefit me throughout my life.

I would also like to extend my sincere thanks to my co-supervisor Prof. Cheng-Chew Lim for your insightful suggestions and for training me on teaching activities and academic writing. I have benefited greatly from your wealth of knowledge and meticulous editing.

Further, yet importantly, I am deeply grateful to my friends from the System and Control Group including Yang Fei, Bing Yan, Zhi Lian, Xin Yuan, Yutong Liu, Di Shen, Tianliang Zhang, Meng Li, Jingbo Fu, Yankai Li, Shiqi Zheng, Yueyuan Zhang and Xinxin Liu for their insightful suggestions and treasured support which widens my research from various perspectives. Additionally, my sincere thanks also go Xiaoyang Yin, Yuan Yao, Qiang Gao, Rui Yuan and Hua Ma for a cherished time spent together in the school and in social settings.

Most importantly, my warm and heartfelt thanks go to my wife Boshu Fan and my parents for the unconditional and tremendous support and hope they had given to me.

Publications

The following is a list of publications that are associated with the contents of this thesis.

Journal publications

YUAN SUN, PENG SHI, CHENG-CHEW LIM (2021). Event-triggered adaptive leaderless consensus control for nonlinear multi-agent systems with unknown backlash-like hysteresis, *International Journal of Robust and Nonlinear Control*, **31**(15), pp. 7409-7424.

YUAN SUN, PENG SHI, CHENG-CHEW LIM (2022). Event-triggered sliding mode scaled consensus control for multi-agent systems, *Journal of the Franklin Institute*, **359**(2), pp. 981–998.

YUAN SUN, PENG SHI, CHENG-CHEW LIM (2022). Adaptive consensus control for output-constrained nonlinear multi-agent systems with actuator faults, *Journal of the Franklin Institute*, **359**(9), pp. 4216–4232.

YUAN SUN, BING YAN, PENG SHI, CHENG-CHEW LIM (2022). Consensus for multi-agent systems under output constraints and unknown control directions, *IEEE Systems Journal*. DOI: 10.1109/JSYST.2022.3192573.

Conference publications

YUAN SUN, PENG SHI, CHENG-CHEW LIM (2019). Sliding mode scaled consensus of multi-agent systems via event triggered approach, *14th International Conference on Innovative Computing, Information and Control (ICICIC)*, **2019-August**.

YUAN SUN, PENG SHI, CHENG-CHEW LIM (2021). Adaptive neural network consensus control of multi-robot systems with output constraints, *IEEE International Conference on Intelligence and Safety for Robotics (ISR)*, **2021-March**, pp. 288–291.

YUAN SUN, PENG SHI, HUIYAN ZHANG (2021). Adaptive fuzzy formation control for nonlinear multi-agent systems with full-state constraints, *15th International Conference on Innovative Computing, Information and Control (ICICIC)*, **2021-September**.

List of Acronyms

QP ..... Quadratic programming

MAS ..... Multi-agent systems

SMC ..... Sliding mode control

BLF ..... Barrier Lyapunov function

CBF ..... Control barrier function

ZBF ..... Zeroing barrier function

LQR ..... Linear–quadratic regulator

LMI ..... Linear matrix inequality

UCD ..... Unknown control directions

MIMO ..... Multiple-input multiple-output

RBFNN ..... Radial basis function neural networks

Notation

$\mathbb{R}^n$ ..... An n-dimensional Euclidean space

$\mathbb{R}^{n\times m}$ ..... An $n \times m$ dimensional vector space

$X > Y$ ..... $X - Y$ is positive definite where X and Y are symmetric matrices

$X \geq Y$ ..... $X - Y$ is positive semi-definite where X and Y are symmetric matrices

$\text{diag}(\cdot)$ ..... A diagonal matrix

$\star$ ..... A symmetric term in a symmetric matrix

$A \otimes B$ ..... The Kronecker product of matrix A and matrix B

$\|\cdot\|$ ..... Euclidean two-norm for matrices

List of Figures

Chapter 1

Introduction

1.1 Background

In this section, we present the subject of multi-agent system (MAS), introduce the classification of MAS, and present distributed consensus control problem in MAS.

1.1.1 Multi-agent Systems

In artificial intelligence research, agent-based systems technology is the mainstream of computer science. An agent is a sophisticated computer program that acts autonomously upon its environment to achieve design objectives (Wooldridge 2009). Figure 1.1 displays the features of an autonomous agent. MAS is a team of multiple intelligent agents that cooperatively accomplish complex tasks while each agent acts towards its own goal in a shared network. In comparison with the abilities of a single agent, MAS has a number of advantages, for instance, robustness, maintainability, responsiveness and flexibility. Hence, a wide variety of applications in MAS range from civilian to military, for example, drone light shows, autonomous vehicles in farming and environmental monitoring and control (Mammarella *et al.* 2021), distributed smart grids and spacecraft formation flying (Ren and Beard 2004). Due to its advantages and broad applications, MAS has emerged as a promising research topic in automatic control in recent decades (Ren and Beard 2008, Shi and Yan 2021).

Generally, MAS is classified into centralized and distributed MAS by control architecture (Lunze 2019). Specifically, in the centralized approach, all agents P_i $(i = 1, \ldots, N)$ are connected to a single central controller C which makes decisions for all agents as shown in Figure 1.2. A large majority of small-size systems adopt this direct approach because of its low cost and slow delays. With the increase in the complexity of tasks, the centralized method is incapable to be applied to autonomous applications. Unlike

1.1.1 Multi-agent Systems

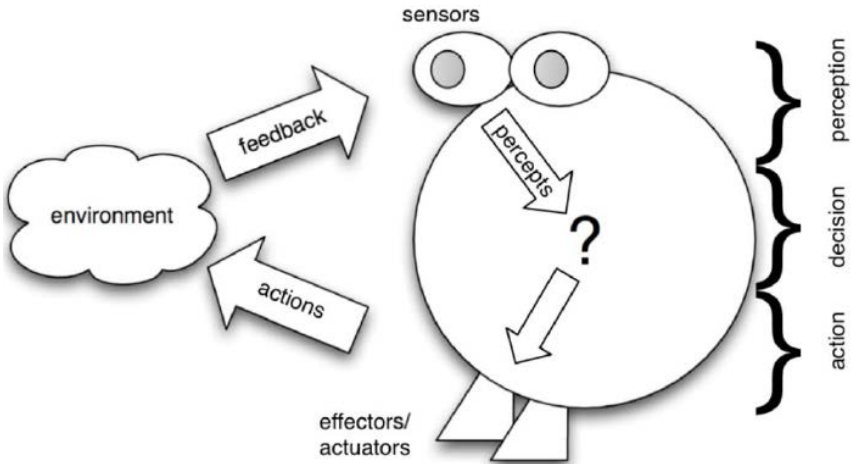

Figure 1.1. Features of an autonomous agent, adopted from (Wooldridge 2009).

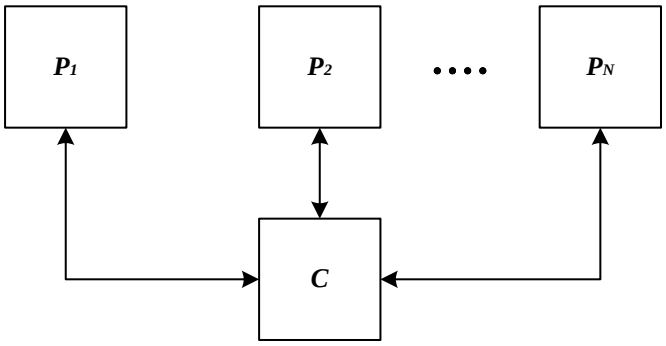

Figure 1.2. Control structure of a centralized MAS.

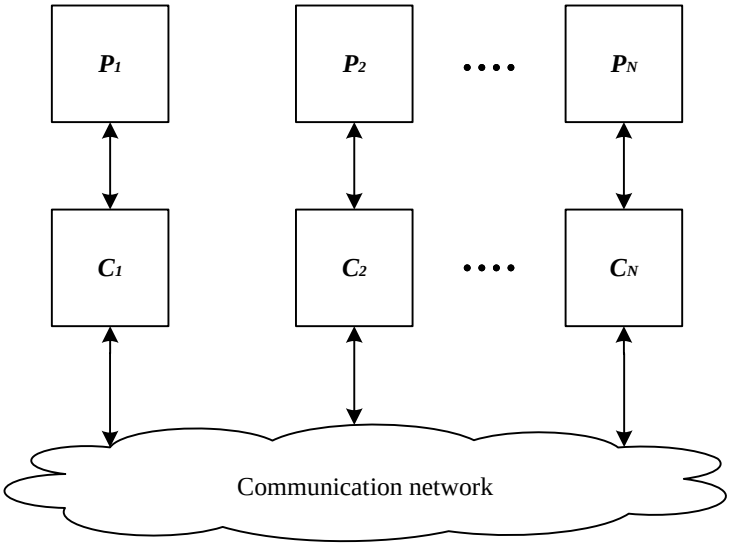

Figure 1.3. Control structure of a distributed MAS.

the centralized one, the distributed MAS is composed of multiple local controllers C_i and a shared communication network as shown in Figure 1.3, thus, a single agent of failure would not risk the whole system. It also has better adaptability and scalability for large-scale systems. Therefore, the distributed MAS can complete more complex tasks autonomously and cooperatively, and it is more effective and reliable than the centralized one.

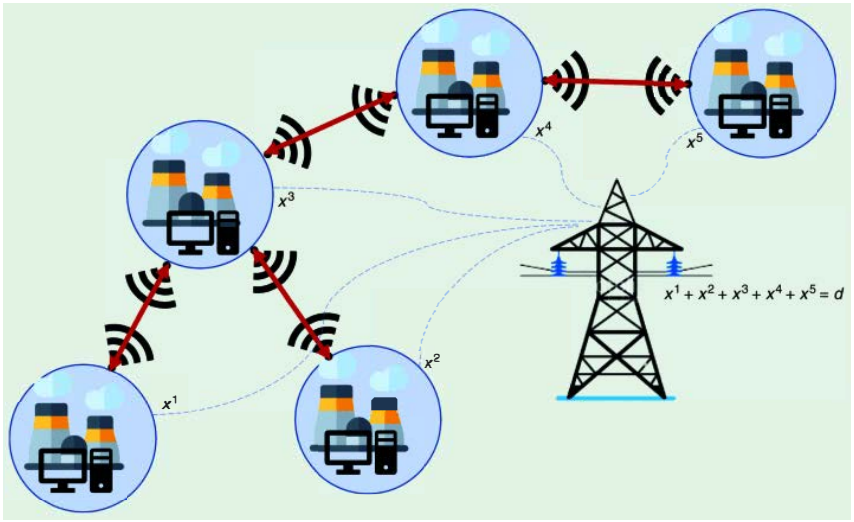

Figure 1.4. Distributed power generation technology is achieved by a distributed consensus control algorithm.

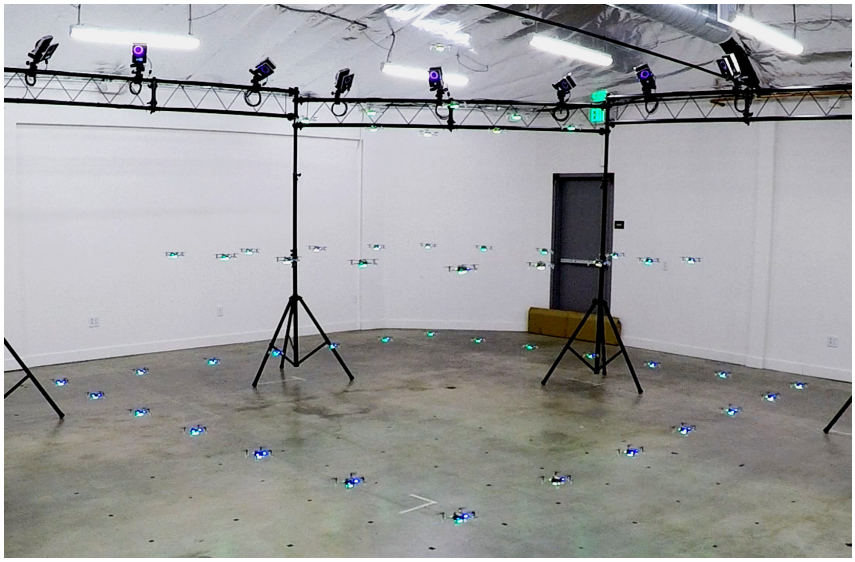

Figure 1.5. Forty-nine crazyflies flying in a 4-layer rotating formation, adopted from (Preiss et al. 2017).

In the distributed MAS, the consensus control problem has emerged as the foundation of MAS, as its basic theoretical framework is widely applied to achieve cooperative behaviour within a networked system. A distributed consensus control algorithm aims to synchronize all states of agents to a common state by exchanging information with its neighbouring agents in a distributed manner (Cao *et al.* 2012). Figure 1.4 indicates a group of five networked generators works cooperatively to meet a common demand d (Kia *et al.* 2019). Another reason for attracting researchers is its variety of practical applications, for instance, rendezvous of mobile multi-vehicles (Ren and Beard 2008), UAVs formation control (Dong *et al.* 2016) and cooperative robotic manipulators (Li *et al.* 2013). Figure 1.5 displays a large nano-quadcopter swarm platform that is based on distributed consensus-based formation control protocol (Preiss *et al.* 2017).

1.2 Literature Review

In this thesis, we have considered distributed consensus control protocols for both linear and nonlinear MAS under different constraints.

For linear MAS, a new type of consensus algorithm named scaled consensus is considered (Roy 2015). The scaled consensus differs from the standard consensus in that the scaled consensus aims to guarantee states of all agents reach assigned ratios instead of a common value. In many practical applications, the states of agents are required to reach predefined ratios, such as water distributed systems, task allocation and web-page-ranking algorithms. Consequently, the scaled consensus can generalize the standard consensus algorithms corresponding to select appropriate scales, namely, bipartite consensus and cluster consensus (Chen *et al.* 2019).

Emerging evidence reveals that the scaled consensus problem has generated raised interest in distributed cooperative control, in particular, a necessary and sufficient condition was established to explore the scaled consensus problems considering time-varying scales and switching networks (Meng and Jia 2016). In the work (Xing and Deng 2018), the continuous-time scaled consensus problem is investigated subject to time-varying communication delay. A sliding mode-based scaled consensus control scheme has been proposed to study the $H\infty$ performance of linear MAS with unknown yet bounded external disturbance (Zhao *et al.* 2017). An alternative scaled consensus algorithm has been presented by employing an integral Lyapunov function to obtain a

necessary and sufficient condition for single-integrator agents with output saturation (Wang 2017). Thus, the scaled consensus control problem is worth investigating and it has not been discovered fully under some specific constraints.

Since inherent nonlinearities exist in all systems in practice, the nonlinear MAS is also investigated in this work. A substantial amount of research has been done on consensus control for nonlinear MAS. For example, the authors presented a smooth distributed adaptive controller to resolve the high-order nonlinear leader-following consensus problem considering unknown parameters and uncertain external disturbances (Huang *et al.* 2017). An adaptive command filtered strategy based on adaptive backstepping was employed to ensure the leader-following consensus tracking errors are semi-globally bounded (Shen and Shi 2015). The output leader-following consensus tracking is asymptotically achieved depending upon locally available interactions and involving mismatched unknown parameters and external disturbances (Wang *et al.* 2017c). A similar distributed adaptive consensus control algorithm with a new Nussbaum-type function was exploited to tackle unknown control directions problems for nonlinear MAS (Huang *et al.* 2018a). The problems of unknown control directions and backlash-like hysteresis for nonlinear MAS under undirected communication topology were addressed by the adaptive neural networks control method (Chen *et al.* 2016). Therefore, the development of distributed consensus control schemes for nonlinear MAS is more complicated than the linear ones, and the investigation of nonlinear MAS with some practical issues has not been studied widely, which motivates us to further explore the nonlinear MAS.

The distributed consensus controller design with some specific constraints can bring more challenges for the discovery of both linear and nonlinear MAS. How to identify the challenges and propose appropriate solutions for MAS are presented in the following section.

1.3 Challenges of Distributed Consensus Control Design

The communication, state and input constraints are the main constraints we have considered, and how to explore the related challenges and properly address the consensus problem drives us to develop effective consensus controllers under such constraints.

Most consensus control algorithms are developed based on a common assumption that the information from one agent towards its neighbours is transmitted continuously and control signals update frequently or at periodic sampling instants. Continuous information exchange between agents and frequent controller updating increase communication effort and energy usage, which may cause unnecessary communication and computing resource consumption. Event-triggered communication mechanism has been developed as an effective method to reduce communication among agents and controller updates frequency considerably during event intervals as well as maintain the desired system performance. In MAS, events are asynchronously generated since distinct event-triggered conditions are embedded in the corresponding subsystems (Dimarogonas *et al.* 2011), which makes theoretical analysis of nonlinear MAS more complicated. The linear leader-following and leaderless consensus problems with external disturbances are investigated by a distributed event-based consensus controller (Xing *et al.* 2016). The adaptive backstepping-based fuzzy event-triggered control algorithm is developed to resolve the consensus tracking problem (Li *et al.* 2018), which reaches the consensus and saves the computation resources. A distributed consensus controller based on a fixed threshold event-triggered strategy is constructed to deal with the difficulty of intermittent actuator faults for nonlinear MAS (Wang *et al.* 2020d). Accordingly, frequently control signal updating escalates the level of difficulty in theoretical analysis and limits the outcomes of the event-triggered consensus control problem for nonlinear MAS.

Output constraint problems are frequently encountered in practical applications due to safety requirements, specific environments and system performances (He *et al.* 2020). For example, inspection drones operating within a tunnel and robot manipulators within a restricted operating zone, etc. Typically, state transformation (Ni and Shi 2021a, Niu *et al.* 2017a, Zheng and Li 2018, Zhao and Song 2020) and barrier Lyapunov function (BLF) (Tee *et al.* 2009) approaches are used to resolve the output constraint problem. The logarithm-type state transformation function is widely applied to transform the constrained state into an unconstrained one. For instance, both constant symmetric and asymmetric cases were analysed for nonlinear output-constrained systems (Niu *et al.* 2017a), yet the lower restricted boundary is assumed to be negative, and the upper boundary is strictly positive. The time-varying asymmetric case was considered with both positive lower and upper boundaries (Zheng and Li 2018). Moreover, a new

nonlinear state-dependent transformation function with positive boundaries was proposed for time-varying asymmetric constraints (Zhao and Song 2020). However, the above transformation functions cannot eliminate the limitation of the boundaries and solve both constrained and unconstrained cases simultaneously. Furthermore, the BLF method requires complex formulations in controller design (Qu *et al.* 2018), especially for the time-varying asymmetric case. Therefore, a more general solution to the output constraint problem is desired to remove the limitations of the state transformation function and simplify the analysis of the BLF approach for nonlinear MAS.

Obstacle avoidance problem is generally converted into equivalent input constraints that are mainly enforced by optimization-based trajectory planning algorithms (Patel and Goulart 2011, Blackmore *et al.* 2011, Ferraguti *et al.* 2020, Rosolia *et al.* 2016, Zeng *et al.* 2021). It is considered impossible to be ignored when the consensus control theory is turned into practice (Zhang *et al.* 2010, Dai *et al.* 2017, Mylvaganam *et al.* 2017, Yan *et al.* 2018). Recently, control barrier function (CBF) is proposed as an important tool to solve constrained-based control problems and is associated with control Lyapunov function to form a QP-based framework with a larger feasibility set (Taylor and Ames 2020, Wang *et al.* 2017a, Kolathaya and Ames 2018). Due to its flexible control design framework and desired real-time optimization performance in safety-critical control areas, CBF has been recognized as a hot research topic (Zeng *et al.* 2021, Xiao and Belta 2019, Choi *et al.* 2021). For example, input constraints decoded from physical constraints are formed as a CBF to combine with a backstepping controller (Hsu *et al.* 2015). Furthermore, a CBF has been constructed based on the avoidable set that is converted into input constraints (Chen *et al.* 2018). Input constraints under high levels of model uncertainty for nonlinear dynamical robotic systems have been addressed by the CBF technique (Nguyen and Sreenath 2021). Although CBF is a promising technique to solve constrained-based control problems, constrained consensus control of MAS with CBF has not been studied yet. More importantly, both the inter-robot collision and static obstacles are necessary to be considered for MAS to ensure that MAS can safely complete complex tasks. Therefore, how to design the synthesis of an optimization-based safe consensus controller, how to transform obstacle avoidance problems into input constraints with a CBF and how to build a multi-robot platform to test the safe consensus controller motivate us to investigate the constrained consensus control of MAS.

The following section has presented the contributions to overcoming the challenges of developing consensus control schemes under communication, output and input constraints for linear and nonlinear MAS, respectively.

1.4 Statement of Contributions

In Chapter 2, the scaled consensus problem for linear discrete-time MAS is investigated via an event-triggered sliding mode control (SMC) approach subject to unknown external bounded disturbance and time-varying state delay. A new event-triggered integral sliding surface function is introduced to handle the external disturbances. Then, a distributed event-triggered control method is integrated with SMC to address the energy-constrained issue in the scaled consensus problem. Subsequently, a sufficient condition is established to ensure a predefined $H\infty$ performance can be achieved for the underlying system. Furthermore, an event-triggered SMC protocol is developed to guarantee the state trajectories of all agents approach the dictated scales in the discrete-time MAS. A numerical example is given to demonstrate the effectiveness of the proposed design techniques.

Chapter 3 aims to investigate the problem of event-triggered adaptive leaderless consensus control for a class of nonlinear MAS with unknown backlash-like hysteresis. Combining adaptive backstepping and event-triggered control techniques, a distributed event-triggered adaptive leaderless consensus controller is designed to compensate for the effects of unknown backlash-like hysteresis and reduce the update frequency of control signals. By the proposed method, we can obtain the desired consensus tracking, ensure the boundedness of all the signals, and exclude the Zeno behaviour from the underlying systems. An example of four robotic manipulators is given to show the effectiveness of the new control design scheme.

Chapter 4 addresses the problem of leader-follower consensus fault-tolerant control for a class of nonlinear MAS with output constraints. Specifically, a new nonlinear state transformation function is proposed to deal with the asymmetric constraint on output. Moreover, by integrating backstepping and radial basis function neural networks (RBFNN) approaches, an adaptive consensus control framework is developed with a single parameter estimator, which mitigates the computation of the control algorithm in comparison with a conventional adaptive approximation-based control technique.

Then, an adaptive compensation method is proposed to eliminate the effect of actuator failure. Under the proposed control scheme, all the closed-loop signals of the systems are bounded and the consensus tracking error converges to an adjustable small neighbourhood of zero. To evaluate the developed control algorithm, a group of four networked two-stage chemical reactors is used to illustrate the effectiveness of the theoretic results obtained.

In Chapter 5, we design an adaptive leader-follower consensus controller for a class of nonlinear MAS in the presence of time-varying asymmetric output constraints and unknown control directions. A new state transformation approach is introduced for each agent to transform the output into an equivalent unconstrained state. An adaptive neural network-based backstepping control method and a Nussbaum function approach are integrated to design the leader-follower consensus controller that compensates for the unknown control directions and guarantees that the consensus tracking error converges to a small compact set. Examples are given to demonstrate the effectiveness of the proposed new design techniques.

Chapter 6 presents a novel framework of safe consensus control by synthesizing the linear–quadratic regulator (LQR) and CBF techniques. The nominal LQR consensus controller is designed by applying a distributed LQR leader-follower consensus control scheme. Furthermore, a special distributed CBF named zeroing barrier function (ZBF) is defined by the constraint in terms of the control input signal, which is introduced to guarantee that the agents can avoid both inter-robot collision and static obstacles. The synthesis of an optimization-based safe consensus controller is tested on a lab-scale multi-robot system in an obstructed environment.

Chapter 2

Event-triggered Consensus Control for Linear Multi-agent Systems

2.1 Introduction

Recently, MAS have been widely studied and applied due to their salient features including large scales of autonomous agents, distributed control actions, shared communication networks and scalability of system architecture. In comparison with the ability of a single agent, MAS have potential applications in various fields, for example, industrial manufacturing, transportation, security surveillance and novel cloud computing. The main objective of MAS is to accomplish complex tasks cooperatively with a group of intelligent agents interacting with their neighbouring agents (Cao *et al.* 2012, Shi and Yan 2021).

As the core component of MAS, distributed cooperative control has been extensively examined concentrating on consensus problem. Consensus problem is treated as the most fundamental and predominant problem in distributed cooperative control. The aim of addressing consensus problem is to develop a distributed consensus algorithm in order to ensure all states of agents approach a common value. In many practical applications, the states of agents are required to reach predefined ratios, such as water distributed systems, task allocation and web-page-ranking algorithms. Author in the work (Roy 2015) introduced a novel notion of scaled consensus. The scaled consensus differs from the standard consensus in that the scaled consensus aims to guarantee

states of all agents to approach assigned ratios instead of a common value. Consequently, the scaled consensus can generalize the standard consensus algorithms corresponding to select appropriate scales, namely, bipartite consensus and cluster consensus (Chen *et al.* 2019). Emerging evidence reveals that the scaled consensus problem has generated raised interest in distributed cooperative control, in particular, a necessary and sufficient condition was established (Meng and Jia 2016) to explore the scaled consensus problems considering time-varying scales and switching networks. The continuous-time scaled consensus problem is investigated subject to time-varying communication delay for MAS (Xing and Deng 2018). A sliding mode based scaled consensus control scheme has been proposed to study H_∞ performance of linear MAS with unknown yet bounded external disturbance (Zhao *et al.* 2017).

Sliding mode control (SMC) is an effective robust approach to reduce the adverse impact of model uncertainties and unknown external disturbances in control system, and it has been widely considered by combining with other control techniques due to its inherent robustness in numerous theoretical and practical engineering systems (Shtessel *et al.* 2014). To illustrate, an adaptive SMC strategy was employed to study switched complex network systems (Li and Chen 2019). A synthesis approach of dynamic event-triggered control and sliding mode observer was proposed to derive stability conditions for time-delayed T-S fuzzy system (Liu *et al.* 2019). It is proven that an asynchronous approach (Fang *et al.* 2021) is implemented to guarantee the stability and improve dissipative performance of nonlinear Markov jump systems. Moreover, a self-triggering-based sliding-mode control algorithm was implemented to analyse stability problem of linear system in the presence of external disturbance (Behera and Bandyopadhyay 2015). The authors (Wang *et al.* 2016b) combined terminal SMC and disturbance observer-based control into a novel combined approach to study finite-time consensus problem for higher-order MAS. However, by our knowledge, little effort has been made to investigate the scaled consensus by SMC method, not to mention event-triggered SMC approach.

Moreover, event-triggered control is a reliable and valid technique for resolving energy-constrained issue in control system. Due to the event-triggered condition implemented, control signals only updates once the measurement error exceeds a predefined threshold, which could significantly lower the high-frequency updates of control signals. Since a unified framework of distributed event-triggered control for MAS was proposed (Dimarogonas *et al.* 2011), on the basis of this method, abundant event-triggered

control strategies have been proposed in MAS. Event-triggered consensus problem was investigated in the presence of model uncertainties and external disturbances for MAS (Liu and Jia 2019). Therefore, the event-triggered SMC method is worth being developed to study discrete-time scaled consensus problem in MAS.

Motivated by the preceding literature in addressing scaled consensus problem in MAS, we study the discrete-time scaled consensus problem subject to time-varying state delay and external disturbance by integrating the SMC approach with an event-triggered scheme. A new sliding surface function is designed to drive the state trajectories to reach a predesigned sliding surface. Besides, for implementing the event-triggered control mechanism, Zeno behavior analysis is inevitable because infinite events are triggered in a finite time interval, therefore, in this work, it is unnecessary to be considered since the triggering instants are generated in a discrete manner. Furthermore, a synthesis SMC controller with the event-triggered control technique is developed to force the trajectories onto the predefined sliding surface. Finally, a sufficient condition is obtained to guarantee the robust scaled consensus with a predefined H_∞ performance adopting linear matrix inequalities (LMIs)-based method.

This chapter is outlined as follows. Some preliminaries on communication topology and MAS dynamics are introduced in Section 2.2. In Section 2.3, a synthetical event-triggered SMC protocol for discrete-time MAS is devised to analyse the stability of scaled consensus problem. In Section 2.4, a simulation example is presented to demonstrate the effectiveness of the proposed new design technique, and Section 2.5 concludes this chapter.

2.2 Problem Formulation and Preliminaries

2.2.1 Basics of Algebraic Graph Theory

Graphs are denoted as $\mathcal{G} = \{\mathcal{V}, \mathcal{E}, \mathcal{A}\}$ to represent information exchange among a cluster of N agents (Godsil and Royle 2013). A graph $\mathcal{G}$ is composed of a finite node set $\mathcal{V} = \{1, 2, ..., N\}$ and a set of edges $\mathcal{E}$, where $\mathcal{E} \subseteq \mathcal{V} \times \mathcal{V}$ represents edges of the graph. A graph with directed or undirected edges names directed or undirected graph, which indicates the allowed information flow between agents.

For an undirected graph, the weighted adjacency matrix $\mathcal{A}$ of the graph $\{\mathcal{V}, \mathcal{E}, \mathcal{A}\}$ is defined such that $\mathcal{A} = [a_{ij}] \in \mathbb{R}^{N\times N}$, if $(i, j) \in \mathcal{E}$, the edge weight $a_{ij} = 1$, otherwise, $a_{ij} = 0$. For an undirected graph, $a_{ij} = a_{ji}$. Denote $\mathcal{D} \triangleq \mathrm{diag}(\mathrm{deg}_1, ..., \mathrm{deg}_N)_{i=1,2,...,N}$, where $\mathrm{deg}_i^{in} = \sum_{j=1}^{N} a_{ij}$ expresses the in-degree of agent i. Consequently, Laplacian matrix $\mathcal{L}$ of graph $\mathcal{G}$ is a symmetric positive semi-definite matrix if and only if graph $\mathcal{G}$ is connected, where $\mathcal{L} = \mathcal{D} - \mathcal{A} = [l_{ij}] \in \mathbb{R}^{N\times N}$, $l_{ii} = \sum_{j=1, i\neq j}^{N} w_{ij}$, and $l_{ij} = -w_{ij}$ for $i \neq j$. Furthermore, zero is a special eigenvalue of the Laplacian matrix $\mathcal{L}$ and $\lambda_i(\mathcal{L})$ denotes the eigenvalue of ith agent in the communication topology of $\mathcal{G}$, where $i \in \{1, 2, \cdots, N\} \triangleq \mathcal{N}$. The graph applied in this chapter is undirected.

For a directed graph, the edges $\mathcal{E}$ indicate a one-way communication between agent j and i, which can be expressed by $(j, i) \in \mathcal{E}$. The Laplacian matrix $\mathcal{L}$ is a key element of the directed graph. It is defined as $\mathcal{L} = \mathcal{D} - \mathcal{A}$, where $\mathcal{A} = [a_{ij}]$ denotes adjacency matrix with $a_{ii} = 0$, when $(j, i) \in \mathcal{E}$, $a_{ij} = 1$, otherwise, $a_{ij} = 0$. For the diagonal degree matrix $\mathcal{D} = [d_{ij}] \in \mathbb{R}^{N\times N}$ is the in-degree matrix and its entries are defined as $d_{ii} = \sum_{j=1}^{N} a_{ij}$ and $d_{ij} = 0$ with $i \neq j$. The desired trajectory of a leader agent is defined as y_r, and the diagonal matrix $\mathcal{B}$ related to the leader is defined as $\mathcal{B} = \mathrm{diag}[b_i, \ldots, b_N]$, where $b_i = 1$ if agent i is able to access the leader, otherwise, $b_i = 0$. In the remaining chapters of this thesis, directed graphs with a leader are considered for leader-follower MAS.

2.2.2 Multi-agent System Dynamics

Consider the following discrete-time MAS for N agents with time-varying state delay and external disturbance. The dynamics of the ith agent is described by:

$$x_i(k+1) = Ax_i(k) + A_d x_i(k - d(k)) + Bu_i(k) + Dw_i(k) \tag{2.1}$$

where $x_i(k) \in \mathbb{R}^n$ and $u_i(k) \in \mathbb{R}^m$ are the system state and control input, $w_i(k) \in \mathbb{R}^p$ is the external disturbance input belonging to $L_2[0, \infty)$, and $i \in \mathcal{N}$. $A \in \mathbb{R}^{n\times n}, A_d \in \mathbb{R}^{n\times n}, B \in \mathbb{R}^{n\times m}, D \in \mathbb{R}^{n\times p}$ are constant matrices with proper dimensions. The time-varying state delay is $d(k) \in [0, \tau_M]$ with an upper bound of $d(k)$ specified as τ_M, and the initial condition is defined as $x_i(k) = \phi(k)$, where $\phi(k)$ is a given function on $[-\tau_M, 0]$, and for all $k \in [-\tau_M, 0]$.

Definition 2.1. (Roy 2015): The scaled consensus of MAS (2.1) is said to achieve or reach by the group of N agents to $(\alpha_1, \alpha_2, \cdots, \alpha_N)$, if

$$\lim_{k\to\infty}\left[\frac{x_i(k)}{\alpha_i} - \frac{x_j(k)}{\alpha_j}\right] = 0$$

for all $i, j \in \mathcal{N}$ and for any initial conditions $x_i(0) \in \mathbb{R}^n$, where scalars $\alpha_1, \alpha_2, \cdots, \alpha_N$ are non-zero constants and indicate the scales of states $x_1(t), x_2(t), \cdots, x_N(t)$. Moreover, a transformation between α_i and α_j is defined as $\alpha_{ij} = \frac{\alpha_i}{\alpha_j}$, which shows agent i and agent j could maintain the same scale α_{ij}.

Define a controlled output function $z_i(k)$ for agent i in MAS (2.1)

$$z_i(k) = x_i(k) - \frac{1}{N}\sum_{j=1}^{N}\alpha_{ij}x_j(k) \tag{2.2}$$

Note that $z_i(k) = 0$, if and only if $\frac{1}{\alpha_i}x_i(k) = \frac{1}{\alpha_j}x_j(k)$ holds for all $i, j \in \mathcal{N}$, which implies that the scaled consensus is reached by the group of N agents.
Denote $z(k) = [z_1^T(k)\ z_2^T(k)\ \ldots\ z_N^T(k)]^T \in \mathbb{R}^{n\times N}$, then, (2.2) can be rewritten in a matrix form as

$$z(k) = (\alpha L_c \alpha^{-1} \otimes I_n)x(k) \tag{2.3}$$

where the symmetric matrix $L_c = \left[l_{c_{ij}}\right] \in \mathbb{R}^{N\times N}$ is specified as

$$l_{c_{ij}} = \begin{cases} \frac{N-1}{N}, & i = j \\ -\frac{1}{N}, & i \neq j, \end{cases}$$

which satisfies $L_c\mathbf{1}_N = 0$. Therefore, the controlled output function $z(k)$ can be employed to analyse the scaled consensus performance.

To proceed, the following assumptions and lemmas are introduced:

Assumption 2.1. *In MAS (2.1), undirected and connected graph $\mathcal{G}$ is imposed to model the communication topology.*

Assumption 2.2. *The unknown external disturbances are bounded, which represents that there exits a positive constant scalar $\overline{\omega}$, so that $\|w_i(k)\| \leq \overline{\omega}$, holds for any $k \geq 0$ and $i \in \mathcal{N}$.*

Lemma 2.1. (Schur's Complement)
For symmetric matrix $F = \begin{bmatrix} F_{11} & F_{12} \\ F_{21} & F_{22} \end{bmatrix}$, and $F_{11} \in \mathbb{R}^{m\times m}$, $F_{22} \in \mathbb{R}^{(n-m)\times(n-m)}$, the following statements are equivalent:

(1) $F_{11} - F_{12}F_{22}^{-1}F_{12}^{T} < 0, F_{22} < 0;$

(2) $F_{22} - F_{12}^{T}F_{11}^{-1}F_{12} < 0, F_{11} < 0;$

(3) $F < 0.$

2.3 Event-triggered Sliding Mode Control Framework

2.3.1 Discrete-time Integral Sliding Surface Design

The sliding mode surface function for agent i is designed as follows:

$$\begin{cases} s_i(k) = Mx_i(k) - Mx_i(0) + b_i(k) \\ b_i(k) = b_i(k-1) - \sigma_i(k-1) \end{cases} \tag{2.4}$$

where $\sigma_i(k-1)$ is given as

$$\begin{aligned} \sigma_i(k-1) =& (MA - M)x_i(k-1) + MA_d x_i(k - d(k-1) - 1) \\ &+ MBK\sum_{j=1}^{N} a_{ij}\Big(\alpha_{ij}x_j(k-1) - x_i(k-1)\Big) \end{aligned}$$

$b_i(0) = 0$, $M \in \mathbb{R}^{m\times n}$, and the protocol gain matrix $K \in \mathbb{R}^{m\times n}$ is to be designed later.

Consider the SMC theory, the trajectories of system state $x_i(k)$ are steered towards the predefined sliding surface, hence, the ideal sliding surface for the discrete-time MAS satisfies

$$\Delta s_i(k) = s_i(k+1) - s_i(k) = 0 \tag{2.5}$$

Then, we obtain

$$s_i(k+1) = Mx_i(k+1) - Mx_i(0) + b_i(k) - \sigma_i(k) \tag{2.6}$$

where $\sigma_i(k)$ is given as

$$\begin{aligned} \sigma_i(k) =& (MA - M)x_i(k) + MA_d x_i(k - d(k)) \\ &+ MBK\sum_{j=1}^{N} a_{ij}\Big(\alpha_{ij}x_j(k) - x_i(k)\Big) \end{aligned}$$

Therefore, we have

$$\Delta s_i(k) = MBu_i(k) - MBK\sum_{j=1}^{N} a_{ij}\Big(\alpha_{ij}x_j(k) - x_i(k)\Big) + MDw_i(k) = 0 \tag{2.7}$$

Without loss of generality, M is selected such that $MB = I$, therefore,the equivalent SMC law is given by

$$u_{eq_i}(k) = K \sum_{j=1}^{N} a_{ij} \Big(\alpha_{ij} x_j(k) - x_i(k) \Big) - MDw_i(k) \tag{2.8}$$

2.3.2 Design of Event-triggered Communication Scheme

In this work, the MAS dynamics (2.1) with event-triggered control is proposed as:

$$x_i(k+1) = Ax_i(k) + A_d x_i(k - d(k)) + Bu_i(k_l^i) + Dw_i(k) \tag{2.9}$$

for $k \in [k_l^i, k_{l+1}^i)$, where k_l^i represents the triggering instants for agent i, and k_{l+1}^i stands for the next triggering instants. The key idea of event-triggered control is to analyse when agent i should interact with its neighbours, then, the following calculation of next triggering instants with event-triggered condition is proposed as

$$k_{l+1}^i = \inf\{k > k_l^i \mid f_i(k) > 0\} \tag{2.10}$$

where $f_i(k) = e_i^T(k)\Psi e_i(k) - \varepsilon x_i^T(k)\Psi x_i(k)$ with the transmission error $e_i(k) = x_i(k_l^i) - x_i(k)$, the threshold parameter $\varepsilon \in [0, 1)$, and Ψ is an undetermined positive-definite weighting matrix. Therefore, from (2.10), we can easily conclude that there is no event triggered for all $k \in [k_l^i, k_{l+1}^i)$, thus, we can obtain

$$e_i^T(k)\Psi e_i(k) \leq \varepsilon x_i^T(k)\Psi x_i(k) \tag{2.11}$$

Therefore, the derived equivalent sliding mode controller considering the event-triggered control strategy can be rewritten as

$$u_{eq_i}(k) = K \sum_{j=1}^{N} a_{ij} \Big(\alpha_{ij} x_j(k_{l'}^j) - x_i(k_l^i) \Big) - MDw_i(k) \tag{2.12}$$

for $k \in [k_l^i, k_{l+1}^i)$, where $x_j(k_{l'}^j)$ represent the latest transmitted states from its neighbouring agent j, and $k_{l'}^j \triangleq arg\, min_{l'} \{k - k_{l'}^j \mid k \geq k_{l'}^j, l' \in N\}$.

Substituting the equivalent SMC law (2.12) to (2.9), then the sliding mode dynamics can be derived as

$$x_i(k+1) = Ax_i(k) + A_d x_i(k - d(k)) + BK \sum_{j=1}^{N} a_{ij} \Big(\alpha_{ij} x_j(k_{l'}^j) - x_i(k_l^i) \Big) + \widetilde{D} w_i(k) \tag{2.13}$$

where $\widetilde{D} = (I_n - BM)D$.

The above sliding mode dynamics (2.13) with the controlled output function (2.2) is formulated in a compact form

$$\begin{aligned} x(k+1) &= (I_N \otimes A - \alpha L \alpha^{-1} \otimes BK)x(k) - (\alpha L \alpha^{-1} \otimes BK)e(k) \\ &\quad + (I_N \otimes A_d)x(k - d(k)) + (I_N \otimes \widetilde{D})w(k) \\ z(k) &= (\alpha L_c \alpha^{-1} \otimes I_n)x(k) \end{aligned} \tag{2.14}$$

Define the following model transformations $\widetilde{x}(k) = (\alpha^{-1} \otimes I_n)x(k)$, $\widetilde{e}(k) = (\alpha^{-1} \otimes I_n)e(k)$, $\widetilde{z}(k) = (\alpha^{-1} \otimes I_n)z(k)$, $\widetilde{w}(k) = (\alpha^{-1} \otimes I_p)w(k)$.

Then from the above transformation, we can obtain

$$\begin{aligned} \widetilde{x}(k+1) &= (I_N \otimes A - L \otimes BK)\widetilde{x}(k) - (L \otimes BK)\widetilde{e}(k) \\ &\quad + (I_N \otimes A_d)\widetilde{x}(k - d(k)) + (I_N \otimes \widetilde{D})\widetilde{w}(k) \\ \widetilde{z}(k) &= (L_c \otimes I_n)\widetilde{x}(k) \end{aligned} \tag{2.15}$$

Denote $\overline{x}(k) = \widetilde{x}(k) - \mathbf{1}_N \otimes (\sum_{j=1}^{N} x_j(k)) = (L_c \otimes I_n)\widetilde{x}(k)$, similarly, $\overline{e}(k) = (L_c \otimes I_n)\widetilde{e}(k)$, note that $L_c\mathbf{1}_N = \mathbf{0}_N$ and $L\mathbf{1}_N = \mathbf{0}_N$. Then we can obtain

$$\begin{aligned} \overline{x}(k+1) &= (L_c \otimes A - L_cL \otimes BK)\overline{x}(k) - (L_cL \otimes BK)\widetilde{e}(k) \\ &\quad + (L_c \otimes A_d)\overline{x}(k - d(k)) + (L_c \otimes \widetilde{D})\widetilde{w}(k) \\ \widetilde{z}(k) &= (L_c \otimes I_n)\overline{x}(k) \end{aligned} \tag{2.16}$$

By considering *Assumption* 1, an orthogonal matrix $U = [U_1, U_2] \in \mathbb{R}^{N \times N}$ with $U_2 = \frac{\mathbf{1}_N}{\sqrt{N}}$ exists for further analysis, we can obtain

$$U^T L_c U = U^T U - \frac{1}{N} U^T \mathbf{1}_N \mathbf{1}_N^T U = \begin{bmatrix} \boldsymbol{I}_{N-1} & \mathbf{0}_{N-1} \\ * & 0 \end{bmatrix} = \overline{L}_c$$

Since $\mathcal{L} \in \mathbb{R}^{N \times N}$ is the Laplacian matrix of undirected communication topology, then

$$U^T \mathcal{L} U = \begin{bmatrix} \boldsymbol{L}_1 & \mathbf{0}_{N-1} \\ * & 0 \end{bmatrix} = \overline{\mathcal{L}}$$

where $\boldsymbol{L}_1 \in \mathbb{R}^{(N-1)\times(N-1)}$ is a positive-definite matrix with nonzero eigenvalues.

Define the following orthogonal transformation, inspired by (Liu and Jia 2012, Liu and Jia 2019):

$$\begin{aligned} \hat{x}(k) &= (U^T \otimes I_n)\overline{x}(k) = \mathrm{col}\{\hat{\mathrm{x}}^1(\mathrm{k}), \hat{\mathrm{x}}^2(\mathrm{k})\} \\ \hat{e}(k) &= (U^T \otimes I_n)\widetilde{e}(k) = \mathrm{col}\{\hat{\mathrm{e}}^1(\mathrm{k}), \hat{\mathrm{e}}^2(\mathrm{k})\} \\ \hat{w}(k) &= (U^T \otimes I_n)\widetilde{w}(k) = \mathrm{col}\{\hat{\mathrm{w}}^1(\mathrm{k}), \hat{\mathrm{w}}^2(\mathrm{k})\} \\ \hat{z}(k) &= (U^T \otimes I_n)\widetilde{z}(k) = \mathrm{col}\{\hat{\mathrm{z}}^1(\mathrm{k}), \hat{\mathrm{z}}^2(\mathrm{k})\} \end{aligned}$$

Thus, we have

$$\begin{aligned}\hat{x}(k+1) &= (\overline{L}_c \otimes A - \overline{L}_c\overline{\mathcal{L}} \otimes BK)\hat{x}(k) - (\overline{L}_c\overline{\mathcal{L}} \otimes BK)\hat{e}(k) \\ &\quad + \overline{L}_c \otimes A_d)\hat{x}(k-d(k)) + (\overline{L}_c \otimes \widetilde{D})\hat{w}(k) \\ \hat{z}(k) &= (\overline{L}_c \otimes I_n)\hat{x}(k)\end{aligned} \tag{2.17}$$

Note that the last rows of matrices $\overline{L}_c$ and $\overline{\mathcal{L}}$ are both $\mathbf{0}_N$, by implementing the above orthogonal transformation, the order of (2.17) can be reduced as the following system

$$\begin{aligned}\hat{x}^1(k+1) &= (I_{N-1} \otimes A - \boldsymbol{L}_1 \otimes BK)\hat{x}^1(k) - (\boldsymbol{L}_1 \otimes BK)\hat{e}^1(k) \\ &\quad + (I_{N-1} \otimes A_d)\hat{x}^1(k-d(k)) + (I_{N-1} \otimes \widetilde{D})\hat{w}^1(k) \\ \hat{z}^1(k) &= \hat{x}^1(k)\end{aligned} \tag{2.18}$$

2.3.3 Scaled Consensus Performance Analysis

Based on the above event-triggered SMC analysis, the following theorem is derived for analysing the scaled consensus performance with a predetermined H_∞ disturbance attenuation index γ.

Theorem 2.1. *For the reduced-order system* (2.18)*, given positive scalars* $\gamma > 0$, $0 \leq \varepsilon < 1$, *and* $\tau_M > 0$*, there exist positive-definite matrices* $\widetilde{P} > 0$, $\widetilde{Q} > 0$, $\widetilde{R} > 0$, $\widetilde{Z} > 0$, *and* $\widetilde{\Phi} > 0$ *such that the following series linear matrix inequalities* (*LMIs*)

$$\widetilde{\Phi} \triangleq \begin{bmatrix} \widetilde{\Upsilon}_{11} & \widetilde{Z} & 0 & 0 & 0 & \widetilde{P} & \widetilde{P}A^T - \lambda_i F^T B^T & \widetilde{P}A^T - \lambda_i F^T B^T - \widetilde{P} \\ \star & \widetilde{\Upsilon}_{22} & \widetilde{Z} & 0 & 0 & 0 & \widetilde{P}A_d^T & \widetilde{P}A_d^T \\ \star & \star & \widetilde{\Upsilon}_{33} & 0 & 0 & 0 & 0 & 0 \\ \star & \star & \star & \widetilde{\Upsilon}_{44} & 0 & 0 & \lambda_i F^T B^T & \lambda_i F^T B^T \\ \star & \star & \star & \star & -\gamma^2 I & 0 & \widetilde{D}^T & \widetilde{D}^T \\ \star & \star & \star & \star & \star & -I & 0 & 0 \\ \star & \star & \star & \star & \star & \star & -\widetilde{P} & 0 \\ \star & \star & \star & \star & \star & \star & \star & \tau_M^{-2}(\widetilde{Z} - 2\widetilde{P}) \end{bmatrix} < 0 \tag{2.19}$$

hold for $i = 1$ *and* $i = N-1$.

where

$$\widetilde{P} = P^{-1},\ F^T = \widetilde{P}K^T,\ \widetilde{D} = D - BMD$$

$$\widetilde{Q} = \widetilde{P}Q\widetilde{P},\ \widetilde{R} = \widetilde{P}R\widetilde{P},\ \widetilde{Z} = \widetilde{P}Z\widetilde{P},\ \widetilde{\Psi} = \widetilde{P}\Psi\widetilde{P},$$
$$\widetilde{\Upsilon}_{11} \triangleq -\widetilde{P} + \widetilde{Q} + \widetilde{R} - \widetilde{Z} + \varepsilon\widetilde{\Psi},$$
$$\widetilde{\Upsilon}_{22} \triangleq -\widetilde{Q} - 2\widetilde{Z},\ \widetilde{\Upsilon}_{33} \triangleq -\widetilde{Z} - \widetilde{R},\ \widetilde{\Upsilon}_{44} \triangleq -\widetilde{\Psi},$$

Therefore, the reduced-order MAS (2.18) *can achieve asymptotically stabilisation with a predetermined H_∞ performance.*

Proof. Firstly, the asymptotically stability condition for the reduced-order MAS in (18) with $\hat{w}^1(k) = 0$ is investigated. Take the following Lyapunov-Krasovskii functions:

$$V(k) = V_1(k) + V_2(k) + V_3(k) + V_4(k) \tag{2.20}$$

where

$$V_1(k) \triangleq \hat{x}^{1T}(k)\mathcal{P}\hat{x}^1(k)$$
$$V_2(k) \triangleq \sum_{s=k-d(k)}^{k-1} \hat{x}^{1T}(s)\mathcal{Q}\hat{x}^1(s)$$
$$V_3(k) \triangleq \sum_{s=k-\tau_M}^{k-1} \hat{x}^{1T}(s)\mathcal{R}\hat{x}^1(s)$$
$$V_4(k) \triangleq \tau_M \sum_{s=-\tau_M}^{-1} \sum_{q=k+s}^{k-1} \eta^T(q)\mathcal{Z}\eta(q)$$
$$\eta(q) \triangleq \hat{x}^1(q+1) - \hat{x}^1(q)$$

where

$$\mathcal{P} = I_{N-1} \otimes P > 0,\ \mathcal{Q} = I_{N-1} \otimes Q > 0$$
$$\mathcal{R} = I_{N-1} \otimes R > 0,\ \mathcal{Z} = I_{N-1} \otimes Z > 0$$

are positive-definite matrices to be determined later.
Thus, the increment of $V(k)$ can be computed as

$$\triangle V(k) = \triangle V_1(k) + \triangle V_2(k) + \triangle V_3(k) + \triangle V_4(k)$$

where

$$\triangle V_1(k) = \hat{x}^{1T}(k+1)\mathcal{P}\hat{x}^1(k+1) - \hat{x}^{1T}(k)\mathcal{P}\hat{x}^1(k)$$
$$\triangle V_2(k) = \hat{x}^{1T}(k)\mathcal{Q}\hat{x}^1(k) - \hat{x}^{1T}(k-d(k))\mathcal{Q}\hat{x}^1(k-d(k))$$
$$\triangle V_3(k) = \hat{x}^{1T}(k)\mathcal{R}\hat{x}^1(k) - \hat{x}^{1T}(k-\tau_M)\mathcal{R}\hat{x}^1(k-\tau_M)$$
$$\triangle V_4(k) = \tau_M^2\eta^T(k)\mathcal{Z}\eta(k) - \tau_M \sum_{s=k-\tau_M}^{k-1} \eta^T(s)\mathcal{Z}\eta(s)$$

For estimating the second term of $\triangle V_4(k)$, we obtain

$$-\tau_M \sum_{s=k-\tau_M}^{k-1} \eta^T(s)\mathcal{Z}\eta(s) = -\tau_M \sum_{s=k-\tau_M}^{k-d(k)-1} \eta^T(s)\mathcal{Z}\eta(s) - \tau_M \sum_{s=k-d(k)}^{k-1} \eta^T(s)\mathcal{Z}\eta(s) \quad (2.21)$$

According to Jensen's inequality, for the first term in (2.21), we can derive

$$\begin{aligned} &-\tau_M \sum_{s=k-\tau_M}^{k-d(k)-1} \eta^T(s)\mathcal{Z}\eta(s) \le -(\tau_M - d(k)) \sum_{s=k-\tau_M}^{k-d(k)-1} \eta^T(s)\mathcal{Z}\eta(s) \\ &= \left[\sum_{s=k-\tau_M}^{k-d(k)-1} \eta^T(s)\right]\mathcal{Z}\left[\sum_{s=k-\tau_M}^{k-d(k)-1} \eta(s)\right] \le \left[\sum_{s=k-\tau_M}^{k-d(k)-1} \eta(s)\right]^T \mathcal{Z}\left[\sum_{s=k-\tau_M}^{k-d(k)-1} \eta(s)\right] \end{aligned} \quad (2.22)$$

Similarly, for the second term in (2.21), we can calculate

$$\begin{aligned} &-\tau_M \sum_{s=k-d(k)}^{k-1} \eta^T(s)\mathcal{Z}\eta(s) \le -d(k) \sum_{s=k-d(k)}^{k-1} \eta^T(s)\mathcal{Z}\eta(s) \\ &= \left[\sum_{s=k-d(k)}^{k-1} \eta^T(s)\right]\mathcal{Z}\left[\sum_{s=k-d(k)}^{k-1} \eta(s)\right] \le \left[\sum_{s=k-d(k)}^{k-1} \eta(s)\right]^T \mathcal{Z}\left[\sum_{s=k-d(k)}^{k-1} \eta(s)\right] \end{aligned} \quad (2.23)$$

Consider the event-triggered conditions in (2.10), for any $k \in [k_l, k_{l+1})$, it satisfies that

$$\mathcal{E}(k) = \varepsilon \hat{x}^{1T}(k)\Psi\hat{x}^1(k) - \hat{e}^{1T}(k)\Psi\hat{e}^1(k) \ge 0 \quad (2.24)$$

Then,

$$\triangle V(k) \le \triangle V(k) + \mathcal{E}(k) = \xi^T(k)\Phi_1\xi(k) \quad (2.25)$$

where

$$\xi(k) \triangleq [\hat{x}^{1T}(k) \quad \hat{x}^{1T}(k-d(k)) \quad \hat{x}^{1T}(k-\tau_M) \quad \hat{e}^{1T}(k)]^T$$

$$\Phi_1 \triangleq \begin{bmatrix} \Upsilon_{11} & \mathcal{Z} & 0 & 0 & \hat{A}^T - \hat{B}^T & \hat{A}^T - \hat{B}^T - I \\ \star & \Upsilon_{22} & \mathcal{Z} & 0 & \hat{A}_d^T & \hat{A}_d^T \\ \star & \star & \Upsilon_{33} & 0 & 0 & 0 \\ \star & \star & \star & \Upsilon_{44} & \hat{B}^T & \hat{B}^T \\ \star & \star & \star & \star & -\mathcal{P}^{-1} & 0 \\ \star & \star & \star & \star & \star & \tau_M^{-2}\mathcal{Z}^{-1} \end{bmatrix}$$

$$\hat{A} = I_{N-1} \otimes A,\ \hat{A}_d = I_{N-1} \otimes A_d,\ \hat{B} = \boldsymbol{L}_1 \otimes BK,$$

$$F^T = P^{-1}K^T,\ \Upsilon_{11} \triangleq -\mathcal{P} + \mathcal{Q} + \mathcal{R} - \mathcal{Z} + \varepsilon(I_{N-1} \otimes \Psi),$$

$$\Upsilon_{22} \triangleq -\mathcal{Q} - 2\mathcal{Z},\ \Upsilon_{33} \triangleq -\mathcal{Z} - \mathcal{R},\ \Upsilon_{44} \triangleq -I_{N-1} \otimes \Psi$$

2.3.3 Scaled Consensus Performance Analysis

Since $\boldsymbol{L}_1 \in \mathbb{R}^{(N-1)\times(N-1)}$ is a positive-definite matrix, an orthogonal matrix T exists with $T^T\boldsymbol{L}_1T \triangleq \text{diag}\{\breve{}_1, \breve{}_2, \ldots, \breve{}_{N-1}\}$, where λ_i are the eigenvalues of $\boldsymbol{L}_1$. Then pre-multiplying and post-multiplying the matrix Φ_2 with $\widetilde{T}^T = \text{diag}\{\text{I}_8 \otimes (\text{T}^\text{T} \otimes \text{I})\}$ and $\widetilde{T}$, therefore, matrix Φ_1 can be rewritten with a series of matrices as follows

$$\Phi_2 \triangleq \begin{bmatrix} \overline{\Upsilon}_{11} & Z & 0 & 0 & A^T - \lambda_i K^T B^T & A^T - \lambda_i K^T B^T - I \\ \star & \overline{\Upsilon}_{22} & Z & 0 & A_d^T & A_d^T \\ \star & \star & \overline{\Upsilon}_{33} & 0 & 0 & 0 \\ \star & \star & \star & \overline{\Upsilon}_{44} & \lambda_i K^T B^T & \lambda_i K^T B^T \\ \star & \star & \star & \star & 0 & 0 \\ \star & \star & \star & \star & -P^{-1} & 0 \\ \star & \star & \star & \star & \star & \tau_M^{-2} Z^{-1} \end{bmatrix}$$

$$\overline{\Upsilon}_{11} \triangleq -P + Q + R - Z + \varepsilon\Psi,\ \overline{\Upsilon}_{22} \triangleq -Q - 2Z,$$

$$\overline{\Upsilon}_{33} \triangleq -Z - R,\ \overline{\Upsilon}_{44} \triangleq -\Psi$$

Moreover, notice that

$$0 \leq (P - Z)Z^{-1}(P - Z) = PZ^{-1}P - P - P + Z$$

which implies

$$-PZ^{-1}P \leq Z - 2P$$

Then, we have

$$\Phi_3 \triangleq \begin{bmatrix} \overline{\Upsilon}_{11} & Z & 0 & 0 & A^TP - \lambda_i K^T B^T P & A^TP - \lambda_i K^T B^T P - P \\ \star & \overline{\Upsilon}_{22} & Z & 0 & A_d^T P & A_d^T P \\ \star & \star & \overline{\Upsilon}_{33} & 0 & 0 & 0 \\ \star & \star & \star & \overline{\Upsilon}_{44} & \lambda_i K^T B^T P & \lambda_i K^T B^T P \\ \star & \star & \star & \star & 0 & 0 \\ \star & \star & \star & \star & -P & 0 \\ \star & \star & \star & \star & \star & \tau_M^{-2}(Z - 2P) \end{bmatrix}$$

Therefore,

$$\Phi_2 \leq \Phi_3$$

It follows from Theorem 1 that $\widetilde{\Phi} < 0$ in (2.19) can guarantee $\Phi_3 < 0$ by applying Schur's complement lemma, which implies that $\triangle V(k) < 0$. Therefore, the reduced-order MAS in (2.18) with $\hat{w}^1(k) = 0$ is asymptotically stable.

Secondly, considering the $\hat{w}^1(k) \neq 0$ scenario under zero initial condition, the reduced-order MAS in (2.18) holds for all non-zero $\hat{w}^1(k) \in L_2[0,\infty)$ with guaranteed H_∞ performance that

$$\left\|\hat{z}^1(k)\right\|_2 < \gamma \left\|\hat{w}^1(k)\right\|_2$$

Then, establishing the following index for all $k \in [k_l, k_{l+1})$:

$$\mathcal{F}(k) \triangleq \xi^T(k)\Phi\xi(k) + \hat{z}^{1T}(k)\hat{z}^1(k) - \gamma^2\hat{w}^{1T}(k)\hat{w}^1(k) \tag{2.26}$$

By implementing the same stability analysis method as above, we can achieve

$$\mathcal{F}(k) \leq \zeta^T(k)\Phi_4\zeta(k)$$

where $\zeta(k) \triangleq [\hat{x}^{1T}(k) \quad \hat{x}^{1T}(k-d(k)) \quad \hat{x}^{1T}(k-\tau_M) \quad \hat{e}^{1T}(k) \quad \hat{w}^{1T}(k)]^T$

$$\Phi_4 \triangleq \begin{bmatrix} \overline{\Upsilon}_{11} & Z & 0 & 0 & 0 & I & A^TP - \lambda_i K^T B^T P & A^TP - \lambda_i K^T B^T P - P \\ \star & \overline{\Upsilon}_{22} & Z & 0 & 0 & 0 & A_d^T P & A_d^T P \\ \star & \star & \overline{\Upsilon}_{33} & 0 & 0 & 0 & 0 & 0 \\ \star & \star & \star & \overline{\Upsilon}_{44} & 0 & 0 & \lambda_i K^T B^T P & \lambda_i K^T B^T P \\ \star & \star & \star & \star & -\gamma^2 I & 0 & \widetilde{D}^T & \widetilde{D}^T \\ \star & \star & \star & \star & \star & -I & 0 & 0 \\ \star & \star & \star & \star & \star & \star & -P & 0 \\ \star & \star & \star & \star & \star & \star & \star & \tau_M^{-2}(Z-2P) \end{bmatrix}$$

with

$$\widetilde{D} = D - BMD$$

By applying Schur's complement lemma, $\Phi_4 < 0$ guarantees $\Phi_3 < 0$, then we can guarantee

$$\triangle V(k) + \hat{z}^{1T}(k)\hat{z}^1(k) - \gamma^2\hat{w}^{1T}(k)\hat{w}^1(k) < 0 \tag{2.27}$$

In order to derive a stabilising equivalent controller gain K, let $\widetilde{P} \triangleq P^{-1}$, $F^T \triangleq \widetilde{P}K^T$, $\widetilde{Q} \triangleq \widetilde{P}Q\widetilde{P}$, $\widetilde{R} \triangleq \widetilde{P}R\widetilde{P}$, $\widetilde{Z} \triangleq \widetilde{P}Z\widetilde{P}$, $\widetilde{\Psi} = \widetilde{P}\Psi\widetilde{P}$, $\widetilde{\Upsilon}_{11} \triangleq -\widetilde{P} + \widetilde{Q} + \widetilde{R} - \widetilde{Z} + \varepsilon\widetilde{\Psi}$, $\widetilde{\Upsilon}_{22} \triangleq -\widetilde{Q} - 2\widetilde{Z}$, $\widetilde{\Upsilon}_{33} \triangleq -\widetilde{Z} - \widetilde{R}$, $\widetilde{\Upsilon}_{44} \triangleq -\widetilde{\Psi}$, then pre-multiplying and post-multiplying Φ_4 by a diagonal matrix $\mathrm{diag}(\mathrm{I}_4 \otimes \mathrm{P}^{-1}, \mathrm{I}, \mathrm{I}, \mathrm{P}^{-1}, \mathrm{P}^{-1})$ and $\mathrm{diag}(\mathrm{I}_4 \otimes \mathrm{P}^{-1}, \mathrm{I}, \mathrm{I}, \mathrm{P}^{-1}, \mathrm{P}^{-1})$, respectively. Therefore, Φ_4 is equivalent to $\widetilde{\Phi}$.
Finally,

$$\Phi_4 \leq \widetilde{\Phi} < 0$$

Note that for the series $LMIs$ in $\widetilde{\Phi}$, we only investigate the smallest λ_1 and largest λ_{N-1} eigenvalues of $\boldsymbol{L}_1$ associated with $LMIs$ in $\widetilde{\Phi}$ because of the convex property of $LMIs$. From the above proof, we can conclude that the reduced-order MAS (2.18) is asymptotically stable. Furthermore, the reduced-order MAS is equivalent to the MAS (2.1). To sum up, the MAS in (2.1) can achieve the scaled consensus with a prescribed H_∞ performance level γ. Therefore, the proof is completed. □

Remark 2.1. *Note that by Theorem* 1*, the linear matrix inequalities in* (2.19) *with the smallest* λ_1 *and largest* λ_{N-1} *eigenvalues of* $\boldsymbol{L}_1$ *can be solved by existing techniques, which convey the* H_∞ *scaled consensus problem subject to unknown external bounded disturbance and time-varying state delay in system* (2.1) *is theoretically feasible. The next step is to design an event-triggered sliding mode controller so that the state trajectories of system* (2.1) *can be maintained on a predefined sliding surface.*

2.3.4 Sliding Mode Control Protocol Synthesis

In this section, the integral sliding mode controller is designed and the sliding mode stability analysis is manifested for the scaled consensus problem.

Specifically, the design of integral sliding mode controller contains an equivalent control law and a nonlinear switching control law to tolerate disturbances or system uncertainties, accordingly, the overall sliding mode controller is designed as follows

Theorem 2.2. *For the MAS described in* (2.1) *along with the sliding surface function designed in* (2.4)*, the event-triggered sliding mode controller in* (2.28) *is proposed, then state trajectories will be steered to arrive the predefined sliding manifold in finite time.*

$$u_i(k) = K\sum_{j=1}^{N} a_{ij}\Big(\alpha_{ij}x_j(k^j_{l'}) - x_i(k^i_l)\Big) - \Omega s_i(k) - \rho_i \cdot \mathrm{sat}\left(s_i(k)\right) \tag{2.28}$$

where $\rho_i = \overline{\omega}\,\|MD\|$ *and for all* $k \in \left[k^i_l, k^i_{l+1}\right)$, $\mathrm{sat}(\cdot)$ *is a saturation function expressed by*

$$\mathrm{sat}\left(s_i(k)\right) = \begin{cases} s_i(k)/\varphi, \ \|s_i(k)\| \le \varphi \\ \mathrm{sign}(s_i(k)), \ \|s_i(k)\| > \varphi. \end{cases}$$

Furthermore, the sliding mode surface function attached event-triggered scheme is derived as

$$\begin{cases} s_i(k) = Mx_i(k^i_l) - Mx_i(0) + b_i(k^i_l) \\ b_i(k^i_l) = b_i(k^i_{l-1}) - \sigma_i(k^i_{l-1}) \end{cases} \tag{2.29}$$

where $\sigma_i(k^i_{l-1})$ *is given as*

$$\sigma_i(k^i_{l-1}) = (MA-M)x_i(k^i_{l-1}) + MA_d x_i(k^i_{l-1}-d(k)) + MBK\sum_{j=1}^{N} a_{ij}\Big(\alpha_{ij}x_j(k^i_{l-1}) - x_i(k^i_{l-1})\Big)$$

and k^i_{l-1} *is the last event-triggering time instant.*

Proof. The following Lyapunov function is selected:

$$\mathcal{V}_i(k) = \frac{1}{2}s_i^T(k)s_i(k)$$

From the derived sliding mode surface function in (2.29), we have

$$\begin{aligned}\Delta s_i(k) &= s_i(k+1) - s_i(k)\\ &= u_i(k) + MDw_i(k) - K\sum_{j=1}^{N} a_{ij}\Big(\alpha_{ij}x_j(k) - x_i(k)\Big)\\ &= MDw_i(k) - \Omega s_i(k) - \rho_i \cdot \mathrm{sat}\,(s_i(k))\end{aligned}$$

Then, deducing the increment of $\mathcal{V}_i(k)$ and considering the event-triggered SMC law in (2.28) and $\Delta s_i(k)$, we obtain

$$\begin{aligned}\Delta\mathcal{V}_i(k) &= \mathcal{V}_i(k+1) - \mathcal{V}_i(k)\\ &= s_i^T(k)\Delta s_i(k) + \frac{1}{2}\Delta s_i^T(k)\Delta s_i(k)\\ &= s_i^T(k)[MDw_i(k) - \rho_i \cdot \mathrm{sat}\,(s_i(k))] - s_i^T(k)\Omega s_i(k) + \frac{1}{2}\Delta s_i^T(k)\Delta s_i(k)\\ &\le -s_i^T(k)\Omega s_i(k) + \frac{1}{2}\Delta s_i^T(k)\Delta s_i(k) + \left\|s_i^T(k)\right\| \|MD\| \|w_i(k)\| - s_i^T(k)\rho_i \cdot \mathrm{sat}\,(s_i(k))\\ &\le -s_i^T(k)\Omega s_i(k) + \frac{1}{2}\Delta s_i^T(k)\Delta s_i(k) + \left\|s_i^T(k)\right\| \rho_i - s_i^T(k)\rho_i \cdot \mathrm{sat}\,(s_i(k))\end{aligned}$$

According to the saturation function sat $(s_i(k))$, we derive that if $\|s_i(k)\| \le \varphi$, with the designed controller (2.28), we obtain

$$\begin{aligned}\Delta\mathcal{V}_i(k) &\le -s_i^T(k)\Omega s_i(k) + \frac{1}{2}\Delta s_i^T(k)\Delta s_i(k) + \rho_i\left(\|s_i(k)\| - \|s_i(k)\|^2/\varphi\right)\\ &\le -s_i^T(k)\Omega s_i(k) + \frac{1}{2}\Delta s_i^T(k)\Delta s_i(k)\end{aligned}$$

If $\|s_i(k)\| > \varphi$, with the designed controller (28), we obtain

$$\Delta\mathcal{V}_i(k) \le -s_i^T(k)\Omega s_i(k) + \frac{1}{2}\Delta s_i^T(k)\Delta s_i(k)$$

Therefore, Ω is a positive-definite matrix to be designed appropriately, which can guarantee that $\Delta\mathcal{V}_i(k) < 0$.

Then, the sliding surface function can be limited within a bounded manifold with an equilibrium point. Finally, the state trajectories of the MAS in (2.1) can be maintained on the sliding surface with the event-triggered sliding mode controller in (2.28). The proof is completed. □

Remark 2.2. *The proposed event-triggered SMC algorithm with a new sliding mode surface can steer the state trajectories to the desired equilibrium point and chattering reduction as well as easily extend to address matched and mismatched disturbances. In order to verify the efficiency of proposed approach, an illustrative example is provided in the following section.*

2.4 Simulation Results

The effectiveness of this proposed event-triggered sliding mode method in this chapter is verified by the following two-stage chemical reactors with delayed streams, see (Li *et al.* 2020). A group of 6 two-stage chemical reactors consisting of MAS (2.1) is modelled as follows:

$$\dot{x}_i = \begin{bmatrix} -\frac{1}{\theta_1} - k_1 & \frac{1-R_2}{V_1} \\ 0 & -\frac{1}{\theta_2} - k_2 \end{bmatrix} x_i + \begin{bmatrix} 0 & 0 \\ \frac{R_1}{V_2} & \frac{R_2}{V_2} \end{bmatrix} x_i(t-d(t)) + \begin{bmatrix} 0 \\ \frac{F_2}{V_2} \end{bmatrix} u_i + \begin{bmatrix} \delta_1 \\ \delta_2 \end{bmatrix} w_i(t) \quad (2.30)$$

where $x_i = [x_{i1}, x_{i2}]^T$ is the state, x_{i1} and x_{i2} are compositions, u_i is the control input, $d(t)$ is the bounded unknown time-varying delay, θ_m indicate reactor residence times, R_m represent recycle flow rates, k_m are reaction constants, F_m mean the feed rates, V_m are reactor volumes and δ_m denote the amplitudes of the external disturbances $w_i(t)$ with $i = 1, \cdots, 6$ and $m = 1, 2$.

To perform our design, we select $\theta_1 = 10$, $\theta_2 = 4$, $k_1 = 19$, $k_2 = 17$, $R_1 = 0.5$ $R_2 = 0.3$, $V_1 = 0.1$, $V_2 = 0.5$, $F_i = 0.6$, $\delta_1 = 0.5$, $\delta_2 = 0.9$, and apply the first-order Taylor expansion with the sampling period $T = 0.1$s, thus, the model of (2.30) is discretised as

$$x_i(k+1) = \begin{bmatrix} -0.91 & 0.65 \\ 0 & -0.73 \end{bmatrix} x_i(k) + \begin{bmatrix} 0 & 0 \\ 0.1 & 0.06 \end{bmatrix} x_i(k-d(k)) + \begin{bmatrix} 0 \\ 0.12 \end{bmatrix} u_i(k) + \begin{bmatrix} 0.05 \\ 0.09 \end{bmatrix} w_i(k) \quad (2.31)$$

where $d(k) = |\sin(k)|$ is the time-varying state delay with upper bound $\tau_M = 1$, and the external disturbances are defined as $w_{i1}(t) = |\sin(k)|$ and $w_{i2}(t) = |\cos(k)|$, respectively.

Moreover, the graph $\mathcal{G}$ models the communication topology of MAS (2.31) with 6 two-stage chemical reactors, which is illustrated in Fig. 2.1. The corresponding Laplacian matrix $\mathcal{L}$ is

$$\mathcal{L} = \begin{bmatrix} 2 & -1 & 0 & 0 & 0 & -1 \\ -1 & 2 & -1 & 0 & 0 & 0 \\ 0 & -1 & 2 & -1 & 0 & 0 \\ 0 & 0 & -1 & 2 & -1 & 0 \\ 0 & 0 & 0 & -1 & 2 & -1 \\ -1 & 0 & 0 & 0 & -1 & 2 \end{bmatrix}$$

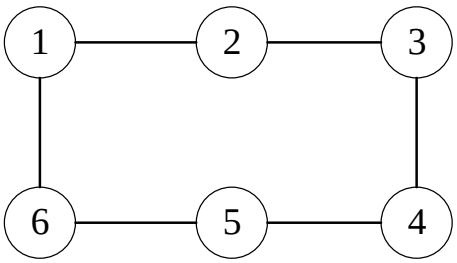

Figure 2.1. Communication topology of multi-agent system.

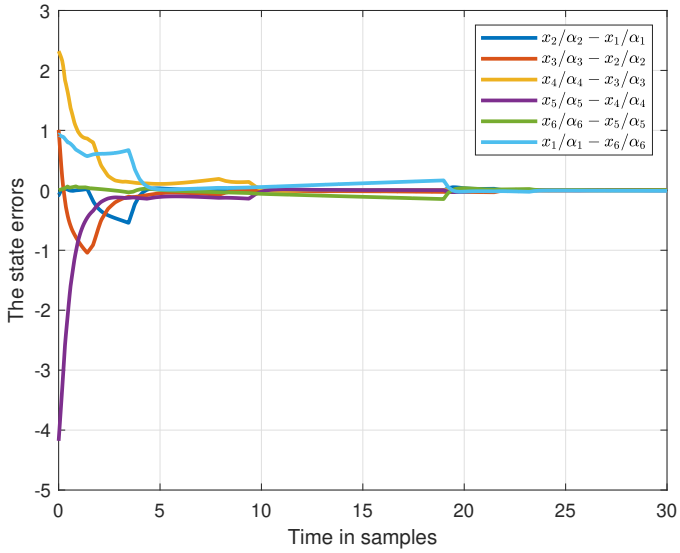

Figure 2.2. State errors of scaled consensus of 6 agents with event-triggered scheme.

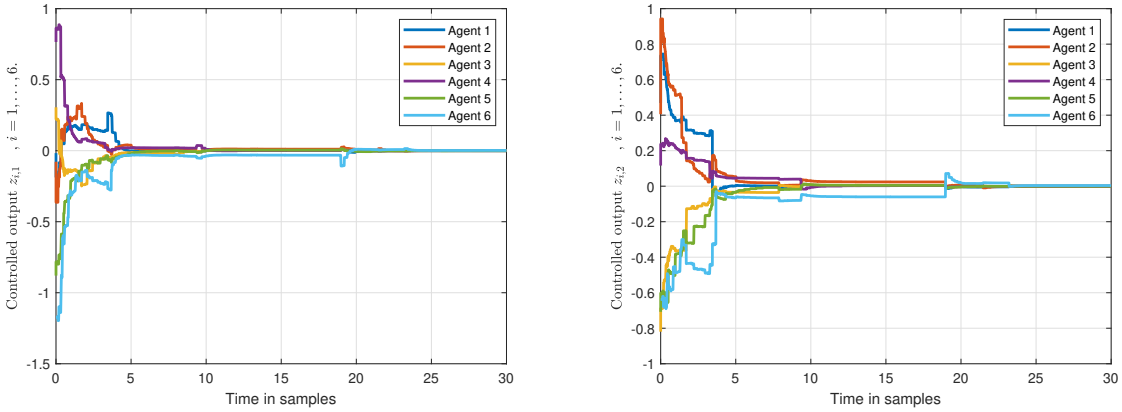

(a) Trajectories of $z_{i1}, i = 1, 2, \ldots, 6$.

(b) Trajectories of $z_{i2}, i = 1, 2, \ldots, 6$.

Figure 2.3. Controlled output trajectories.

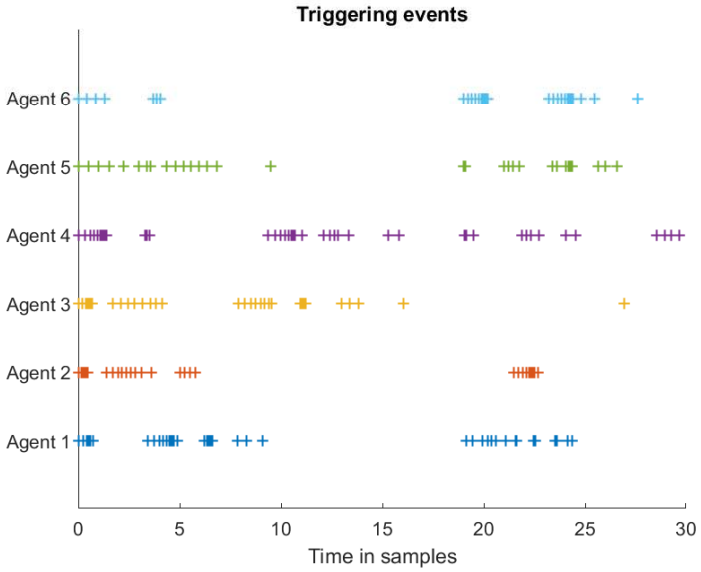

Figure 2.4. Event-based release instants k_l^i of agents.

The designed controller output function $z_i(k)$ is described as

$$z_i(k) = x_i(k) - \frac{1}{6}\sum_{j=1}^{6} \alpha_{ij} x_j(k) \tag{2.32}$$

In this case, the state trajectories of $z_i(k)$ under the event-triggered sliding mode scheme are depicted in Fig. 2.3. For the scaled consensus problem in MAS (2.31), the scaled scalars are selected as $\alpha_i = \{0.5, 0.8, 0.4, 0.3, 0.6, 0.9\}$. The initial conditions of each agent are randomly selected within $[-1, 1]$. The threshold parameter of event-triggered condition is given as $\varepsilon = 0.8$. Then, by solving the corresponding LMIs in(2.19), and considering the above given parameters, the controller gain matrix is computed as

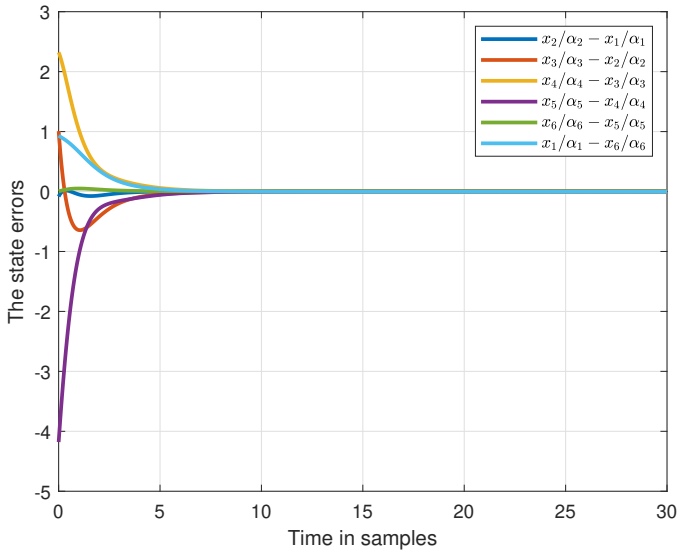

Figure 2.5. State errors of scaled consensus with 6 agents without event-triggered scheme.

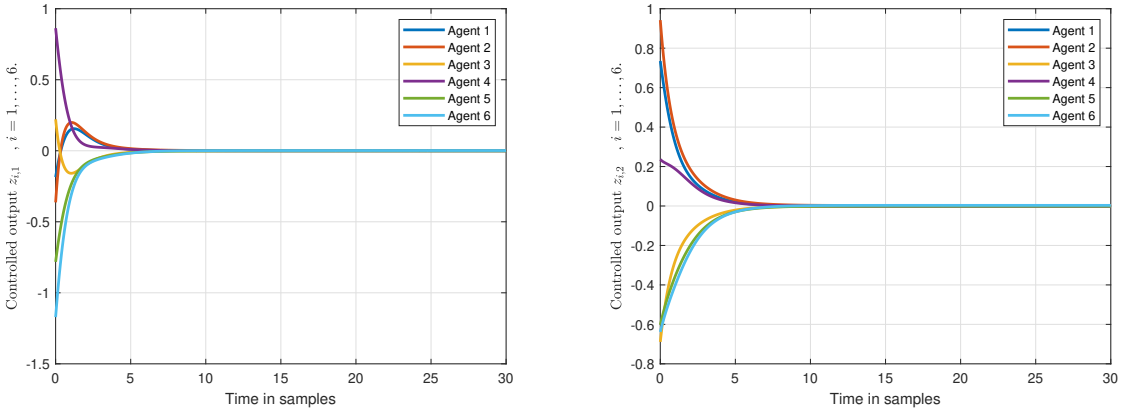

(a) Trajectories of z_{i1}, $i = 1, 2, \ldots, 6$.

(b) Trajectories of z_{i2}, $i = 1, 2, \ldots, 6$.

Figure 2.6. Controlled output trajectories without event-triggered scheme.

$K = \begin{bmatrix} -0.3525 & 0.1705 \end{bmatrix}$ and the minimal H_∞ disturbance attenuation index is $\gamma = 0.17$. Consequently, Figs 2.2-2.4 can be obtained by deploying the event-triggered sliding mode controller in (2.28). Fig. 2.2 indicates the state errors of the six agents which demonstrates the reachability of scaled consensus of MAS, and Fig. 2.4 shows the event-based release instants for each agent. Comparison with Figs. 2.5 and 2.6 shows the later reaches the scaled consensus with faster convergence speed. However, from Figs 2.2-2.4, transmitted states are significantly degraded from the desired scaled consensus performance. Therefore, the simulation results conclude that the closed-loop MAS presented in this work is robust stable and the discrete-time scaled consensus

problem in the presence of the state time-varying delay and external bounded disturbance is solvable.

2.5 Chapter Summary

In this chapter, we have studied the discrete-time scaled consensus problem subject to the time-varying state delay and bounded external disturbance in MAS. The integral SMC method is employed to handle the external disturbance and improve the robustness of MAS. Then, a feasible solution to the limited energy issue in the scaled consensus problem is introduced, which is the event-triggered control scheme. Under the proposed event-triggered SMC strategy, the discrete-time scaled consensus problem is converted into a stability analysis problem of a reduced-order MAS. Sufficient conditions are presented for the system to guarantee that a minimised H_∞ performance index is satisfied. A practical example is presented to show the effectiveness of the developed new design method in term of the event-triggered SMC. Future research direction includes considering this framework with an online optimization problem rather than solving LMIs offline, which can achieve an online optimal solution and does not require the entire input in advance.

Chapter 3

Event-triggered Consensus Control for Nonlinear Multi-agent Systems

3.1 Introduction

A distributed consensus controller aims to steer the state of all agents to approach a common goal by only requiring local interactions among the adjacent agents. Due to the introduction of a distributed controller and local information exchange, each subsystem lacks information on the system parameters and external disturbances. For this reason, the consensus problem involving parametric uncertainties and unknown external disturbances are typically challenging to study.

Hysteresis nonlinearities are incorporated in many physical devices, materials and systems, such as electrical relays, memory metal, mechanical actuators. The ubiquitous effects of hysteresis nonlinearities often degrade the performance of control systems and it can be mathematically complicated to investigate. There are two different methods to deal with the impact of unknown hysteresis. The first technique is to cancel the hysteresis impacts in controller design by constructing an inverse model of hysteresis (Rakotondrabe 2010, Zhou *et al.* 2012). Another method is to model the hysteresis by a differential equation, then treat the hysteresis effects as a bounded disturbance (Chen *et al.* 2013a). Although the ubiquitous influences of hysteresis phenomenon present in uncertain nonlinear systems, the results of consensus control with unknown hysteresis are still very limited in nonlinear MAS. Therefore, leaderless consensus control problem with unknown backlash-like hysteresis is worth investigating.

Adaptive backstepping control (Krstic *et al.* 1995, Zhou and Wen 2008) is a promising technique to design distributed controller and handle parametric uncertainties for uncertain nonlinear MAS, see e.g. (Wang *et al.* 2020c). The authors (Huang *et al.* 2017) presented a smooth distributed adaptive controller to resolve the high-order nonlinear leader-following consensus problem considering unknown parameters and uncertain external disturbances. Adaptive command filtered strategy based on adaptive backstepping (Shen and Shi 2015) was employed to ensure the leader-following consensus tracking errors are semi-globally bounded. The output leader-following consensus tracking is asymptotically achieved depending upon locally available interactions and involving mismatched unknown parameters and external disturbances (Wang *et al.* 2017c). A similar distributed adaptive consensus control algorithm with a new Nussbaum-type function (Huang *et al.* 2018a) was exploited to tackle unknown control directions problem for nonlinear MAS. The problems of unknown control directions and backlash-like hysteresis for nonlinear MAS under undirected communication topology were addressed by adaptive neural networks control method (Chen *et al.* 2016).

Noted that the above consensus control algorithms are all developed based on a common assumption that the information from one agent towards its neighbours is transmitted continuously and control signals update frequently or at periodic sampling instants. Continuous information exchange between agents and frequent controller updating increase communication effort and energy usage, which may cause unnecessary communication and computing resources consumption. Event-triggered communication mechanism has been developed as an effective method to reduce communication among agents and controller updates frequency considerably during event intervals as well as maintain a desired system performance. In MAS, events are asynchronously generated since distinct event-triggered conditions are embedded in the corresponding subsystems (Dimarogonas *et al.* 2011), which makes theoretical analysis of nonlinear MAS more complicated. The linear leader-following and leaderless consensus problems with external disturbances are investigated by a distributed event-based consensus controller (Xing *et al.* 2016). The adaptive backstepping based fuzzy event-triggered control algorithm is developed to resolve the consensus tracking problem, which reaches the consensus and saves the computation resources (Li *et al.* 2018). A distributed consensus controller based on a fixed threshold event-triggered strategy is constructed to deal with the difficulty of intermittent actuator faults for nonlinear

MAS (Wang *et al.* 2020d). Accordingly, frequently control signals updating and unknown backlash nonlinearity escalate the level of difficulty in theoretical analysis and limit the outcomes of event-triggered leaderless consensus control problem for nonlinear MAS.

Motivated by the above observation, we explore the event-triggered leaderless consensus tracking problem with unknown backlash-like hysteresis for MAS. Most consensus schemes require the global information of a predetermined leader or exosystem, which decreases the degree of autonomy in MAS. On the contrary, leaderless consensus can be reached without a predefined global exosystem. Moreover, an auxiliary system represented by local information interactions is introduced to overcome the barrier brought by the asymmetric semi-definite positive Laplacian matrix. Likewise, an event-triggered strategy based on a dynamic threshold is proposed to achieve considerable reduction of controller update. The designed event-triggered adaptive leaderless consensus control protocol is applicable to improve the leaderless consensus tracking performance of the nonlinear MAS by compensating for impact of the unknown backlash-like hysteresis. Moreover, the controller can ensure the leaderless consensus tracking error asymptotically converges to zero. An example is given to show the effectiveness of the new control design method.

The reminder of the chapter is as follows. Section 3.2 presents problem formulation and preliminaries. Event-triggered adaptive leaderless consensus controller is designed in Section 3.3. In Section 3.4, the tracking performance of leaderless consensus control is evaluated. A group of four robotic manipulators is used in Section 3.5 to verify the new control scheme and Section 3.6 summarises this study.

3.2 Problem Formulation

A set of N nonlinear agents are modelled as

$$\begin{aligned} \dot{x}_{i,q} &= x_{i,q+1} + \varphi_{i,q}(\bar{x}_{i,q})^T\theta_i \\ \dot{x}_{i,n} &= b_i u_i(\omega) + \varphi_{i,n}(x_i)^T\theta_i + d_i(t) \\ y_i &= x_{i,1} \end{aligned} \tag{3.1}$$

where $\bar{x}_{i,q} = (x_{i,1}, \ldots, x_{i,q})$, for $i = 1, \ldots, N$ and $q = 1, \ldots, n-1$. The function $\varphi_{i,j}$ is known nonlinear function for $j = 1, \ldots, n$, and yet $\theta_i \in \mathbb{R}^{q_i}$ represents a column vector

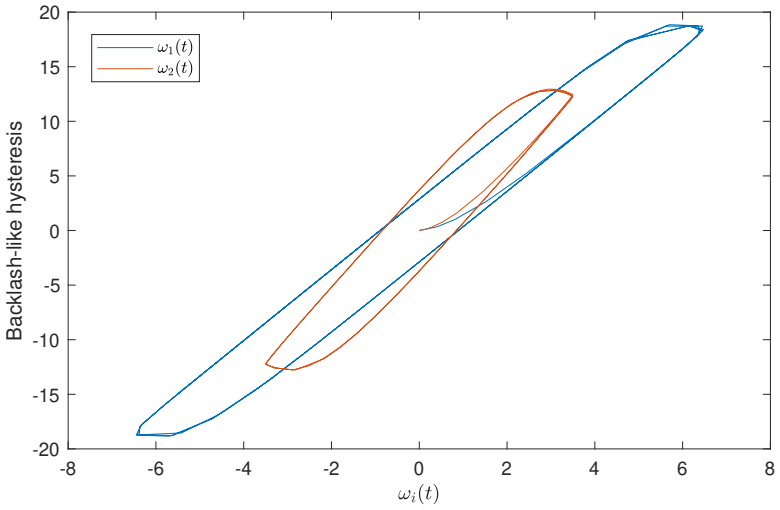

Figure 3.1. Backlash-like hysteresis curve for each agent..

of unknown parameters. $x_i = [x_{i,1}, \ldots, x_{i,n}]^T \in \mathbb{R}^n$ are system states. $u_i, y_i \in \mathbb{R}$ are the inputs and system outputs.

The control gain b_i is a vector of non-zero constants, $d_i(t)$ denotes the unknown time-varying bounded disturbances, and $u_i(\omega)$ indicates the backlash-like hysteresis type of nonlinearity impacts on actuators. The dynamics of backlash-like hysteresis is defined by

$$\frac{du_i}{dt} = a_i \left| \frac{d\omega_i}{dt} \right| (c_i\omega_i - u_i) + H_i \frac{d\omega_i}{dt} \tag{3.2}$$

where H_i, a_i and c_i are constants, c_i represents the gradient of the lines and the $c_i > H_i$ holds. According to the results (Su *et al.* 2000), the solution of (3.2) can be obtained as

$$\begin{aligned} u_i(t) =& c_i\omega_i(t) + g_i(\omega) \\ g_i(\omega) =& \left[u_i(0) - c_i\omega_i(0)\right] e^{-a_i(\omega_i - \omega_i(0))sgn(\dot{\omega}_i)} \\ &+ e^{-a_i\omega_i sgn(\dot{\omega}_i)} \int_{\omega_i(0)}^{\omega_i} \left[H_i - c_i\right] e^{a_i\xi(sgn(\dot{\omega}_i))} d\xi \end{aligned} \tag{3.3}$$

The solution implies that backlash-like hysteresis type of nonlinearities can be modelled by (3.2) as illustrated in Figure 3.1. The parameters are given as $a_1 = a_2 = 1$, $c_1 = 3.2$, $c_2 = 4.5$, $H_1 = 0.35$ and $H_2 = 0.6$, the input signals are set as $\omega_1(t) = 6.4\sin(2.4t)$ and $\omega_2(t) = 3.5\sin(1.5t)$, and the initial condition $u_i(0) = 0$. From Figure 3.1, $g_i(\omega)$ is bounded but the bound is unknown.

Next, we substitute the structure of solution (3.3) for the control input $u_i(\omega)$, the uncertain nonlinear MAS (3.1) are restructured as

$$\begin{aligned} \dot{x}_{i,q} &= x_{i,q+1} + \varphi_{i,q}(\bar{x}_{i,q})^T\theta_i, \quad q = 1, \ldots, n-1 \\ \dot{x}_{i,n} &= \beta_i\omega_i(t) + \varphi_{i,n}(x_i)^T\theta_i + b_i g_i(\omega) + d_i(t) \\ y_i &= x_{i,1} \end{aligned} \tag{3.4}$$

where $\beta_i = b_i c_i$ and $c_i > 0$ for $i = 1, \ldots, N$.

Our objective in this chapter is *to design distributed event-triggered adaptive leaderless consensus control such that all the signals from system* (2.1) *are bounded, while guaranteeing the consensus tracking errors asymptotically tend to zero.*

To develop our main results in the next section, we introduce the following assumptions:

Assumption 3.1. *(Ren* et al. *2007) The directed communication graph $\mathcal{G}$ is strongly connected, which implies that the Laplacian matrix $\mathcal{L}$ consists of a zero eigenvalue and the remaining eigenvalues locating in the open right half-plane.*

Assumption 3.2. *The unknown time-varying disturbance $d_i(t)$ is bounded by D_i, where D_i is an unknown constant satisfying $|d_i(t)| \leq D_i$.*

Assumption 3.3. *The sign of parameter b_i is known and $b_i \neq 0$.*

Lemma 3.1. *(Ren* et al. *2009) The hyperbolic tangent function* $\tanh(\cdot)$ *with a given positive function $\eta(t) > 0$ and $\lambda \in \mathbb{R}$ satisfies the following inequality:*

$$0 \leq |\lambda| - \lambda \tanh(\frac{\lambda}{\eta(t)}) \leq \kappa\varepsilon \tag{3.5}$$

where κ represents a positive constant satisfying $\kappa = e^{-(\kappa+1)}$, which obtains $\kappa = 0.2785$.

Remark 3.1. *Leader-following consensus algorithms are designed (Shi and Shen 2017, Huang* et al. *2018b), specifically, the desired trajectories are described by leaders or exosystems which bring additional assumption that the leader knowledge and its n-th order derivatives are accessible to all subsystems. Second, the establishment of leaders could lower the degree of autonomy in numerous practical applications. Conversely, the leaderless consensus control is an alternative to avoid adding exosystems and decreasing the degree of autonomy.*

Remark 3.2. *Unlike assumptions on nonlinear functions under the Lipschitz-like or global Lipschitz conditions (Zheng* et al. *2019, Niu* et al. *2017b), the nonlinear functions $\varphi_{i,j}(x_i)^T\theta_i$ constructed in* (3.1) *help eliminate the assumptions, which ensures that system model* (3.1) *can represent the majority of practical applications.*

3.3 Event-triggered Controller Design

An adaptive backstepping approach is implemented to construct the event-triggered adaptive leaderless consensus controller. To start, we introduce the following auxiliary system

$$\dot{z}_i = -\sum_{j=1}^{N} a_{i,j}(y_i - y_j), \quad i = 1, \ldots, N \tag{3.6}$$

Let the leaderless consensus tracking error variables $e_{i,1}$ and $e_{i,q}$ be

$$\begin{aligned} e_{i,1} =& x_{i,1} - z_i \\ e_{i,q} =& x_{i,q} - \alpha_{i,q-1}, \quad q = 2, \ldots, n \end{aligned} \tag{3.7}$$

where $\alpha_{i,q-1}, i = 1, \ldots, N$ are virtual control laws and z_i represents the auxiliary system states. The adaptive backstepping control design procedure consists of n steps.

Step 1: From (3.7), the derivative of the leaderless consensus tracking error $e_{i,1}$ is derived as

$$\dot{e}_{i,1} = e_{i,2} + \alpha_{i,1} + \varphi_{i,1}^T \theta_i - \dot{z}_i \tag{3.8}$$

Then, selecting the virtual controller $\alpha_{i,1}$ as follows:

$$\alpha_{i,1} = -k_1 e_{i,1} - \varphi_{i,1}^T \hat{\theta}_i + \dot{z}_i \tag{3.9}$$

where k_1 is a positive prescribed parameter, $\hat{\theta}_i$ denotes the parameter estimation of θ_i for the ith agent. Substituting (3.6) and (3.7) into (3.8), we obtain

$$\dot{e}_{i,1} = e_{i,2} - k_1 e_{i,1} + \varphi_{i,1}^T \tilde{\theta}_i \tag{3.10}$$

The Lyapunov function is selected as

$$V_1 = \frac{1}{2}\sum_{i=1}^{N} e_{i,1}^2 + \frac{1}{2}\sum_{i=1}^{N} \tilde{\theta}_i^T \Gamma_i^{-1} \tilde{\theta}_i \tag{3.11}$$

where $\tilde{\theta}_i = \theta_i - \hat{\theta}_i$, Γ_i is a positive definite matrix. Then, the resulting $\dot{V}_1$ is

$$\begin{aligned} \dot{V}_1 =& \sum_{i=1}^{N} e_{i,1}\dot{e}_{i,1} - \sum_{i=1}^{N} \tilde{\theta}_i^T \Gamma_i^{-1} \dot{\hat{\theta}}_i \\ =& -\sum_{i=1}^{N} k_1 e_{i,1}^2 + \sum_{i=1}^{N} e_{i,1} e_{i,2} + \sum_{i=1}^{N} \tilde{\theta}_i^T \Gamma_i^{-1} \left(\Gamma_i \tau_{i,1} - \dot{\hat{\theta}}_i \right) \end{aligned} \tag{3.12}$$

We select the adaptive law for $\dot{\hat{\theta}}_i$ as

$$\dot{\hat{\theta}}_i = \Gamma_i \tau_{i,1}, \quad \tau_{i,1} = e_{i,1}\varphi_{i,1} \tag{3.13}$$

where $\tau_{i,1}$ is the first tuning function.

Step 2: We derive the second error variable as

$$e_{i,2} = x_{i,2} - \alpha_{i,1} \tag{3.14}$$

so the $e_{i,2}$ dynamics can be derived

$$\begin{aligned}\dot{e}_{i,2} =& \dot{x}_{i,2} - \dot{\alpha}_{i,1} \\ =& e_{i,3} + \alpha_{i,2} + \left(\varphi_{i,2} - \frac{\partial \alpha_{i,1}}{\partial x_{i,1}}\varphi_{i,1}\right)^T \theta_i - \frac{\partial \alpha_{i,1}}{\partial x_{i,1}} x_{i,2} \\ & - \frac{\partial \alpha_{i,1}}{\partial \hat{\theta}_i}\dot{\hat{\theta}}_i - \sum_{j=1}^{N} a_{ij}\frac{\partial \alpha_{i,1}}{\partial x_{j,1}}\left(x_{j,2} + \varphi_{j,1}^T \theta_j\right)\end{aligned} \tag{3.15}$$

Thus, the virtual controller $\alpha_{i,2}$ is given by

$$\begin{aligned}\alpha_{i,2} =& -e_{i,1} - k_2 e_{i,2} - \left(\varphi_{i,2} - \frac{\partial \alpha_{i,1}}{\partial x_{i,1}}\varphi_{i,1}\right)^T \hat{\theta}_i + \frac{\partial \alpha_{i,1}}{\partial x_{i,1}} x_{i,2} \\ & + \sum_{j=1}^{N} a_{ij}\frac{\partial \alpha_{i,1}}{\partial x_{j,1}}\left(x_{j,2} + \varphi_{j,1}^T \hat{\theta}_{ij}\right) + \frac{\partial \alpha_{i,1}}{\partial \hat{\theta}_i}\Gamma_i \tau_{i,2}\end{aligned} \tag{3.16}$$

where k_2 is a positive design constant, and the second tuning function $\tau_{i,2}$ is determined as

$$\tau_{i,2} = \tau_{i,1} + \left(\varphi_{i,2} - \frac{\partial \alpha_{i,1}}{\partial x_{i,1}}\varphi_{i,1}\right) e_{i,2} \tag{3.17}$$

Substituting the virtual controller $\alpha_{i,2}$ into (3.15), the $e_{i,2}$ dynamics can be derived as

$$\begin{aligned}\dot{e}_{i,2} =& -e_{i,1} - k_2 e_{i,2} + e_{i,3} + \left(\varphi_{i,2}^T - \frac{\partial \alpha_{i,1}}{\partial x_{i,1}}\varphi_{i,1}^T\right)\tilde{\theta}_i \\ & - \sum_{j=1}^{N} a_{ij}\frac{\partial \alpha_{i,1}}{\partial x_{j,1}}\varphi_{j,1}^T \tilde{\theta}_{i,j} + \frac{\partial \alpha_{i,1}}{\partial \hat{\theta}_i}\left(\Gamma_i \tau_{i,2} - \dot{\hat{\theta}}_i\right)\end{aligned} \tag{3.18}$$

Constructing the Lyapunov function as:

$$V_2 = V_1 + \frac{1}{2}\sum_{i=1}^{N} e_{i,2}^2 + \frac{1}{2}\sum_{i=1}^{N}\sum_{j=1}^{N} a_{ij}\tilde{\theta}_{i,j}^T \Gamma_{ij}^{-1}\tilde{\theta}_{ij} \tag{3.19}$$

Its derivative is

$$\begin{aligned}\dot{V}_2 =&\dot{V}_1 + \sum_{i=1}^{N} e_{i,2}\dot{e}_{i,2} - \sum_{i=1}^{N}\sum_{j=1}^{N} a_{ij}\tilde{\theta}_{i,j}^T\Gamma_{i,j}^{-1}\dot{\hat{\theta}}_{i,j}\\ =&-k_1\sum_{i=1}^{N} e_{i,1}^2 - k_2\sum_{i=1}^{N} e_{i,2}^2 + \sum_{i=1}^{N} e_{i,2}e_{i,3}\\ &+\sum_{i=1}^{N} e_{i,2}\frac{\partial\alpha_{i,1}}{\partial\hat{\theta}_i}\left(\Gamma_i\tau_{i,2} - \dot{\hat{\theta}}_i\right) + \sum_{i=1}^{N}\tilde{\theta}_i^T\Gamma_i^{-1}\left(\Gamma_i\tau_{i,2} - \dot{\hat{\theta}}_i\right)\\ &+\sum_{i=1}^{N}\sum_{j=1}^{N} a_{ij}\tilde{\theta}_{i,j}^T\Gamma_{i,j}^{-1}\left(\Gamma_{i,j}\tau_{ij,1} - \dot{\hat{\theta}}_{i,j}\right)\end{aligned} \tag{3.20}$$

where the $\hat{\theta}_{i,j} = \theta_j - \hat{\theta}_{ij}$ is the estimate of θ_j. The parameter $\hat{\theta}_{i,j}$ is introduced to indicate the dynamics of i-th agent's neighbour, agent j when $a_{ij} = 1$. Then, $\dot{\hat{\theta}}_{i,j}$ and $\tau_{ij,1}$ are stated as

$$\dot{\hat{\theta}}_{i,j} = \Gamma_{i,j}\tau_{ij,1}, \quad \tau_{ij,1} = -\frac{\partial\alpha_{i,1}}{\partial x_{j,1}}\varphi_{j,1}e_{i,2}, \quad \text{if} \quad a_{ij} = 1 \tag{3.21}$$

Step p $(3 \le p \le n-1)$: The i-th leaderless consensus tracking error $e_{i,p}$ is derived as

$$e_{i,p} = x_{i,p} - \alpha_{i,p-1} \tag{3.22}$$

Then, the derivative of $e_{i,p}$ is obtained as

$$\begin{aligned}\dot{e}_{i,p} =&e_{i,p+1} + \alpha_{i,p} + \theta_i^T\left(\varphi_{i,p} - \sum_{m=1}^{p-1}\frac{\partial\alpha_{i,p-1}}{\partial x_{i,m}}\varphi_{i,m}\right) - \sum_{m=1}^{p-1}\frac{\partial\alpha_{i,p-1}}{\partial x_{i,m}}x_{i,m+1} - \frac{\partial\alpha_{i,p-1}}{\partial\hat{\theta}_i}\dot{\hat{\theta}}_i\\ &-\theta_j^T\left(\sum_{j=1}^{N} a_{ij}\sum_{m=1}^{p-1}\frac{\partial\alpha_{i,p-1}}{\partial x_{j,m}}\varphi_{j,m+1}\right) - \sum_{j=1}^{N} a_{ij}\sum_{m=1}^{p-1}\frac{\partial\alpha_{i,p-1}}{\partial x_{j,m}}x_{j,m} - \sum_{j=1}^{N} a_{ij}\frac{\partial\alpha_{i,p-1}}{\partial\hat{\theta}_{i,j}}\dot{\hat{\theta}}_{i,j}\end{aligned} \tag{3.23}$$

Then, the virtual controller $\alpha_{i,p}$ is formed as

$$\begin{aligned}\alpha_{i,p} =& - e_{i,p-1} - k_p e_{i,p}\\ &+\sum_{m=1}^{p-1}\frac{\partial\alpha_{i,p-1}}{\partial x_{i,m}}x_{i,m+1} - \hat{\theta}_i^T\left(\varphi_{i,p} - \sum_{m=1}^{p-1}\frac{\partial\alpha_{i,p-1}}{\partial x_{i,m}}\varphi_{i,m}\right) + \frac{\partial\alpha_{i,p-1}}{\partial\hat{\theta}_i}\Gamma_i\tau_{i,p}\\ &+\left(\sum_{m=2}^{p-1}\frac{\partial\alpha_{i,m-1}}{\partial\hat{\theta}_i}e_{i,m}\right)\Gamma_i\left(\varphi_{i,p} - \sum_{m=1}^{p-1}\frac{\partial\alpha_{i,p-1}}{\partial x_{i,m}}\varphi_{i,m}\right)\\ &+\sum_{j=1}^{N} a_{ij}\left[\sum_{m=1}^{p-1}\frac{\partial\alpha_{i,p-1}}{\partial x_{j,m}}x_{j,m+1} + \left(\sum_{m=1}^{p-1}\frac{\partial\alpha_{i,p-1}}{\partial x_{j,m}}\varphi_{j,m}\right)^T\hat{\theta}_{i,j} + \frac{\partial\alpha_{i,p-1}}{\partial\hat{\theta}_{i,j}}\Gamma_{ij}\tau_{ij,p-1}\right.\\ &\left.-\left(\sum_{m=3}^{p-1}\frac{\partial\alpha_{i,m-1}}{\partial\hat{\theta}_{i,j}}e_{i,m}\right)\Gamma_{ij}\left(\sum_{m=1}^{p-1}\frac{\partial\alpha_{i,p-1}}{\partial x_{j,m}}\varphi_{j,m}\right)\right]\end{aligned} \tag{3.24}$$

where k_p is a positive design parameter, $\tau_{i,p}$ and $\tau_{ij,p-1}$ are the tuning functions defined as

$$\tau_{i,p} = \tau_{i,p-1} + \left(\varphi_{i,p} - \sum_{m=1}^{p-1} \frac{\partial \alpha_{i,p-1}}{\partial x_{i,m}} \varphi_{i,m}\right) e_{i,p}, \quad \tau_{ij,p-1} = \tau_{ij,p-2} - \left(\sum_{m=1}^{p-1} \frac{\partial \alpha_{i,p-1}}{\partial x_{j,m}} \varphi_{j,m}\right) e_{i,p} \tag{3.25}$$

The Lyapunov function V_p is introduced as

$$V_p = V_{p-1} + \frac{1}{2} \sum_{i=1}^{N} e_{i,p}^2 \tag{3.26}$$

Then, its derivative is obtained as

$$\begin{aligned} \dot{V}_p = \sum_{i=1}^{N} \Bigg[& - \sum_{m=1}^{p} \left(k_m e_{i,m}^2\right) + e_{i,p} e_{i,p+1} + \tilde{\theta}_i^T \Gamma_i^{-1} \left(\Gamma_i \tau_{i,p} - \dot{\hat{\theta}}_i\right) \\ & + \left(\sum_{m=2}^{p} \frac{\partial \alpha_{i,m-1}}{\partial \hat{\theta}_i} e_{i,m}\right) \left(\Gamma_i \tau_{i,p} - \dot{\hat{\theta}}_i\right) + \sum_{j=1}^{N} a_{ij} \tilde{\theta}_{i,j}^T \Gamma_{i,j}^{-1} \left(\Gamma_{i,j} \tau_{ij,p-1} - \dot{\hat{\theta}}_{i,j}\right) \\ & + \sum_{j=1}^{N} a_{ij} \sum_{m=3}^{p} \left(e_{i,m} \frac{\partial \alpha_{i,m-1}}{\partial \hat{\theta}_{i,j}}\right) \left(\Gamma_{i,j} \tau_{ij,p-1} - \dot{\hat{\theta}}_{i,j}\right) \Bigg] \end{aligned} \tag{3.27}$$

where the parameter update laws for $\dot{\hat{\theta}}_i$ and $\dot{\hat{\theta}}_{i,j}$ are designed as

$$\dot{\hat{\theta}}_i = \Gamma_i \tau_{i,p}, \quad \dot{\hat{\theta}}_{i,j} = \Gamma_{i,j} \tau_{ij,p-1} \tag{3.28}$$

Step *n*: In the final step n, the event-triggered leaderless consensus controller is at our disposal. Inspired by the idea (Yu *et al.* 2018, Xing *et al.* 2018), the event-triggered mechanism is implemented to obtain a time-varying threshold, while aiming to reduce unnecessary controller updates in the leaderless consensus control. Additionally, flexible time intervals can be generated based on the time-varying threshold. Therefore, the event-triggered strategy is designed as

$$\begin{aligned} w_i(t) &= v_i(t_k^i), \quad \text{for all } t \in [t_k^i, t_{k+1}^i) \\ t_{k+1}^i &= \inf\left\{t > t_k^i \mid f_i\left(\varepsilon_i(t), w_i(t), t\right) \geq 0\right\} \end{aligned} \tag{3.29}$$

where $v_i(t)$ is the event-triggered controller to be planned, t_k^i, $k \in \mathbb{Z}^+$ are the controller update instants. The controller signals $v_i(t_k^i)$ remain the same during the period

$[t_k^i, t_{k+1}^i)$. When the next event instant t_{k+1}^i is triggered, the updated controller signals $v_i(t_{k+1}^i)$ will be employed to MAS. The event-triggered condition f_i for each agent i is designed as $f_i(\varepsilon_i(t), w_i(t), t) = |\varepsilon_i(t)| - \delta_i|w_i(t)| - \mu_i e^{-\alpha t}$, the measurement error is prescribed as $\varepsilon_i(t) = v_i(t) - w_i(t)$, $0 < \delta_i < 1$, $\mu_i > 0$ and $\alpha > 0$ are all design parameters.

Therefore, as stated in the definition of $f_i(t, \varepsilon_i(t))$, we introduce two continuous time-varying parameters $\lambda_1^i(t)$ and $\lambda_2^i(t)$ which satisfy $|\lambda_1^i(t)| \leq 1$ and $|\lambda_2^i(t)| \leq 1$, during the time interval $[t_k^i, t_{k+1}^i)$, we derive $v_i(t) = (1 + \lambda_1^i(t)\sigma_i) w_i(t) + \lambda_2^i(t)\mu_i$ which is identical to the following equation

$$w_i(t) = \frac{v_i(t)}{1 + \lambda_1^i(t)\sigma_i} - \frac{\lambda_2^i(t)\mu_i}{1 + \lambda_1^i(t)\sigma_i} \tag{3.30}$$

Based on (3.4), (3.7) and (3.30), we derive the $e_{i,n}$ dynamics as follows

$$\begin{aligned}
\dot{e}_{i,n} =& \beta_i w_i(t) + \varphi_{i,n}(x_i)^T\theta_i + b_i g_i(\omega) + d_i(t) - \dot{\alpha}_{i,n-1} \\
=& \frac{\beta_i v_i(t)}{1 + \lambda_1^i(t)\sigma_i} + \xi_i(t) + \varphi_{i,n}(x_i)^T\theta_i + d_i(t) - \frac{\partial \alpha_{i,n-1}}{\partial \hat{\theta}_i}\dot{\hat{\theta}}_i - \sum_{j=1}^{N} a_{ij}\frac{\partial \alpha_{i,n-1}}{\partial \hat{\theta}_{i,j}}\dot{\hat{\theta}}_{i,j} \\
& - \sum_{j=1}^{N} a_{ij} \sum_{m=1}^{n-1} \left(\frac{\partial \alpha_{i,n-1}}{\partial x_{j,m}} \left(x_{j,m+1} + \varphi_{j,m}^T\theta_j \right) \right) - \sum_{m=1}^{n-1} \left(\frac{\partial \alpha_{i,n-1}}{\partial x_{i,m}} \left(x_{i,m+1} + \varphi_{i,m}^T\theta_i \right) \right)
\end{aligned} \tag{3.31}$$

where $\xi_i(t)$ is described as

$$\xi_i(t) = b_i g_i(\omega) - \frac{\beta_i \lambda_2^i(t)\mu_i}{1 + \lambda_1^i(t)\sigma_i} \tag{3.32}$$

From the definition of backlash-like hysteresis and event-triggered condition, we know that $\xi_i(t)$ is bounded. For this reason, we define $p_i = \psi_i \sup_{t \geq 0} |\xi_i(t)|$, $\hat{p}_i$ is an estimate of p_i with $\tilde{p}_i = \hat{p}_i - p_i$ and $\psi_i = 1/|\beta_i|$. Thus, we obtain

$$\begin{aligned}
\xi_i(t)e_{i,n} &\leq |\beta_i| p_i |e_{i,n}| \\
&= |\beta_i||e_{i,n}|\hat{p}_i - |\beta_i||e_{i,n}|\tilde{p}_i
\end{aligned} \tag{3.33}$$

Then, applying Lemma 1 to $|\beta_i||e_{i,n}|\hat{p}_i$ with a positive function $\eta_i(t)$, it yields

$$\xi_i(t)e_{i,n} \leq |\beta_i| \left(e_{i,n}\hat{p}_i \tanh\left(\frac{e_{i,n}\hat{p}_i}{\eta_i(t)} \right) + \kappa\eta_i(t) \right) - |\beta_i||e_{i,n}|\tilde{p}_i \tag{3.34}$$

We consider the Lyapunov function by introducing

$$V_n = V_{n-1} + \frac{1}{2}\sum_{i=1}^{N}\left(e_{i,n}^2 + \frac{1}{\rho_i}\tilde{D}_i^2 + \frac{|\beta_i|}{\gamma_i}\tilde{\psi}_i^2 + \frac{|\beta_i|}{\zeta_i}\tilde{p}_i^2\right) \tag{3.35}$$

where ρ_i, γ_i and ζ_i are positive parameters to be given, $\hat{D}_i$ is an estimate of D_i with $\hat{D}_i = D_i - \tilde{D}_i$ and $\hat{\psi}_i$ is an estimate of ψ_i with $\tilde{\psi}_i = \hat{\psi}_i - \psi_i$. Substituting (3.31), (3.34) and (3.35) into the time derivative of V_n yields

$$\begin{aligned}
\dot{V}_n =& \dot{V}_{n-1} + \sum_{i=1}^{N}\left(e_{i,n}\dot{e}_{i,n} - \frac{1}{\rho_i}\tilde{D}_i\dot{\hat{D}}_i + \frac{|\beta_i|}{\gamma_i}\tilde{\psi}_i\dot{\hat{\psi}}_i + \frac{|\beta_i|}{\zeta_i}\tilde{p}_i\dot{\hat{p}}_i\right)\\
=& \sum_{i=1}^{N}\Bigg[-\sum_{m=1}^{n-1}k_m e_{i,m}^2 + e_{i,n-1}e_{i,n} + \tilde{\theta}_i^T\Gamma_i^{-1}\left(\Gamma_i\tau_{i,n-1} - \dot{\hat{\theta}}_i\right)\\
&+ \left(\sum_{m=2}^{n-1}\frac{\partial\alpha_{i,m-1}}{\partial\hat{\theta}_i}e_{i,m}\right)\left(\Gamma_i\tau_{i,n-1} - \dot{\hat{\theta}}_i\right) + \sum_{j=1}^{N}a_{ij}\tilde{\theta}_{i,j}^T\Gamma_{i,j}^{-1}\left(\Gamma_{i,j}\tau_{ij,n-2} - \dot{\hat{\theta}}_{i,j}\right)\\
&+ \sum_{j=1}^{N}a_{ij}\sum_{m=3}^{n-1}\left(e_{i,m}\frac{\partial\alpha_{i,m-1}}{\partial\hat{\theta}_{i,j}}\right)\left(\Gamma_{i,j}\tau_{ij,n-2} - \dot{\hat{\theta}}_{i,j}\right) + \frac{\beta_i v_i(t)e_{i,n}}{1+\lambda_1^i(t)\sigma_i} + \xi_i(t)e_{i,n}\\
&+ \varphi_{i,n}(x_i)^T\theta_i e_{i,n} + e_{i,n}d_i(t) - e_{i,n}\dot{\alpha}_{i,n-1} - \frac{1}{\rho_i}\tilde{D}_i\dot{\hat{D}}_i + \frac{|\beta_i|}{\gamma_i}\tilde{\psi}_i\dot{\hat{\psi}}_i + \frac{|\beta_i|}{\zeta_i}\tilde{p}_i\dot{\hat{p}}_i\Bigg]\\
=& \sum_{i=1}^{N}\Bigg[-\sum_{m=1}^{n}k_m e_{i,m}^2 + \tilde{\theta}_i^T\Gamma_i^{-1}\left(\Gamma_i\tau_{i,n} - \dot{\hat{\theta}}_i\right) + \left(\sum_{m=2}^{n}\frac{\partial\alpha_{i,m-1}}{\partial\hat{\theta}_i}e_{i,m}\right)\left(\Gamma_i\tau_{i,n} - \dot{\hat{\theta}}_i\right)\\
&+ \sum_{j=1}^{N}a_{ij}\tilde{\theta}_{i,j}^T\Gamma_{i,j}^{-1}\left(\Gamma_{i,j}\tau_{ij,n-1} - \dot{\hat{\theta}}_{i,j}\right) + \sum_{j=1}^{N}a_{ij}\left(\sum_{m=3}^{n}\frac{\partial\alpha_{i,m-1}}{\partial\hat{\theta}_{i,j}}e_{i,m}\right)\left(\Gamma_{i,j}\tau_{ij,n-1} - \dot{\hat{\theta}}_{i,j}\right)\\
&+ \frac{\beta_i v_i(t)e_{i,n}}{1+\lambda_1^i(t)\sigma_i} + \xi_i(t)e_{i,n} + \varphi_{i,n}(x_i)^T\theta_i e_{i,n} + e_{i,n}d_i(t) - e_{i,n}\alpha_{i,n} - \frac{1}{\rho_i}\tilde{D}_i\dot{\hat{D}}_i\\
&+ \frac{|\beta_i|}{\gamma_i}\tilde{\psi}_i\dot{\hat{\psi}}_i + \frac{|\beta_i|}{\zeta_i}\tilde{p}_i\dot{\hat{p}}_i\Bigg]
\end{aligned} \tag{3.36}$$

where the virtual controller $\alpha_{i,n}$ is given as

$$\begin{aligned}\alpha_{i,n} =& -e_{i,n-1} - k_n e_{i,n} + \sum_{m=1}^{n-1} \frac{\partial \alpha_{i,n-1}}{\partial x_{i,m}} x_{i,m+1} - \hat{\theta}_i^T \left(\varphi_{i,n} - \sum_{m=1}^{n-1} \frac{\partial \alpha_{i,n-1}}{\partial x_{i,m}} \varphi_{i,m} \right) + \frac{\partial \alpha_{i,n-1}}{\partial \hat{\theta}_i} \Gamma_i \tau_{i,n} \\ &+ \left(\sum_{m=2}^{n-1} \frac{\partial \alpha_{i,m-1}}{\partial \hat{\theta}_i} e_{i,m} \right) \Gamma_i \left(\varphi_{i,n} - \sum_{m=1}^{n-1} \frac{\partial \alpha_{i,n-1}}{\partial x_{i,m}} \varphi_{i,m} \right) \\ &+ \sum_{j=1}^{N} a_{ij} \left[\sum_{m=1}^{n-1} \frac{\partial \alpha_{i,n-1}}{\partial x_{j,m}} x_{j,m+1} + \left(\sum_{m=1}^{n-1} \frac{\partial \alpha_{i,n-1}}{\partial x_{j,m}} \varphi_{j,m} \right)^T \hat{\theta}_{i,j} + \frac{\partial \alpha_{i,n-1}}{\partial \hat{\theta}_{i,j}} \Gamma_{ij} \tau_{ij,n-1} \right. \\ &\left. - \left(\sum_{m=3}^{n-1} \frac{\partial \alpha_{i,m-1}}{\partial \hat{\theta}_{i,j}} e_{i,m} \right) \Gamma_{ij} \left(\sum_{m=1}^{n-1} \frac{\partial \alpha_{i,n-1}}{\partial x_{j,m}} \varphi_{j,m} \right) \right] \end{aligned} \tag{3.37}$$

The actual event-triggered controller $v_i(t)$ is designed as

$$\begin{aligned} v_i(t) =& -\operatorname{sign}(b_i)(1+\sigma_i) \left[\bar{\alpha}_{i,n} \hat{\psi}_i \tanh\left(\frac{e_{i,n} \bar{\alpha}_{i,n} \hat{\psi}_i}{\eta_i(t)} \right) + \hat{p}_i \tanh\left(\frac{e_{i,n} \hat{p}_i}{\eta_i(t)} \right) \right] \\ \bar{\alpha}_{i,n} =& \hat{D}_i \tanh\left(\frac{e_{i,n}}{\eta_i(t)} \right) - \alpha_{i,n} \end{aligned} \tag{3.38}$$

The local parameter adaptive laws are

$$\begin{aligned} \dot{\hat{\theta}}_i &= \Gamma_i \tau_{i,n}, \ \dot{\hat{\theta}}_{i,j} = \Gamma_{i,j} \tau_{ij,n-1}, \ \dot{\hat{\psi}}_i = \gamma_i e_{i,n} \bar{\alpha}_{i,n} \\ \dot{\hat{D}}_i &= \rho_i e_{i,n} \tanh\left(\frac{e_{i,n}}{\eta_i(t)} \right), \ \dot{\hat{p}}_i = \zeta_i |e_{i,n}| \end{aligned} \tag{3.39}$$

where the tuning functions $\tau_{i,n}$ and $\tau_{ij,n-1}$ are defined as

$$\tau_{i,n} = \tau_{i,n-1} + \left(\varphi_{i,n} - \sum_{m=1}^{n-1} \frac{\partial \alpha_{i,n-1}}{\partial x_{i,m}} \varphi_{i,m} \right) e_{i,n}, \quad \tau_{ij,n-1} = \tau_{ij,n-2} - \left(\sum_{m=1}^{n-1} \frac{\partial \alpha_{i,n-1}}{\partial x_{j,m}} \varphi_{j,m} \right) e_{i,n}$$

3.4 Stability Analysis

In this section, the boundedness of all the signals in the closed-loop system and the leaderless consensus tracking performance are evaluated.

Theorem 3.1. *For the closed-loop system of* (3.1) *with the controller* (3.38) *and the parameter update law* (3.39)*, all the signals are globally bounded and the leaderless consensus can be asymptotically achieved.*

Proof. Considering event-triggered controller $v_i(t)$, Lemma 1 and $1+\lambda_1^i(t)\sigma_i \le 1+\sigma_i$, the following term in (3.36) yields

$$\begin{aligned}\frac{\beta_i v_i(t) e_{i,n}}{1+\lambda_1^i(t)\sigma_i} \le & -|\beta_i| e_{i,n}\bar{\alpha}_{i,n}\hat{\psi}_i \tanh\left(\frac{e_{i,n}\bar{\alpha}_{i,n}\hat{\psi}_i}{\eta_i(t)}\right) - |\beta_i| e_{i,n}\hat{p}_i \tanh\left(\frac{e_{i,n}\hat{p}_i}{\eta_i(t)}\right) \\ \le & -|\beta_i|\hat{\psi}_i e_{i,n}\bar{\alpha}_{i,n} + \kappa\eta_i(t)|\beta_i| - |\beta_i| e_{i,n}\hat{p}_i \tanh\left(\frac{e_{i,n}\hat{p}_i}{\eta_i(t)}\right) \\ = & -e_{i,n}\bar{\alpha}_{i,n} - |\beta_i|\tilde{\psi}_i e_{i,n}\bar{\alpha}_{i,n} + \kappa\eta_i(t)|\beta_i| - |\beta_i| e_{i,n}\hat{p}_i \tanh\left(\frac{e_{i,n}\hat{p}_i}{\eta_i(t)}\right)\end{aligned} \tag{3.40}$$

Substituting (3.38), (3.39) and (3.40) into (3.36), it yields

$$\begin{aligned}\dot{V}_n \le & \sum_{i=1}^{N}\Bigg[-\sum_{m=1}^{n} k_m e_{i,m}^2 + \tilde{\theta}_i^T\Gamma_i^{-1}\left(\Gamma_i\tau_{i,n} - \dot{\hat{\theta}}_i\right) + \left(\sum_{m=2}^{n}\frac{\partial\alpha_{i,m-1}}{\partial\hat{\theta}_i}e_{i,m}\right)\left(\Gamma_i\tau_{i,n} - \dot{\hat{\theta}}_i\right) \\ & + \sum_{j=1}^{N} a_{ij}\tilde{\theta}_{i,j}^T\Gamma_{i,j}^{-1}\left(\Gamma_{i,j}\tau_{ij,n-1} - \dot{\hat{\theta}}_{i,j}\right) + \sum_{j=1}^{N} a_{ij}\left(\sum_{m=3}^{n}\frac{\partial\alpha_{i,m-1}}{\partial\hat{\theta}_{i,j}}e_{i,m}\right)\left(\Gamma_{i,j}\tau_{ij,n-1} - \dot{\hat{\theta}}_{i,j}\right) \\ & - e_{i,n}\bar{\alpha}_{i,n} - |\beta_i|\tilde{\psi}_i e_{i,n}\bar{\alpha}_{i,n} + 2\kappa\eta_i(t)|\beta_i| - |\beta_i||e_{i,n}|\tilde{p}_i + e_{i,n}d_i(t) - e_{i,n}\alpha_{i,n} \\ & - \frac{1}{\rho_i}\tilde{D}_i\dot{\hat{D}}_i + \frac{|\beta_i|}{\gamma_i}\tilde{\psi}_i\dot{\hat{\psi}}_i + \frac{|\beta_i|}{\zeta_i}\tilde{p}_i\dot{\hat{p}}_i\Bigg] \\ \le & \sum_{i=1}^{N}\Bigg[-\sum_{m=1}^{n} k_m e_{i,m}^2 + \tilde{\theta}_i^T\Gamma_i^{-1}\left(\Gamma_i\tau_{i,n} - \dot{\hat{\theta}}_i\right) + \left(\sum_{m=2}^{n}\frac{\partial\alpha_{i,m-1}}{\partial\hat{\theta}_i}e_{i,m}\right)\left(\Gamma_i\tau_{i,n} - \dot{\hat{\theta}}_i\right) \\ & + \sum_{j=1}^{N} a_{ij}\tilde{\theta}_{i,j}^T\Gamma_{i,j}^{-1}\left(\Gamma_{i,j}\tau_{ij,n-1} - \dot{\hat{\theta}}_{i,j}\right) + \sum_{j=1}^{N} a_{ij}\left(\sum_{m=3}^{n}\frac{\partial\alpha_{i,m-1}}{\partial\hat{\theta}_{i,j}}e_{i,m}\right)\left(\Gamma_{i,j}\tau_{ij,n-1} - \dot{\hat{\theta}}_{i,j}\right) \\ & + \frac{|\beta_i|}{\gamma_i}\tilde{\psi}_i\left(\dot{\hat{\psi}}_i - \gamma_i e_{i,n}\bar{\alpha}_{i,n}\right) + \frac{1}{\rho_i}\tilde{D}_i\left(\rho_i e_{i,n}\tanh\left(\frac{e_{i,n}}{\eta_i(t)}\right) - \dot{\hat{D}}_i\right) \\ & + \frac{|\beta_i|}{\zeta_i}\tilde{p}_i\left(\dot{\hat{p}}_i - \zeta_i|e_{i,n}|\right) + \kappa\eta_i(t)(D_i + 2|\beta_i|)\Bigg] \\ \le & -\sum_{i=1}^{N}\sum_{m=1}^{n} k_m e_{i,m}^2 + \sum_{i=1}^{N}\kappa\eta_i(t)\left(D_i + 2|\beta_i|\right)\end{aligned} \tag{3.41}$$

Integrating both sides of (3.41) over $[t_0, t]$, and we obtain

$$\begin{aligned}V_n(t) \le & V_n(0) - \int_{t_0}^{t}\sum_{i=1}^{N}\sum_{m=1}^{n} k_m e_{i,m}^2 ds + \int_{t_0}^{t}\sum_{i=1}^{N}\kappa\left(D_i + 2|\beta_i|\right)\eta_i(s)ds \\ \le & V_n(0) + \kappa\left(D_i + 2|\beta_i|\right)\bar{\eta}_i\end{aligned} \tag{3.42}$$

We can conclude that the signals of $e_{i,n}$, $\hat{\theta}_i$, $\hat{\theta}_{i,j}$, $\hat{\psi}_i$, $\hat{D}_i$ and $\hat{p}_i$ are bounded because of the definition of V_n. The virtual control laws $\alpha_{i,n}$ and event-triggered controller v_i are also bounded from (3.37) and (3.38). Overall, the boundedness of all signals is established. Applying Barbalat Lemma, we can achieve $\lim_{t\to\infty} e_{i,m}(t) = 0$ for $i = 1,\ldots,N$ and $m = 1,\ldots,n$.

Then by defining $z = [z_1,\ldots,z_N]^T$, $e_1 = [e_{1,1}, e_{2,1}\ldots,e_{N,1}]^T$ and $x_1 = [x_{1,1}, x_{2,1}\ldots,x_{N,1}]^T$, and deriving the differential equation of z, we have

$$\dot{z} = -\mathcal{L}x_1 = -\mathcal{L}(z + e_1) \tag{3.43}$$

To analyse the above equation, we define a positive definite matrix P and treat P and P^{-1} as the right and left eigenvectors of $\mathcal{L}$, respectively, as stated in Assumption 1, we can obtain $\mathcal{L} = PJP^{-1}$ where $J = \text{diag}(0, J_1)$ is the Jordan canonical form of $\mathcal{L}$ and $-J_1 \in \mathbb{R}^{(N-1)\times(N-1)}$ is a Hurwitz matrix. By defining $\chi = P^{-1}z$ in which $\chi = [\chi_1,\ldots,\chi_N]^T$, the derivative of z can be transformed as

$$\dot{\chi} = -J\chi - JP^{-1}e_1 \tag{3.44}$$

We derive $\chi_1 = -p^T x_1(0)$, where p^T is the first row of P^{-1} and $\dot{\chi}_1 = 0$ implies the first row of J are zero. According to Theorem 4.6 (Khalil 2002) with Hurwitz matrix $-J_1$ and bounded signal e_1, the vector $[\chi_2,\ldots,\chi_N]$ is bounded and the following equation with a positive definite matrix T is attained as

$$QJ_1 + J_1^T Q = -T \tag{3.45}$$

Therefore, applying the Hurwitz linear system stability analysis (Khalil 2002), we obtain that $[\chi_2,\ldots,\chi_N]$ can converge to zero. Since the first column of P is 1_N, we obtain

$$\lim_{t\to\infty} x_1 = 1_N p^T x_1(0) \tag{3.46}$$

which means that z converges to zero, and it is equivalent to the output of each subsystem asymptotically achieve leaderless consensus, then we have

$$\lim_{t\to\infty} y_i - y_j = 0 \tag{3.47}$$

Next, we aim to avert the infinite number of controller updates occurs in a finite time period, which implies that there exists a $t^* > 0$ satisfying $t^i_{k+1} - t^i_k \geq t^*$ for any $k \in \mathbb{Z}^+$ and $\varepsilon_i(t) = v_i(t) - w_i(t)$ for all $t \in [t^i_k, t^i_{k+1})$

$$\frac{d}{dt}|\varepsilon_i| = \frac{d}{dt}(\varepsilon_i \cdot \varepsilon_i)^{\frac{1}{2}} = \text{sign}(\varepsilon_i)\dot{\varepsilon}_i \leq |\dot{v}_i| \tag{3.48}$$

It is seen from (3.38) that the actual event-triggered controller $v_i(t)$ is differentiable and the function of $\dot{v}_i$ consists of bounded signals. Then, inequality $|\dot{v}_i| \leq \bar{v}_i$ holds, where $\bar{v}$ represents a positive constant. From the event-triggered condition, we derive that $\varepsilon_i(t^i_k) = 0$ and $\lim_{t \to t^i_{k+1}} \varepsilon_i(t) = \mu_i e^{-\alpha t}$. Consequently, the lower bound of the triggered interval $t^* \geq \mu_i e^{-\alpha t}/\bar{v}_i > 0$. This completes the proof. □

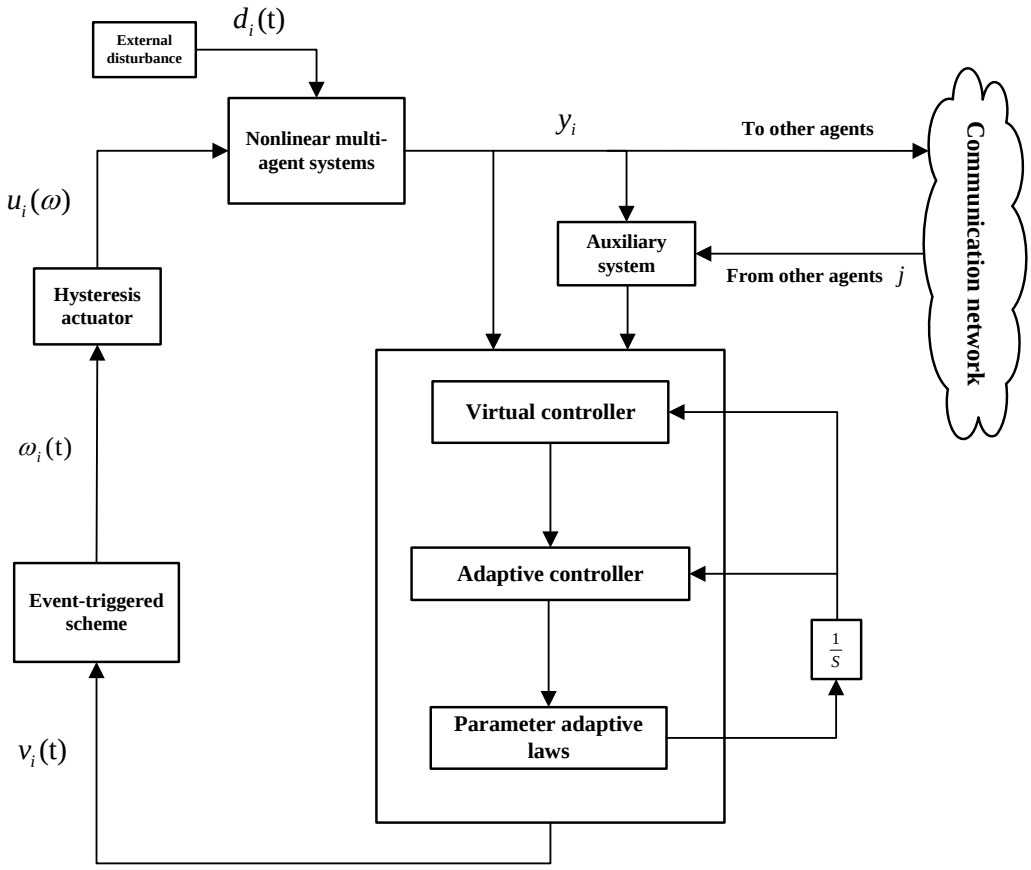

Figure 3.2. Block diagram of the event-triggered adaptive leaderless consensus control framework.

For clarity, Figure 3.2 displays the block diagram of the proposed control framework.

Remark 3.3. *The consensus tracking control problem has been addressed (Shen and Shi 2015, Shi and Shen 2015, Zhang and Lewis 2012), which conclude that the leader-following consensus tracking errors converge to a small region which means semi-globally uniformly bounded. In contrast, our proposed control scheme shows that the leaderless consensus tracking and a considerable reduction in controller update can be both satisfied.*

3.5 Simulation Results

To evaluate the performance of controller (3.38) designed in this chapter, a group of four second-order robotic manipulators is considered. The four manipulators are completely coupled, which is modelled by a directed graph displayed in Figure 3.3. The dynamics of each manipulator is modelled as

$$\begin{aligned} \dot{x}_{i,1} &= x_{i,2} \\ \dot{x}_{i,2} &= \frac{1}{M_i} u_i(\omega_i) - \frac{m_i}{2M_i} l_i g \sin(x_{i,1}) + d_i(t) \\ y_i &= x_{i,1}, \quad i = 1, \ldots, 4 \end{aligned} \tag{3.49}$$

where M_i is the moment of inertia, $x_{i,1}$ represents the angular position, $x_{i,2}$ is the angular velocity, m_i describes the mass of the manipulator link, $g = 9.8\text{m/s}^2$ is the gravity acceleration and the length of the robotic manipulator is l_i. The term $d_i(t)$ denotes the bounded external disturbance, ω_i is the input torque, $u_i(\omega)$ indicates that the backlash-like nonlinearity impacts on the robotic manipulator and y_i represents the output signal.

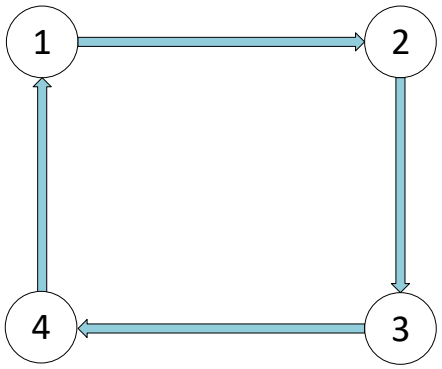

Figure 3.3. Directed communication topology among robotic manipulators.

The manipulator system parameters are given as

$$M_1 = 1.1\text{Nm},\ m_1 = 0.5\text{kg},\ l_1 = 0.85\text{m}$$
$$M_2 = 0.9\text{Nm},\ m_2 = 0.6\text{kg},\ l_2 = 0.80\text{m}$$
$$M_3 = 0.8\text{Nm},\ m_3 = 0.4\text{kg},\ l_3 = 0.90\text{m}$$
$$M_4 = 1.0\text{Nm},\ m_4 = 0.6\text{kg},\ l_4 = 0.75\text{m}$$

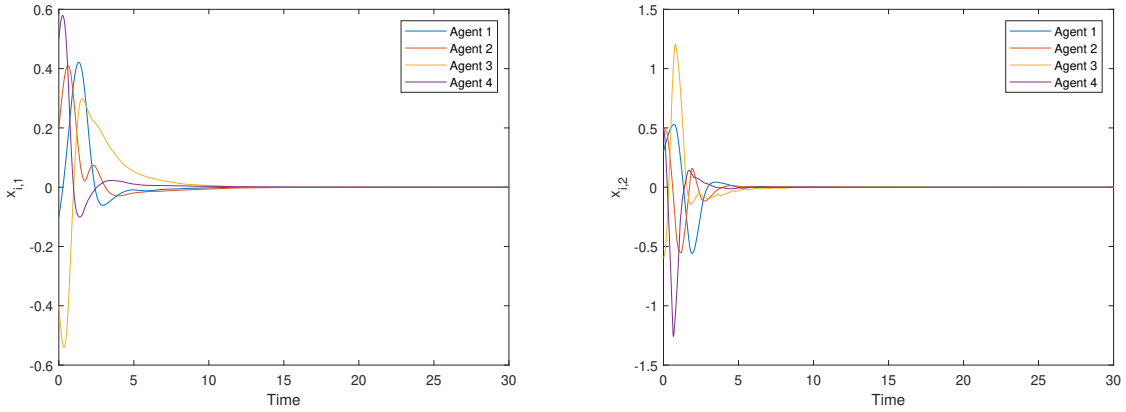

(a) States of x_{i1} (b) States of x_{i2}

Figure 3.4. Evolution of states x_i under controller u_i.

The backlash-like hysteresis nonlinearities are modelled as

$$\frac{du_i}{dt} = a_i \left| \frac{d\omega_i}{dt} \right| (c_i\omega_i - u_i) + H_i \frac{d\omega_i}{dt} \tag{3.50}$$

where the backlash-like hysteresis parameters a_i, c_i and H_i are selected as

$$a_i = [2,\ 2.2,\ 2.4,\ 2.5]^T,\ c_i = [0.5,\ 0.6,\ 0.4,\ 0.7]^T,\ H_i = [1,\ 1,\ 0.9,\ 0.8]^T.$$

All the initial states of the robotic manipulators and the design parameters are prescribed as

$$x_1(0) = [-0.1,\ 0.3]^T,\ x_2(0) = [0.2,\ 0.5]^T,\ x_3(0) = [-0.4,\ -0.6]^T,\ x_4(0) = [0.5,\ 0.5]^T$$
$$k_1 = k_2 = 0.5,\ \rho_i = 0.1,\ \gamma_i = \zeta_i = \Gamma_i = 1,\ \mu_i = \alpha = 1,\ \varepsilon_i = 0.5,\ \eta_i(t) = 0.2e^{-0.01t}.$$

The bounded external disturbance is taken as $d_i(t) = \cos(t)x_{i,2}(t)$. Figures 3.4 shows the states of all the robotic manipulators, which indicates the leaderless consensus is reached asymptotically with the designed controller (3.38). The adaptive parameter states of $\hat{\theta}_i$, $\hat{\psi}_i$, $\hat{D}_i$ and $\hat{p}_i$ are shown in Figures 3.5 and 3.6, which confirm that the adaptive parameters are bounded and maintain constant as the leaderless consensus

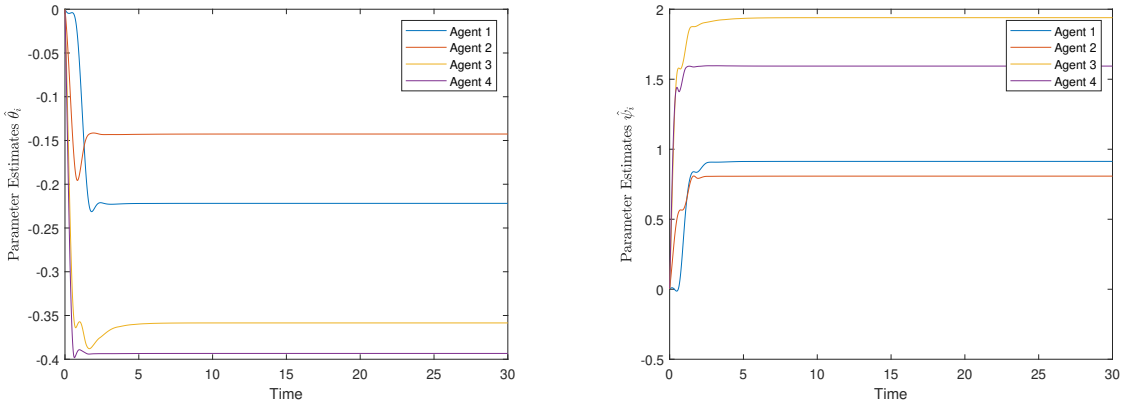

(a) $\hat{\theta}_i$ (b) $\hat{\psi}_i$

Figure 3.5. Adaptive laws of $\hat{\theta}_i$ and $\hat{\psi}_i$.

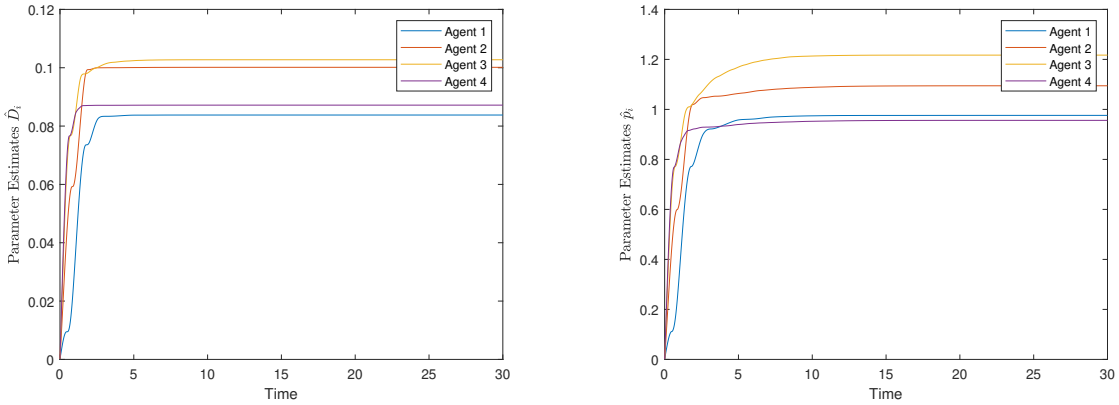

(a) $\hat{D}_i$ (b) $\hat{p}_i$

Figure 3.6. Adaptive laws of $\hat{D}_i$ and $\hat{p}_i$.

is achieved. The control signals u_i for all agents are plotted in Figure 3.7. The triggering events of each agent are presented in Figure 3.8, which reveals that the controller updates are considerably reduced compared with the periodic sampling on designed controller. The results demonstrate that by implementing the proposed event-triggered adaptive controller, the leaderless consensus is achieved asymptotically under the impact of backlash-like hysteresis.

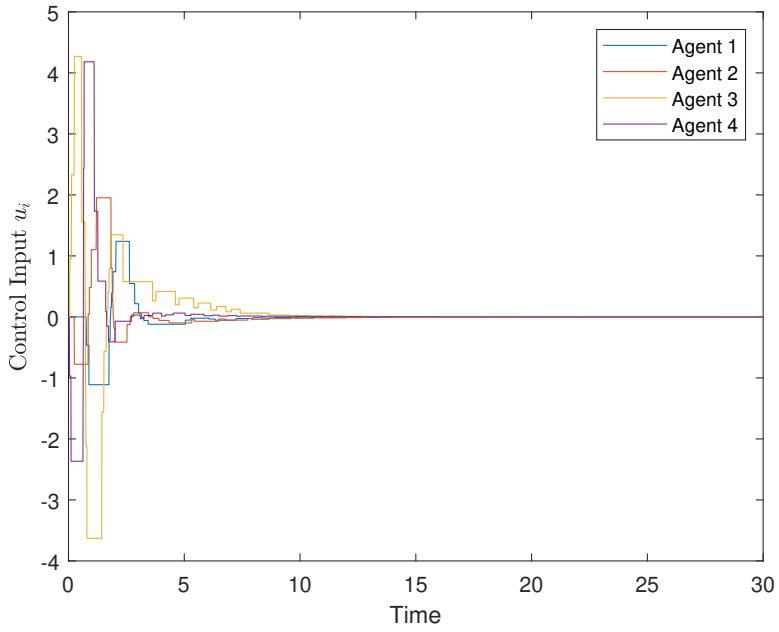

Figure 3.7. Control signals u_i of the agents.

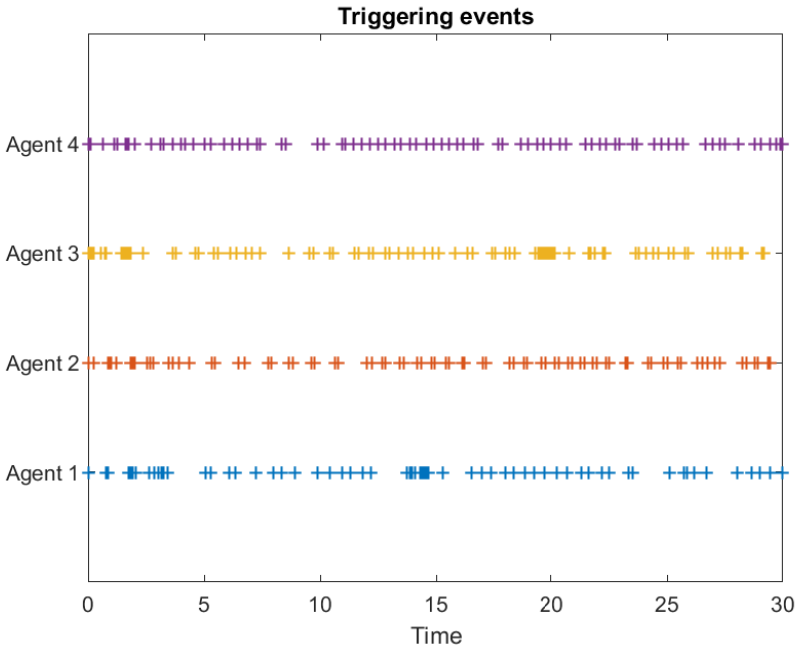

Figure 3.8. The triggering events of each agent.

3.6 Chapter Summary

In this chapter, the problem of control has been studied for nonlinear MAS with unknown backlash-like hysteresis. We have proposed an event-triggered adaptive leaderless consensus controller to compensate for the impacts of unknown backlash-like hysteresis and reduce the unnecessary update of control signals. By applying the new control scheme, all the state trajectories from the nonlinear MAS are guaranteed to be globally bounded and the leaderless consensus tracking has been achieved asymptotically. Furthermore, a considerable reduction of the unnecessary update of controller has been attained. Simulation results have verified the effectiveness of the proposed design technique.

Chapter 4

Constrained Consensus Control with Actuator Faults

4.1 Introduction

Some practical issues remain to be challenging to maintain the desired system performance, such as communication network faults, sensor and actuator failures and state constraints, to name a few. In practice, actuator faults are often encountered, particularly for multiple networked actuators in MAS, as faulty actuators cause drastic oscillations in subsystem behaviours, instability or even system failures.

Some fault-tolerant control approaches have been developed to prevent MAS from actuator failures, which can be divided into passive and active strategies. A passive fault-tolerant controller based on distributed estimation algorithm (Deng *et al.* 2020) was deployed to tackle the actuator outage and loss-of-effectiveness faults for linear MAS. Similarly, the same fault model was considered with a passive adaptive event-triggered fault-tolerant consensus controller to compensate the actuator faults (Ye *et al.* 2019). The passive methods require a fixed controller which guarantees robustness for a class of presumed faults. On the contrary, active fault-tolerant control schemes are developed based on the estimated fault information provided by individual fault isolation or detection module. An active distributed fault compensation controller was proposed to solve discrete-time heterogeneous MAS formation problem with a fault estimator unit (Yan *et al.* 2019). Nevertheless, none of these fault-tolerant control protocols is applicable to nonlinear MAS. A second-order nonlinear MAS with integral quadratic constrained uncertainties was studied to develop an active fault-tolerant consensus controller (Jin *et al.* 2018). An active fault-tolerant consensus controller with a fault

detection module was applied to address a first-order nonlinear MAS satisfying Lipschitz continuity condition (Li and Wang 2020). Therefore, how to design an effective fault-tolerant controller for a more general nonlinear MAS subject to frequent actuator failure is one of our motivations.

Many practical applications require system states to be restricted in a certain range such that the system states cannot violate critical constraints. In detail, enforcing constraints on the output of a system state ensures that the output cannot exceed a safe bound, thus, the safe behaviour can be improved by considering the output constraint problem.

Barrier Lyapunov functions (BLF) (Tee *et al.* 2009) and state transformation approaches (Zhao and Song 2019) are widely used to deal with the output constraint problem. The output constraint problem of heterogeneous MAS was addressed by a γ-type BLF (Shen and Xu 2018), which has been defined as a general form of BLF compared with the conventional types of logarithmic or tangent BLF (Zhang *et al.* 2018b). However, the BLF approach to the output constraint problem has some limitations. First, the controller design with an asymmetric BLF is complicated. Second, since the preset constraints are related to the system tracking error instead of the system state, initial value selection of the constraints is a relatively conservative condition. Compared with the BLF method, a log-type nonlinear state transformation function was introduced to map the constrained consensus tracking error rather than the constrained state (Ni and Shi 2021a), thus it cannot directly transform the constrained output into a constraint-free state. Despite this state transformation technique can simplify the controller design procedure, it cannot avert the limitations of the BLF method and solve constrained and unconstrained cases uniformly, which drives us to investigate the constraint problem for nonlinear MAS.

In this work, motivated by the limitations outlined in actuator fault and output constraint problems for nonlinear MAS, we propose a distributed fault-tolerant consensus control scheme for nonlinear MAS under output constraint by synthesizing the adaptive backstepping and neural network methods. More specifically, we introduce a new state transformation function for each agent to directly map the constrained output into a constraint-free one, which averts the limitations of the BLF method and is able to cope with constrained and unconstrained cases uniformly. The proposed state transformation strategy greatly differs from the BLF method (Shen and Xu 2018) and (Zhang *et al.* 2018b) in design and analysis process. Since the conventional adaptive

approximation based control techniques require one adaptive law at each design step, a single parameter estimator is introduced to mitigate the computation of controller. Furthermore, compared with (Deng *et al.* 2020) and (Ye *et al.* 2019), a more general fault model is used to represent four operating modes of actuator for each agent. The adaptive compensation technique is applied to tackle the actuator fault problem for nonlinear MAS, which is unlike the fault-tolerant approaches (Deng *et al.* 2020, Ye *et al.* 2019, Yan *et al.* 2019, Jin *et al.* 2018). Consequently, an effective fault-tolerant consensus control framework is proposed to improve the consensus control performance and reliability of the nonlinear MAS.

The rest of the chapter is structured into five sections. Section 4.2 covers preliminaries and problem formulation. In Section 4.3, the adaptive leader-follower consensus control scheme is developed and the stability is analysed. A group of four networked two-stage chemical reactors is modelled in Section 4.4 to prove the validity of the designed control scheme and Section 4.5 concludes this chapter.

4.2 Problem Formulation and Preliminaries

4.2.1 Problem Formulation

Suppose that MAS consists of N followers and one leader. The nonlinear dynamics of i-th follower is modelled in strict-feedback form:

$$\begin{aligned} \dot{x}_{i,k} &= x_{i,k+1} + f_{i,k}(\bar{x}_{i,k}), \quad k = 1, \ldots, n-1 \\ \dot{x}_{i,n} &= g_i u_i^F + f_{i,n}(\bar{x}_{i,n}) \\ y_i &= x_{i,1}, \quad \text{for } i = 1, \ldots, N \end{aligned} \tag{4.1}$$

subject to the output constraint:

$$x_{i,1} \in \mathcal{C}_{x_{i,1}} := \{x_{i,1} \in \mathbb{R} : -k_{a_{i,1}} < x_{i,1} < k_{b_{i,1}}\} \tag{4.2}$$

where $x_{i,m} \in \mathbb{R}$ with $m = 1, \ldots, n$, $u_i^F \in \mathbb{R}$, $y_i \in \mathbb{R}$ are the system state, the control input and the output, respectively. $f_{i,m}(\bar{x}_{i,m})$ is unknown smooth nonlinear function with $\bar{x}_{i,m} = [x_{i,1}, x_{i,2}, \cdots, x_{i,m}]^{\mathrm{T}} \in \mathbb{R}^m$, g_i is an unknown bounded control coefficient function. $k_{a_{i,1}}$ and $k_{b_{i,1}}$ are predefined constants to ensure the output in a constrained set $\mathcal{C}_{x_{i,1}}$.

Table 4.1. Cases of actuator faults.

Actuator fault of the ith agent	$\rho_i(t)$	$h_i(t)$
Loss of effectiveness	$0 < \rho_i(t) < 1$	0
Actuator bias fault	1	$h_i(t) \neq 0$
Loss of effectiveness with bias	$0 < \rho_i(t) < 1$	$h_i(t) \neq 0$

To formulate the actuator fault problem, we apply a general actuator fault model (Li and Wang 2020) for each follower subsystem as follows

$$u_i^F = \rho_i(t)\omega_i + h_i(t) \tag{4.3}$$

where the unknown continuous functions $\rho_i(t)$ and $h_i(t)$ indicate the severity of loss of effectiveness actuator fault and the biased fault severity for the i-th agent, respectively. u_i^F is the actual output of unhealthy actuator and ω_i is the control input to be designed. Three cases of actuator faults are summarized in Table 4.1.

Our aim in this study is to develop an adaptive consensus controller subject to actuator faults and output constraints for (4.1) such that:

- The output of each agent $y_i(t)$ can closely follow a desired trajectory $y_r(t)$, accordingly, its consensus tracking error reaches to an adjustable small neighborhood of zero and all signals in the closed-loop MAS are bounded;
- The output asymmetric constraint is enforced within the constrained set $\mathcal{C}_{x_{i,1}}$ and the impact of actuator failure is compensated by the proposed controller.

The following lemma and assumptions are needed to achieve the above control objective.

Assumption 4.1. *The communication topology is modelled by a directed graph which contains a spanning tree with $b_i = 1$ for the root agent i.*

Assumption 4.2. *The desired leader $y_r(t) \in \mathbb{R}$ and its kth derivative are continuous and bounded. Its trajectory enforces the same constraint in the constrained set $\mathcal{C}_{x_{i,1}}$, satisfying $y_r(t) \in \mathbb{R} := \{-k_{a_{i,1}} < y_r(t) < k_{b_{i,1}}\}$.*

Assumption 4.3. *(Liu and Tong 2016) Consider the control gain function $g_i(\cdot)$ with a given sign, there exist two unknown constants $\bar{g}_i$ and $\underline{g}_i$ that yield: $0 < \underline{g}_i \leq |g_i(\cdot)| < \bar{g}_i$.*

Remark 4.1. *Since the trajectory of the leader is related to the output and the consensus tracking error aims to converge to a small region, its trajectory should be within the same set $\mathcal{C}_{x_{i,1}}$. In order to ensure the controllability for system* (4.1)*, Assumption* 4.3 *indicates that the control gain function $g_i(\cdot)$ is bounded away from zero. Furthermore, such assumption has been widely applied in the framework of adaptive control design (Krstic* et al. *1995, Zhao* et al. *2020).*

Lemma 4.1 ((Huang *et al.* 2020))**.** *For any $z \in \mathbb{R}$ and $\eta > 0$, the following inequality holds:*

$$0 \leq z - \frac{z^2}{\sqrt{z^2 + \eta^2}} \leq \eta$$

4.2.2 Radial Basis Function Neural Networks (RBFNN)

The RBFNN technique is commonly employed to approximate unknown smooth functions due to its effective approximation performance. Any unknown smooth function $f(Z) : \mathbb{R}^l \to \mathbb{R}$ can be approximated over a compact set $\Omega_Z \subset \mathbb{R}^l$ as follows:

$$f(Z) = W^{\mathrm{T}}\varphi(Z) + \sigma, \quad \forall Z \in \Omega_Z$$

where $Z \in \Omega_Z \subset \mathbb{R}^l$ is a input vector, $W \in \mathbb{R}^q$ denotes an optimal weight vector, $q \geq 1$ represents the neuron node number of RBFNN, $\varphi(Z) = [\varphi_1(Z), \cdots, \varphi_q(Z)]^{\mathrm{T}} \in \mathbb{R}^q$ is a known activation function vector and $\sigma \in \mathbb{R}$ is the approximation error. A general type of Gaussian function is selected as the entry of $\varphi(Z)$ such that $\varphi_i(Z) = \exp[-(Z - c_i)^{\mathrm{T}}(Z - c_i)/w_i^2]$, $i = 1, \ldots, q$, where c_i and w_i are the center and width of the Gaussian function, respectively. Moreover, the smooth functions can be approximated to arbitrary accuracy and the compact set $\Omega_Z \subset \mathbb{R}^l$ can be selected as large as desired by adding large enough neuron nodes q. Furthermore, the stability analysis based on RBFNN control is in a semi-global manner, which means that the proposed controller ensures that all signals in the closed-loop system are bounded.

4.3 Main Results

4.3.1 Nonlinear State Transformation Function

In order to enforce the asymmetric constant constraint on the output of i-th agent, a new nonlinear state transformation function is constructed as follows:

$$\chi_{i,1} = \frac{k_{a_{i,1}} x_{i,1} + \bar{k}_{a_{i,1}}}{2\left(k_{a_{i,1}} + x_{i,1}\right)} + \frac{k_{b_{i,1}} x_{i,1} - \bar{k}_{b_{i,1}}}{2\left(k_{b_{i,1}} - x_{i,1}\right)} \tag{4.4}$$

with initial condition of $x_{i,1}(0) \in \mathcal{C}_{x_{i,1}}$, where $\bar{k}_{a_{i,1}}$ and $\bar{k}_{b_{i,1}}$ are constants satisfying the following conditions:

$$k_{a_{i,1}}^2 > \bar{k}_{a_{i,1}}, \quad k_{b_{i,1}}^2 > \bar{k}_{b_{i,1}} \tag{4.5}$$

From the state transformation function (4.4), state $\chi_{i,1}$ tends to infinity as $x_{i,1}$ ap-

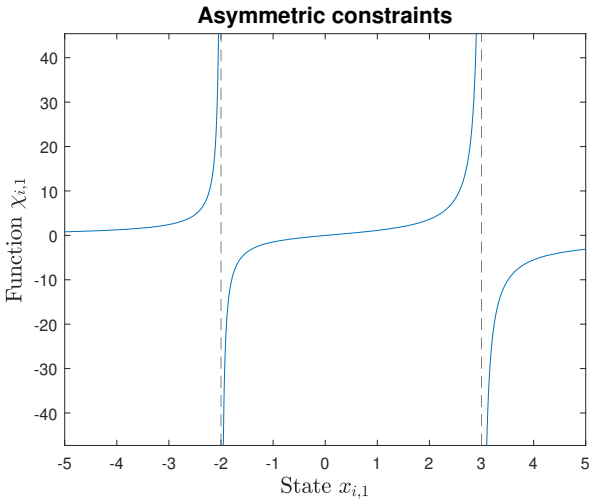

Figure 4.1. Asymmetric constraint case of function $\chi_{i,1}$ on state $x_{i,1}$.

proaches to the boundaries of $\mathcal{C}_{x_{i,1}}$, which implies that the boundedness of $\chi_{i,1}$ is maintained as $x_{i,1}$ stays in the constrained set $\mathcal{C}_{x_{i,1}}$. Accordingly, the output constraint enforcement problem for nonlinear MAS converts to the proof of boundedness for $\chi_{i,1}$. Figure 4.1 shows asymmetric constraint case of function (4.4), i.e., $-2 < x_{i,1} < 3$. Furthermore, if the constraints on output do not exist, i.e., $K_i = k_{a_{i,1}} = k_{b_{i,1}} \to \infty$, applying the L'Hôpital rule, we obtain $\lim_{K_i \to \infty} \chi_{i,1} = x_{i,1}$, which proves this function can address constrained and unconstrained cases uniformly.

Remark 4.2. *The nonlinear state transformation function for MAS is inspired by (Zhao* et al. *2020) and (Zhao* et al. *2021). Unlike the log-type nonlinear function (Ni and Shi 2021a) and the BLF method (Tee* et al. *2009), this approach can solve constrained and unconstrained cases uniformly and transform a constrained output into a constraint-free one, consequently, the control design and analysis can be simplified significantly. Moreover, this function can readily be extended to solve the time-varying case of output constraint problem.*

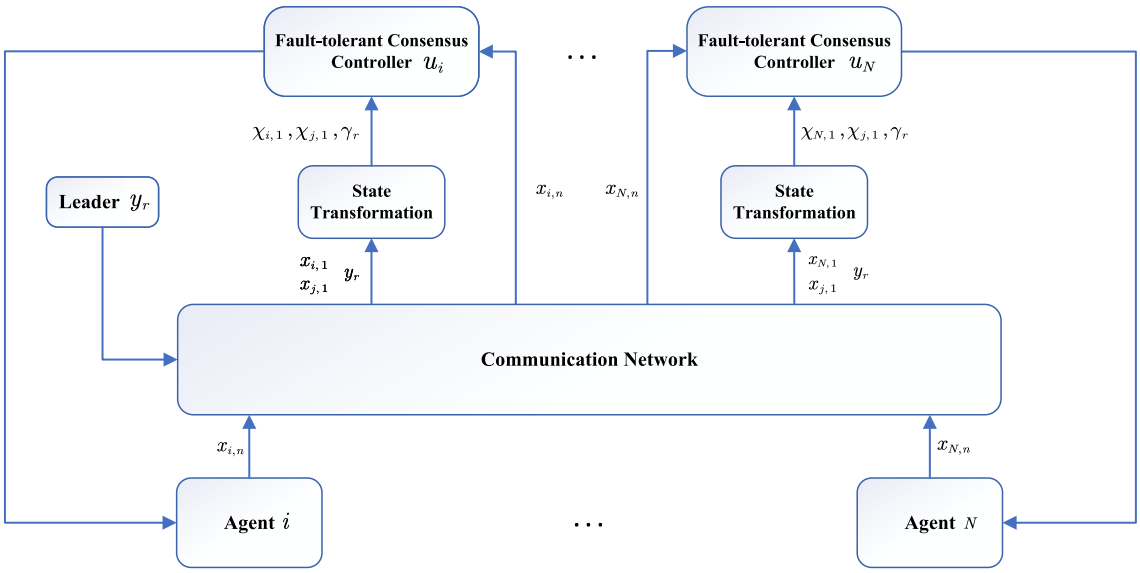

Figure 4.2. The fault-tolerant consensus control diagram for nonlinear MAS.

4.3.2 Fault-tolerant Consensus Controller Design

In this subsection, a fault-tolerant consensus controller is proposed to achieve consensus tracking for nonlinear MAS that is subject to actuator fault. Figure 4.2 displays the structure of the fault-tolerant consensus control design.

Define the following coordinate transformation:

$$\begin{aligned} z_{i,1} &= \sum_{j=1}^{N} a_{ij}(\chi_{i,1} - \chi_{j,1}) + b_i(\chi_{i,1} - \gamma_r), \quad i = 1, \ldots, N \\ z_{i,k} &= x_{i,k} - \alpha_{i,k-1}, \quad k = 2, \ldots, n \end{aligned} \tag{4.6}$$

where

$$\gamma_r = \frac{k_{a_{i,1}} y_r + \bar{k}_{a_{i,1}}}{2\left(k_{a_{i,1}} + y_r\right)} + \frac{k_{b_{i,1}} y_r - \bar{k}_{b_{i,1}}}{2\left(k_{b_{i,1}} - y_r\right)}$$

is a known function, under Assumption 1 and the conditions in (4.5), and $\alpha_{i,k-1}$ is virtual control law.

The adaptive backstepping control design procedure is given by the following steps:

Step 1: The derivative of $\chi_{i,1}$ is calculated as

$$\dot{\chi}_{i,1} = \psi_{i,1}\dot{x}_{i,1} \tag{4.7}$$

where

$$\psi_{i,1} = \frac{k_{a_{i,1}}^2 - \bar{k}_{a_{i,1}}}{2\left(k_{a_{i,1}} + x_{i,1}\right)^2} + \frac{k_{b_{i,1}}^2 - \bar{k}_{b_{i,1}}}{2\left(k_{b_{i,1}} - x_{i,1}\right)^2}$$

is available for the controller design based on the conditions in (4.5).

Taking the derivative of $z_{i,k}$ and considering (4.7), we obtain

$$\begin{aligned} \dot{z}_{i,1} &= (d_i + b_i)\dot{\chi}_{i,1} - \sum_{j=1}^{N} a_{ij}\dot{\chi}_{j,1} - b_i\dot{\gamma}_r \\ &= (d_i + b_i)\left(\psi_{i,1}x_{i,2} + \psi_{i,1}f_{i,1}\right) - b_i\dot{\gamma}_r - \sum_{j=1}^{N} a_{ij}\left(\psi_{j,1}x_{j,2} + \psi_{j,1}f_{j,1}\right) \end{aligned} \tag{4.8}$$

Since the nonlinear functions $f_{i,1}$, $f_{j,1}$ and $\dot{\gamma}_r$ are unavailable for the controller design, we define a function $F_{i,1}\left(Z_{i,1}\right)$ that represents the lumped unknown terms, then apply RBFNN approach, we have

$$F_{i,1}\left(Z_{i,1}\right) = W_{i,1}^{\mathrm{T}}\varphi_{i,1}(Z_{i,1}) + \sigma_{i,1} \tag{4.9}$$

where $Z_{i,1} = [x_{i,1}, x_{j,1}, y_r]^{\mathrm{T}} \in \Omega_{i,1} \subset \mathbb{R}^3$ is the input vector, the approximation error $\sigma_{i,1}$ satisfies that $|\sigma_{i,1}|$ is bounded and $|\sigma_{i,1}| \leq \varepsilon_{i,1}$ where $\varepsilon_{i,1}$ is a positive constant.

Thus, (4.8) becomes

$$\begin{aligned} \dot{z}_{i,1} &= (d_i + b_i)\psi_{i,1}x_{i,2} + F_{i,1}\left(Z_{i,1}\right) - \sum_{j=1}^{N} a_{ij}\psi_{j,1}x_{j,2} \\ &= (d_i + b_i)\psi_{i,1}z_{i,2} + (d_i + b_i)\psi_{i,1}\alpha_{i,1} + F_{i,1}\left(Z_{i,1}\right) - \sum_{j=1}^{N} a_{ij}\psi_{j,1}x_{j,2} \end{aligned}$$

Considering the following Lyapunov function $V_{i,1}$ as

$$V_{i,1} = \frac{1}{2}z_{i,1}^2 + \frac{1}{2\mu_i}\tilde{\theta}_i^2 \tag{4.10}$$

Its derivative yields

$$\begin{aligned} \dot{V}_{i,1} &= z_{i,1}\dot{z}_{i,1} - \frac{1}{\mu_i}\tilde{\theta}_i\dot{\hat{\theta}}_i \\ &= (d_i + b_i)\psi_{i,1}z_{i,1}z_{i,2} + (d_i + b_i)\psi_{i,1}z_{i,1}\alpha_{i,1} \\ &\quad + z_{i,1}F_{i,1}\left(Z_{i,1}\right) - \sum_{j=1}^{N} a_{ij}\psi_{j,1}x_{j,2}z_{i,1} - \frac{1}{\mu_i}\tilde{\theta}_i\dot{\hat{\theta}}_i \end{aligned} \tag{4.11}$$

Substituting (4.9) into (4.11) and applying Young's inequality, it yields

$$\begin{aligned} z_{i,1}F_{i,1}\left(Z_{i,1}\right) &= z_{i,1}W_{i,1}^{\mathrm{T}}\varphi_{i,1}(Z_{i,1}) + z_{i,1}\sigma_{i,1} \\ &\leq \frac{1}{2\mu_i^2}z_{i,1}^2\left\|W_{i,1}\right\|^2\varphi_{i,1}^{\mathrm{T}}(Z_{i,1})\varphi_{i,1}(Z_{i,1}) + \frac{\mu_i^2}{2} + z_{i,1}\sigma_{i,1} \\ &\leq \frac{1}{2\mu_i^2}z_{i,1}^2\theta_i\varphi_{i,1}^{\mathrm{T}}(Z_{i,1})\varphi_{i,1}(Z_{i,1}) + \frac{\mu_i^2}{2} + \frac{1}{2}z_{i,1}^2 + \frac{\varepsilon_{i,1}^2}{2} \end{aligned} \tag{4.12}$$

where $\theta_{i,m} = \left\{\left\|W_{i,1}\right\|^2, \cdots, \left\|W_{i,m}\right\|^2\right\}$, $m = 1, \ldots, n$, $\theta_i = \max\left\{\theta_{i,1}, \cdots, \theta_{i,n}\right\}$, and $\tilde{\theta}_i = \theta_i - \hat{\theta}_i$ where $\hat{\theta}_i$ is the estimate of parameter θ_i, μ_i is a design parameter.

Only one parameter estimator in RBFNN for θ_i is designed to mitigate the computational burden of our proposed control strategy as follows

$$\dot{\hat{\theta}}_i = \sum_{k=1}^{n}\frac{1}{2\mu_i}z_{i,k}^2\varphi_{i,k}^{\mathrm{T}}(Z_{i,k})\varphi_{i,k}(Z_{i,k}) - \kappa_i\hat{\theta}_i \tag{4.13}$$

Then, designing the virtual control law $\alpha_{i,1}$ as follows:

$$\alpha_{i,1} = \frac{1}{(d_i + b_i)\psi_{i,1}}\left(-\frac{1}{2\mu_i^2}z_{i,1}\hat{\theta}_i\varphi_{i,1}^{\mathrm{T}}(Z_{i,1})\varphi_{i,1}(Z_{i,1}) - c_{i,1}z_{i,1} - \frac{1}{2}z_{i,1} + \sum_{j=1}^{N}a_{ij}\psi_{j,1}x_{j,2}\right) \tag{4.14}$$

Substituting (4.12), (4.13) and (4.14) into (4.11), it becomes

$$\begin{aligned} \dot{V}_{i,1} \leq & -c_{i,1}z_{i,1}^2 + (d_i + b_i)\psi_{i,1}z_{i,1}z_{i,2} \\ & - \sum_{k=2}^{n}\frac{1}{2\mu_i}z_{i,k}^2\varphi_{i,k}^{\mathrm{T}}(Z_{i,k})\varphi_{i,k}(Z_{i,k}) + \beta_{i,1} + \frac{\kappa_i}{\mu_i}\tilde{\theta}_i\hat{\theta}_i \end{aligned} \tag{4.15}$$

where $\beta_{i,1} = \frac{1}{2}\mu_i^2 + \frac{1}{2}\varepsilon_{i,1}^2$ is unknown constant.

Step 2: Considering $z_{i,2}$ in (4.6) and taking its derivative, we have

$$\begin{aligned} \dot{z}_{i,2} &= x_{i,3} + f_{i,2} - \dot{\alpha}_{i,1} \\ &= z_{i,3} + \alpha_{i,2} + f_{i,2} - \dot{\alpha}_{i,1} \end{aligned} \tag{4.16}$$

Since the nonlinear functions $f_{i,2}$ and $\dot{\alpha}_{i,1}$ are unavailable, applying RBFNN approach, we have $F_{i,2}\left(Z_{i,2}\right) = W_{i,2}^{\mathrm{T}}\varphi_{i,2}(Z_{i,2}) + \sigma_{i,2}$, where $Z_{i,2} = [x_{i,1}, x_{i,2}, \alpha_{i,1}]^{\mathrm{T}} \in \Omega_{i,2} \subset \mathbb{R}^3$ is the input vector.

Choosing the Lyapunov candidate function $V_{i,2} = \frac{1}{2}z_{i,2}^2$ and calculating its derivative, we obtain

$$\dot{V}_{i,2} = z_{i,2}z_{i,3} + z_{i,2}\alpha_{i,2} + z_{i,2}F_{i,2}\left(Z_{i,2}\right) \tag{4.17}$$

Then, the virtual control law $\alpha_{i,2}$ is obtained as

$$\alpha_{i,2} = -c_{i,2}z_{i,2} - (d_i + b_i)\psi_{i,1}z_{i,1} - \frac{1}{2}z_{i,2} - \frac{1}{2\mu_i^2}z_{i,2}\hat{\theta}_i\varphi_{i,2}^{\mathrm{T}}(Z_{i,2})\varphi_{i,2}(Z_{i,2}) \tag{4.18}$$

Applying Young's inequality, we have

$$\begin{aligned} z_{i,2}F_{i,2}\left(Z_{i,2}\right) &= z_{i,2}W_{i,2}^{\mathrm{T}}\varphi_{i,2}(Z_{i,2}) + z_{i,2}\sigma_{i,2} \\ &\leq \frac{1}{2\mu_i^2}z_{i,2}^2\theta_i\varphi_{i,2}^{\mathrm{T}}(Z_{i,2})\varphi_{i,2}(Z_{i,2}) + \frac{1}{2}\mu_i^2 + \frac{1}{2}z_{i,2}^2 + \frac{1}{2}\varepsilon_{i,2}^2 \end{aligned}$$

Substituting (4.18) into (4.17), it yields

$$\begin{aligned} \dot{V}_{i,2} \leq & -(d_i + b_i)\psi_{i,1}z_{i,2}z_{i,1} + z_{i,2}z_{i,3} - c_{i,2}z_{i,2}^2 \\ & - \frac{1}{2}z_{i,2}^2 - \frac{1}{2\mu_i^2}z_{i,2}^2\hat{\theta}_i\varphi_{i,2}^{\mathrm{T}}(Z_{i,2})\varphi_{i,2}(Z_{i,2}) + \frac{1}{2}z_{i,2}^2 \\ & + \frac{1}{2\mu_i^2}z_{i,2}^2\theta_i\varphi_{i,2}^{\mathrm{T}}(Z_{i,2})\varphi_{i,2}(Z_{i,2}) + \frac{1}{2}\mu_i^2 + \frac{1}{2}\varepsilon_{i,2}^2 \\ \leq & -c_{i,2}z_{i,2}^2 - (d_i + b_i)\psi_{i,1}z_{i,1}z_{i,2} + z_{i,2}z_{i,3} \\ & + \frac{1}{2\mu_i^2}z_{i,2}^2\tilde{\theta}_i\varphi_{i,2}^{\mathrm{T}}(Z_{i,2})\varphi_{i,2}(Z_{i,2}) + \beta_{i,2} \end{aligned} \tag{4.19}$$

where $\beta_{i,2} = \frac{1}{2}\mu_i^2 + \frac{1}{2}\varepsilon_{i,2}^2$.

Step k: $(3 \leq k \leq n-1)$ Considering $z_{i,k}$ in (4.6) and taking its derivative, we have

$$\begin{aligned} \dot{z}_{i,k} &= x_{i,k+1} + f_{i,k} - \dot{\alpha}_{i,k-1} \\ &= z_{i,k+1} + \alpha_{i,k} + f_{i,k} - \dot{\alpha}_{i,k-1} \end{aligned} \tag{4.20}$$

Applying the RBFNN approach for the unknown terms $f_{i,k} - \dot{\alpha}_{i,k-1}$ in (4.20), we derive $F_{i,k}\left(Z_{i,k}\right) = W_{i,k}^{\mathrm{T}}\varphi_{i,k}(Z_{i,k}) + \sigma_{i,k}$, where the input vector is defined as $Z_{i,k} = [x_{i,1}, \cdots, x_{i,k}, \alpha_{i,k-1}]^{\mathrm{T}} \in \Omega_{i,k} \subset \mathbb{R}^{k+1}$.

Selecting the Lyapunov candidate function $V_{i,k} = \frac{1}{2}z_{i,k}^2$, then, calculating its derivative, we have

$$\dot{V}_{i,k} = z_{i,k}z_{i,k+1} + z_{i,k}\alpha_{i,k} + z_{i,k}F_{i,k}\left(Z_{i,k}\right) \tag{4.21}$$

Next, the virtual control law $\alpha_{i,k}$ is given by

$$\alpha_{i,k} = -c_{i,k}z_{i,k} - z_{i,k-1} - \frac{1}{2}z_{i,k} - \frac{1}{2\mu_i^2}z_{i,k}\hat{\theta}_i\varphi_{i,k}^{\mathrm{T}}(Z_{i,k})\varphi_{i,k}(Z_{i,k}) \tag{4.22}$$

Implementing Young's inequality, we obtain

$$\begin{aligned} z_{i,k}F_{i,k}\left(Z_{i,k}\right) &= z_{i,k}W_{i,k}^{\mathrm{T}}\varphi_{i,k}(Z_{i,k}) + z_{i,k}\sigma_{i,k} \\ &\leq \frac{1}{2\mu_i^2}z_{i,k}^2\theta_i\varphi_{i,k}^{\mathrm{T}}(Z_{i,k})\varphi_{i,k}(Z_{i,k}) + \frac{1}{2}\mu_i^2 + \frac{1}{2}z_{i,k}^2 + \frac{1}{2}\varepsilon_{i,k}^2 \end{aligned}$$

Substituting (4.22) into (4.21), it yields

$$\dot{V}_{i,k} \leq -c_{i,k}z_{i,k}^2 - z_{i,k}z_{i,k-1} + z_{i,k}z_{i,k+1} + \frac{1}{2\mu_i^2}z_{i,k}^2\tilde{\theta}_i\varphi_{i,k}^{\mathrm{T}}(Z_{i,k})\varphi_{i,k}(Z_{i,k}) + \beta_{i,k} \tag{4.23}$$

where $\beta_{i,k} = \frac{1}{2}\mu_i^2 + \frac{1}{2}\varepsilon_{i,k}^2$.

Step n: Considering $z_{i,n}$ and the actuator fault model in (4.3) and taking its derivative, we obtain

$$\begin{aligned} \dot{z}_{i,n} &= \dot{x}_{i,n} - \dot{\alpha}_{i,n-1} \\ &= g_i\rho_i(t)\omega_i + g_ih_i(t) + f_{i,n} - \dot{\alpha}_{i,n-1} \end{aligned} \tag{4.24}$$

Since the nonlinear functions $g_ih_i(t)$, $f_{i,n}$ and $\dot{\alpha}_{i,n-1}$ are unavailable for the actual controller design, applying the RBFNN approach and introducing an intermediate control law v_i to compensate the effect of the actuator fault, it yields

$$\dot{z}_{i,n} = g_i\rho_i(t)\omega_i + F_{i,n}\left(Z_{i,n}\right) + v_i - v_i \tag{4.25}$$

where $Z_{i,n} = [x_{i,1}, \cdots, x_{i,n}, \alpha_{i,n-1}]^{\mathrm{T}} \in \Omega_{i,n} \subset \mathbb{R}^{n+1}$ is the input vector.

Then, designing the intermediate control law v_i as

$$v_i = c_{i,n}z_{i,n} + z_{i,n-1} + \frac{1}{2}z_{i,n} + \frac{1}{2\mu_i^2}z_{i,n}\hat{\theta}_i\varphi_{i,n}^{\mathrm{T}}(Z_{i,n})\varphi_{i,n}(Z_{i,n}) \tag{4.26}$$

Furthermore, according to the actuator fault model, the boundedness of $\rho_i(t)$ is ensured such that $0 < \underline{\rho}_i \leq \rho_i(t)$. Thus, we have

$$\lambda_i = \inf_{t\geq 0}|g_i|\,\rho_i(t) = \underline{g}_{i,n}\underline{\rho}_i \tag{4.27}$$

where λ_i is an unknown parameter.

Selecting the Lyapunov candidate function $V_{i,n}$ as

$$V_{i,n} = \frac{1}{2}z_{i,n}^2 + \frac{\lambda_i}{2\tau_i}\tilde{\vartheta}_i^2 \tag{4.28}$$

where $\tilde{\vartheta}_i = \vartheta_i - \hat{\vartheta}_i$ and $\hat{\vartheta}_i$ is the estimate of parameter $\vartheta_i = 1/\lambda_i$.

Taking its derivative, it yields

$$\begin{aligned}\dot{V}_{i,n} &= z_{i,n}\dot{z}_{i,n} - \frac{\lambda_i}{\tau_i}\tilde{\vartheta}_i\dot{\hat{\vartheta}}_i \\ &= g_i\rho_i(t)\omega_i z_{i,n} + z_{i,n}F_{i,n}\left(Z_{i,n}\right) + z_{i,n}v_i - c_{i,n}z_{i,n}^2 \\ &\quad - z_{i,n-1}z_{i,n} - \frac{1}{2\mu_i^2}z_{i,n}^2\hat{\theta}_i\varphi_{i,n}^{\mathrm{T}}(Z_{i,n})\varphi_{i,n}(Z_{i,n}) - \frac{1}{2}z_{i,n}^2 - \frac{\lambda_i}{\tau_i}\tilde{\vartheta}_i\dot{\hat{\vartheta}}_i\end{aligned} \tag{4.29}$$

Applying Young's inequality, we obtain

$$\begin{aligned}z_{i,n}F_{i,n}\left(Z_{i,n}\right) &= z_{i,n}W_{i,n}^{\mathrm{T}}\varphi_{i,n}(Z_{i,n}) + z_{i,n}\sigma_{i,n} \\ &\leq \frac{1}{2\mu_i^2}z_{i,n}^2\theta_i\varphi_{i,n}^{\mathrm{T}}(Z_{i,n})\varphi_{i,n}(Z_{i,n}) + \frac{1}{2}z_{i,n}^2 + \beta_{i,n}\end{aligned}$$

where $\beta_{i,n} = \frac{1}{2}\mu_i^2 + \frac{1}{2}\varepsilon_{i,n}^2$.

Substituting (4.26) into (4.29), we derive

$$\begin{aligned}\dot{V}_{i,n} &\leq g_i\rho_i(t)\omega_i z_{i,n} + z_{i,n}v_i - c_{i,n}z_{i,n}^2 \\ &\quad - z_{i,n-1}z_{i,n} + \frac{1}{2\mu_i^2}z_{i,n}^2\tilde{\theta}_i\varphi_{i,n}^{\mathrm{T}}(Z_{i,n})\varphi_{i,n}(Z_{i,n}) + \beta_{i,n} - \frac{\lambda_i}{\tau_i}\tilde{\vartheta}_i\dot{\hat{\vartheta}}_i\end{aligned} \tag{4.30}$$

The fault-tolerant controller ω_i is given by

$$\omega_i = -\frac{\mathrm{sgn}(g_i)z_{i,n}\hat{\vartheta}_i^2 v_i^2}{\sqrt{z_{i,n}^2\hat{\vartheta}_i^2 v_i^2 + \epsilon_i^2}} \tag{4.31}$$

where ϵ_i is a constant.

Substituting controller (4.31) into the term $g_i\rho_i(t)\omega_i z_{i,n}$, then according to Lemma 1 and (4.27), we have the following inequality:

$$\begin{aligned}g_i\rho_i(t)\omega_i z_{i,n} &= -\frac{g_i\rho_i(t)\mathrm{sgn}(g_i)z_{i,n}^2\hat{\vartheta}_i^2 v_i^2}{\sqrt{z_{i,n}^2\hat{\vartheta}_i^2 v_i^2 + \epsilon_i^2}} \\ &\leq -\frac{\underline{g}_{i,n}\underline{\rho}_i z_{i,n}^2\hat{\vartheta}_i^2 v_i^2}{\sqrt{z_{i,n}^2\hat{\vartheta}_i^2 v_i^2 + \epsilon_i^2}} \\ &\leq \lambda_i\epsilon_i - \lambda_i z_{i,n}\vartheta_i v_i + \lambda_i z_{i,n}\tilde{\vartheta}_i v_i \\ &= \lambda_i\epsilon_i - z_{i,n}v_i + \lambda_i\tilde{\vartheta}_i z_{i,n}v_i\end{aligned} \tag{4.32}$$

The adaptive law for $\hat{\vartheta}_i$ is developed as follows

$$\dot{\hat{\vartheta}}_i = \tau_i z_{i,n} v_i - \delta_i \hat{\vartheta}_i \tag{4.33}$$

where τ_i and δ_i are design constants.

Then, substituting (4.32) and (4.33) into (4.30) yields

$$\begin{aligned}\dot{V}_{i,n} &\leq \lambda_i \epsilon_i - z_{i,n} v_i + \lambda_i \tilde{\vartheta}_i z_{i,n} v_i + z_{i,n} v_i - c_{i,n} z_{i,n}^2 \\ &\quad - z_{i,n-1} z_{i,n} + \frac{1}{2\mu_i^2} z_{i,n}^2 \tilde{\theta}_i \varphi_{i,n}^{\mathrm{T}}(Z_{i,n}) \varphi_{i,n}(Z_{i,n}) + \beta_{i,n} - \frac{\lambda_i}{\tau_i} \tilde{\vartheta}_i \dot{\hat{\vartheta}}_i \\ &\leq -c_{i,n} z_{i,n}^2 + \frac{1}{2\mu_i^2} z_{i,n}^2 \tilde{\theta}_i \varphi_{i,n}^{\mathrm{T}}(Z_{i,n}) \varphi_{i,n}(Z_{i,n}) - z_{i,n-1} z_{i,n} + \beta_{i,n} + \lambda_i \epsilon_i + \frac{\delta_i \lambda_i}{\tau_i} \tilde{\vartheta}_i \hat{\vartheta}_i\end{aligned} \tag{4.34}$$

Remark 4.3. *The fault-tolerant technique in this chapter differs from other methods (Yan* et al. *2019, Zhang* et al. *2018a). First, no additional fault diagnosis module is introduced. Second, multiple faults of different types can be considered rather than simply solving for one type of faults. From* (4.32) *and* (4.33)*, a robust structure consisting of an adaptive law is implemented to compensate for the actuator failure without auxiliary dynamic filter.*

Remark 4.4. *The explicit formula of partial derivative of virtual controller was calculated at each step, which increases the complexity of the design process (Huang* et al. *2020, Sun* et al. *2021). However, the integration of adaptive RBFNN and backstepping approaches eliminates the problem of repeated differentiations of virtual control laws known as "explosion of complexity" in backstepping control. Furthermore, compared with (Yoo 2018, Xiao* et al. *2020), one adaptive law for the unknown parameter of RBFNN is adequate instead of containing an adaptive law at each step of the backstepping control design, which significantly mitigates the computation of control design.*

4.3.3 Stability Analysis on Closed-loop Systems

In this subsection, the following theorem describes the stability analysis of the closed-loop MAS under the proposed adaptive laws (4.13), (4.33) and fault-tolerant consensus controller (4.31).

Theorem 4.1. *Consider system* (4.1) *with* (4.2) *and* (4.3) *for any initial conditions in the set* $\mathcal{C}_{x_{i,1}}$*, there exist a desired compact sets* $\Omega_{i,p}$ *with enough neural nodes such that* $Z_{i,p} \in \Omega_{i,p}$ *where* $i = 1, \ldots, N$*, and* $p = 1, \ldots, n$*. Let Assumptions 1-3 hold. Then, controller* (4.31)

together with (4.13) *and* (4.33) *will make all the signals in the closed-loop MAS bounded, the output constraints are enforced and the consensus tracking error converges to an adjustable small neighborhood of zero.*

Proof. Choosing the total Lyapunov function as

$$V = \sum_{i=1}^{N} \left(\sum_{k=1}^{n} V_{i,k} \right) \tag{4.35}$$

Calculating the derivative of V and substituting (4.15), (4.19), (4.23) and (4.34) into its derivative, we have

$$\dot{V} \leq \sum_{i=1}^{N} \left(-\sum_{k=1}^{n} c_{i,k} z_{i,k}^2 + \sum_{k=1}^{n} \beta_{i,k} + \lambda_i \epsilon_i + \frac{\kappa_i}{\mu_i} \tilde{\theta}_i \hat{\theta}_i + \frac{\delta_i \lambda_i}{\tau_i} \tilde{\vartheta}_i \hat{\vartheta}_i \right) \tag{4.36}$$

Then, applying Young's inequality yields

$$\frac{\kappa_i}{\mu_i} \tilde{\theta}_i \hat{\theta}_i = \frac{\kappa_i}{\mu_i} \left(\tilde{\theta}_i \theta_i - \tilde{\theta}_i^2 \right) \leq \frac{\kappa_i}{2\mu_i} \left(\theta_i^2 - \tilde{\theta}_i^2 \right) \tag{4.37}$$

Similarly,

$$\frac{\delta_i \lambda_i}{\tau_i} \tilde{\vartheta}_i \hat{\vartheta}_i = \frac{\delta_i \lambda_i}{\tau_i} \left(\tilde{\vartheta}_i \vartheta_i - \tilde{\vartheta}_i^2 \right) \leq \frac{\delta_i \lambda_i}{2\tau_i} \left(\vartheta_i^2 - \tilde{\vartheta}_i^2 \right) \tag{4.38}$$

Finally, (4.36) can be rearranged as

$$\dot{V} \leq \sum_{i=1}^{N} \left(-\sum_{k=1}^{n} c_{i,k} z_{i,k}^2 - \frac{\kappa_i}{2\mu_i} \tilde{\theta}_i^2 - \frac{\delta_i \lambda_i}{2\tau_i} \tilde{\vartheta}_i^2 + \sum_{k=1}^{n} \beta_{i,k} + \lambda_i \epsilon_i + \frac{\kappa_i}{2\mu_i} \theta_i^2 + \frac{\delta_i \lambda_i}{2\tau_i} \vartheta_i^2 \right) \tag{4.39}$$

implies that

$$\dot{V} \leq -aV + b \tag{4.40}$$

where $a = \min\{2c_{i,1}, \ldots, 2c_{i,n}, \kappa_i, \delta_i\}$, $b = \sum_{i=1}^{N} \left(\sum_{k=1}^{n} \beta_{i,k} + \lambda_i \epsilon_i + \frac{\kappa_i}{2\mu_i} \theta_i^2 + \frac{\delta_i \lambda_i}{2\tau_i} \vartheta_i^2 \right)$. From (4.40) and the definitions of Lyapunov functions at each step, we obtain that for any initial conditions in the constrained set $\mathcal{C}_{x_{i,1}}$, all signals $z_{i,n}$, θ_i and ϑ_i of the closed-loop MAS are bounded. Then, we derive that the signal $\chi_{i,1}$ is bounded and there exist constants $\underline{k}_{a_{i,1}}$ and $\underline{k}_{a_{i,1}}$ in (4.5) such that $-k_{a_{i,1}} < -\underline{k}_{a_{i,1}} \leq x_{i,1} \leq \underline{k}_{a_{i,1}} < k_{b_{i,1}}$, therefore, the output constraints are enforced.

Furthermore, solving (4.40), we obtain

$$0 \leq V(t) < \frac{a}{b} + \left(V(0) - \frac{a}{b} \right) \mathrm{e}^{-at} \tag{4.41}$$

From (4.41), we have

$$\begin{aligned}\sum_{i=1}^{N}\sum_{k=1}^{n}\frac{1}{2}z_{i,k}^{2} &< \frac{a}{b}+\left(V(0)-\frac{a}{b}\right)\mathrm{e}^{-at}\\ &< \frac{a}{b}+V(0)\mathrm{e}^{-at}\end{aligned} \tag{4.42}$$

that is,

$$\sum_{i=1}^{N}\sum_{k=1}^{n}z_{i,k}^{2} < 2\frac{a}{b}+2V(0)\mathrm{e}^{-at} \tag{4.43}$$

which implies that for a given $\eta > \sqrt{2a/b}$, thus, the consensus tracking error satisfies $|z_{i,1}| < \eta$, where η is the adjustable small residual set which is determined by the appropriate design parameters a and b. Therefore, the consensus tracking error can approach to a small set around zero. This completes the proof. □

Remark 4.5. *From the proof of Theorem 1, it can be seen that the design parameters in MAS satisfy the following requirements: increasing the parameter $c_{i,n}$ from the virtual control law at each step, the parameter τ_i in the adaptive law* (4.33) *and decreasing μ_i from the adaptive law* (4.13) *result in larger a in* (4.41)*, which narrows the bound of the tracking error. Smaller values of the parameters κ_i, δ_i in the designed two adaptive laws* (4.13) *and* (4.33) *can reduce the value of b.*

4.4 Simulation Results

In this section, a group of four two-stage chemical reactors is provided to demonstrate the viability and effectiveness of the proposed fault-tolerant consensus controller. The four networked two-stage chemical reactors consisting of MAS (4.1) is modeled as follows :

$$\begin{aligned}\dot{x}_{i,1} &= -\frac{1}{T_{i,1}}x_{i,1}-C_{i,1}x_{i,1}+\frac{1-R_{i,2}}{v_{i,1}}x_{i,2}+f_{i,1}\\ \dot{x}_{i,2} &= -\frac{1}{T_{i,2}}x_{i,2}-C_{i,2}x_{i,2}+\frac{g_i}{v_{i,2}}u_i^F+f_{i,2}\\ y_i &= x_{i,1}, \quad \text{for } i=1,\ldots,4\end{aligned} \tag{4.44}$$

where states $x_{i,1}$ and $x_{i,2}$ represent chemical compositions, y_i is the output, $T_{i,1}$ and $T_{i,2}$ are reactor residence times, $C_{i,1}$ and $C_{i,2}$ indicate reaction constants, $v_{i,1}$ and $v_{i,2}$ are reaction volumes, $R_{i,2}$ is the recycle flow rate, g_i is the feed rate, u_i^F stands for actuator fault, $f_{i,1}$ and $f_{i,2}$ are unknown functions. The networked two-stage chemical reactors model is borrowed from (Li *et al.* 2021).

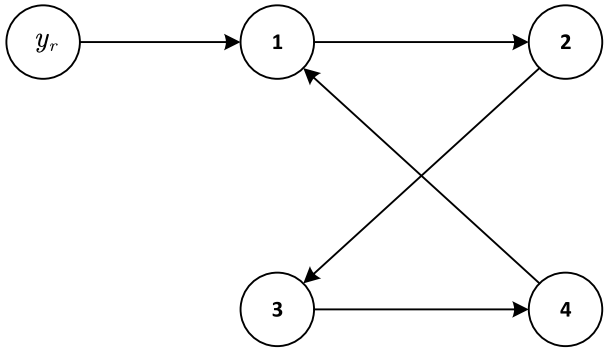

Figure 4.3. Communication topology of the MAS with a leader.

To demonstrate the communication network between the four chemical reactors, a directed graph is listed in Figure 4.3 with a leader.

In the simulation, the corresponding system parameters are chosen as $T_{i,1} = T_{i,2} = 5$, $C_{i,1} = 0.3$, $C_{i,2} = 0.2$, $v_{i,1} = v_{i,2} = R_{i,2} = g_i = 0.5$, $f_{i,1} = 0.6 \sin x_{i,1}$ and $f_{i,2} = x_{i,1} + 0.1x_{i,2}$. The design parameters are given by $k_{a_{i,1}} = 2.2$, $k_{b_{i,1}} = 2$, $\bar{k}_{a_{i,1}} = \bar{k}_{b_{i,1}} = -0.2$, $c_{i,1} = 16$ $c_{i,2} = 11$, $\mu_i = \tau_i = 1$ and $\kappa_i = \delta_i = \epsilon_i = 0.01$. Moreover, the RBFNN contains 41 neural nodes evenly distributed in $[-2, 2]$ with width $w_i = 0.1$, Gaussian function is selected as the activation function of RBFNN. Furthermore, consider the following actuator fault case occurs after 5 seconds:

- The loss of effectiveness actuator fault with bias in the 1st reactor with $u_1^F = \rho_1(t)\omega_1 + h_1(t)$, where $\rho_1(t) = 0.4 \sin t + 0.3$ and $h_1(t) = 0.5t$.
- The loss of effectiveness actuator fault in the 3nd reactor with $u_3^F = \rho_3(t)\omega_3$, where $\rho_3(t) = 0.3 \sin t + 0.3$.

Figure 4.4 shows the trajectories of state $x_{i,1}$ with the asymmetric output constraint and includes two scenarios of actuator faults that occur in the actuators of distinct reactors. Figure 4.5 presents state $x_{i,2}$ of each chemical reactor. Adaptive laws $\hat{\theta}_i$ in (4.13) and $\hat{\vartheta}_i$ in (4.33) are demonstrated in Figure 4.6. Figure 4.7 displays the response of the proposed fault-tolerant consensus controller u_i subject to two cases of actuator faults. Figure 4.8 shows the evolution of consensus tracking errors $z_{i,1}$ and $z_{i,2}$. Therefore, from the simulation results, the upper and lower bounds of the output constraint are enforced, the designed fault-tolerant consensus controller guarantees that the output trajectories can closely follow the leader and the consensus tracking error convergences to a small region.

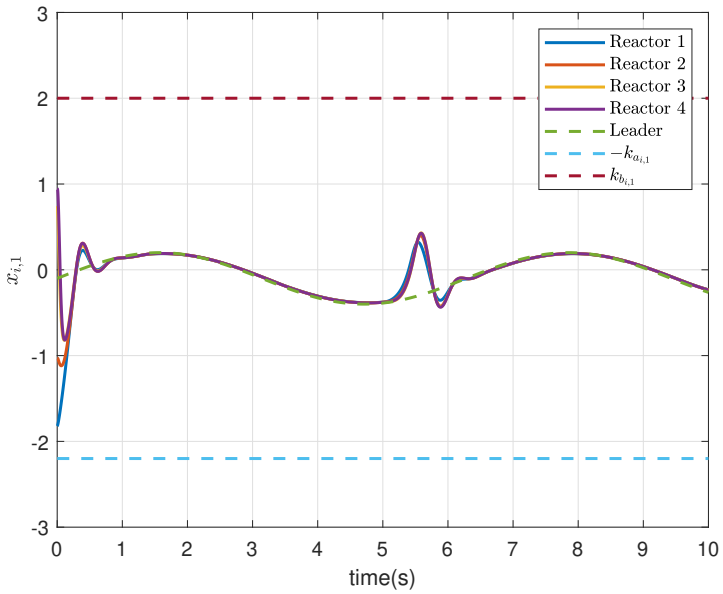

Figure 4.4. Output trajectories with asymmetric constraint and actuator fault.

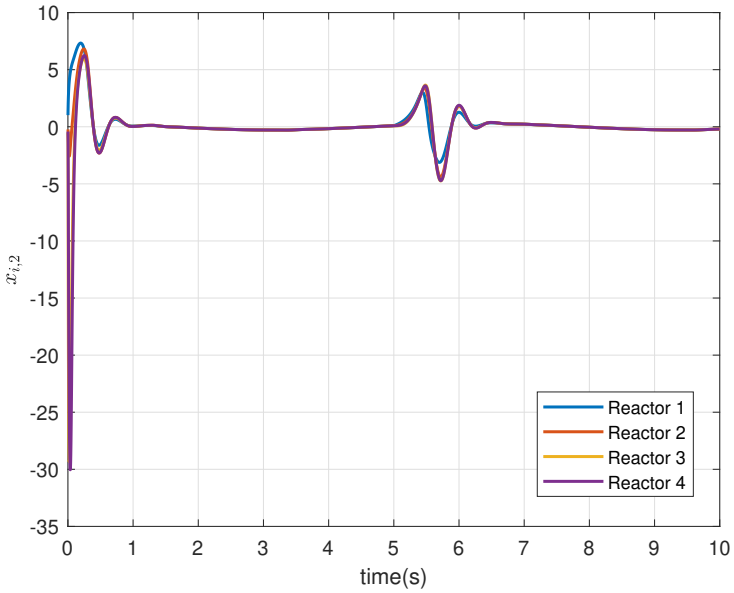

Figure 4.5. Trajectories of the states $x_{i,2}$ under actuator fault.

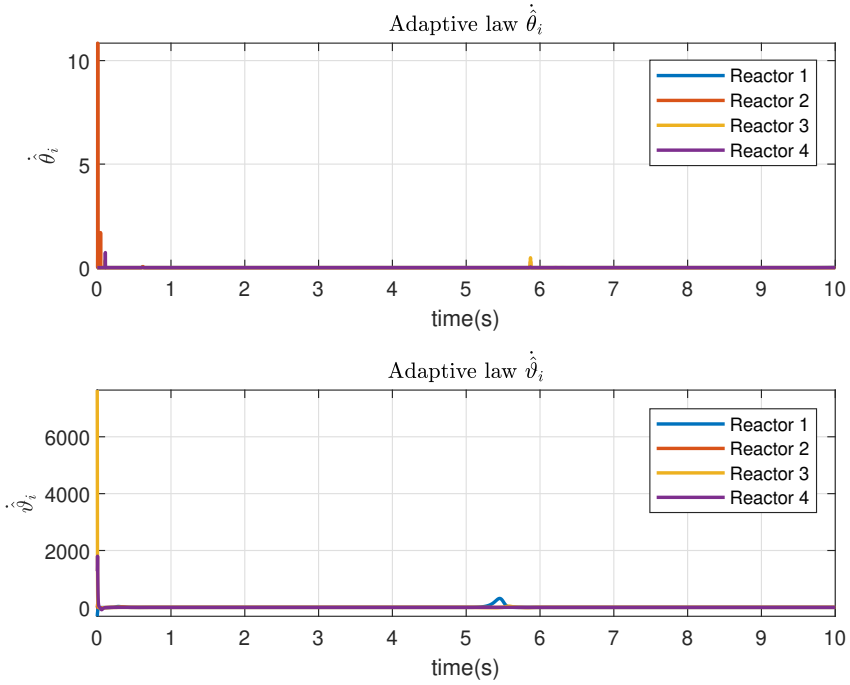

Figure 4.6. Adaptive laws under the proposed controller.

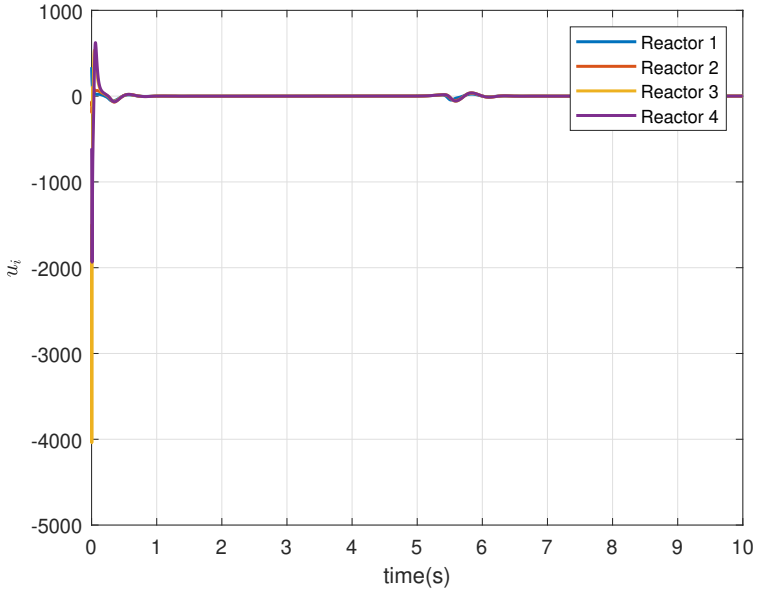

Figure 4.7. Fault-tolerant consensus controller u_i.

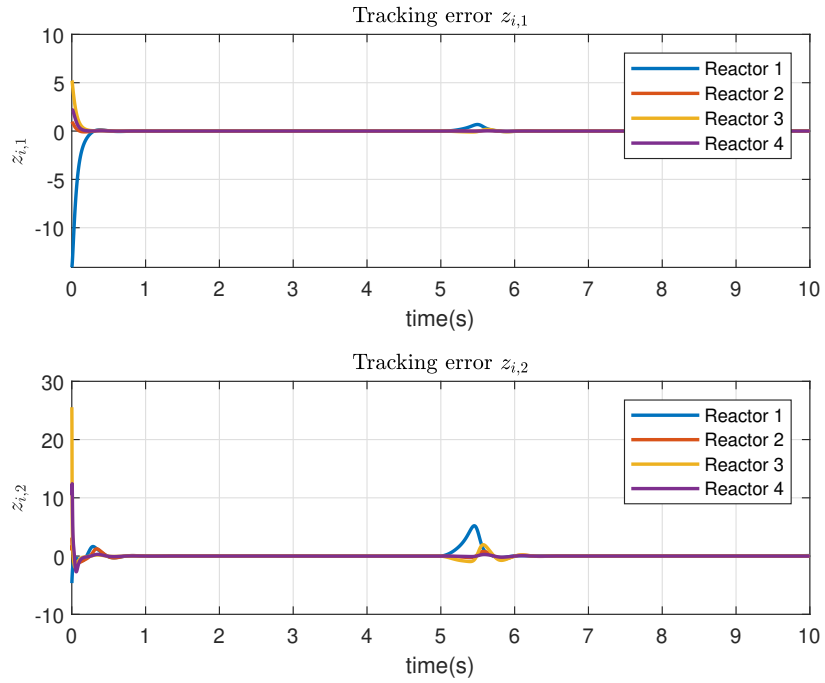

Figure 4.8. Consensus tracking errors $z_{i,1}$ and $z_{i,2}$.

4.5 Chapter Summary

In this chapter, a fault-tolerant leader-follower consensus control scheme subject to output constraint has been proposed for nonlinear MAS. By integrating adaptive RBFNN and backstepping control approaches, a single parameter estimator has been designed with the control scheme. We also introduced a new state transformation technique to solve the output constraint for each agent. Furthermore, an adaptive compensation method has been adopted to eliminate the effect of actuator failure.

Chapter 5

Constrained Consensus Control with Unknown Control Directions

5.1 Introduction

Consensus control problem has emerged as the foundation of MAS, as its basic theoretical framework is widely applied to achieve cooperative behaviour within a networked system. A consensus control algorithm aims to synchronize all states of agents to a common state by exchanging information with its neighboring agents in a distributed manner (Lunze 2019, Cao *et al.* 2012, Sun *et al.* 2022b). Another reason for attracting a number of researchers is due to its variety of practical applications (Ren and Beard 2008), for instance, drone light shows, satellite clusters, vehicle platooning, etc. Normally, consensus control methods are classified into leaderless and leader-follower consensus control approaches (Shi and Yan 2021). The objective of leader-follower consensus control is to drive all following agents to track the predefined trajectory of a leader.

In recent years, many leader-follower consensus control studies have been conducted for MAS. A fully distributed leader-follower consensus controller (Li *et al.* 2014) was proposed for linear MAS without acquiring the global information of a directed communication graph. Furthermore, a leader-follower consensus controller was designed with a distributed extended state observer to compensate unknown external disturbances for a class of linear MAS (Cao *et al.* 2015). A distributed consensus control algorithm was developed for linear MAS subject to a periodic intermittent communication constraint along with switching directed topologies (Wen *et al.* 2014). The above

consensus control protocols are challenging to be employed for nonlinear MAS, even though they can achieve desired control performance for linear MAS.

For nonlinear MAS, a substantial amount of research has been done on consensus control (Rezaee and Abdollahi 2020, Chen *et al.* 2020, Huang *et al.* 2020, Shi and Yu 2021, Fu *et al.* 2022). The unknown control directions (UCD) problem is of paramount importance in practical control systems. Recently, significant results have been published to tackle this problem by applying various Nussbaum functions and making different assumptions on unknown control gain for nonlinear MAS. The solution to the UCD problem for MAS was first developed by proposing a new type of Nussbaum function, and all control gains were assumed to be unknown constants with the same sign (Chen *et al.* 2013b). An alternative Nussbaum function with a condition inequality (Xie *et al.* 2018) was proposed to handle both unknown actuator failures and non-identical control directions simultaneously. Despite the above studies that have concentrated on UCD for MAS, few attempts are practicable to solve the UCD problem with less restrictive assumption on control gain matrix for multiple-input multiple-output (MIMO) nonlinear MAS.

Output constraint problems are frequently encountered in practical applications due to safety requirements, specific environment and system performances (He *et al.* 2020). For example, inspection drones operating within a tunnel and robot manipulators within a restricted operating zone, etc. Typically, state transformation (Ni and Shi 2021a, Niu *et al.* 2017a, Zheng and Li 2018, Sun *et al.* 2022a) and barrier Lyapunov function (BLF) (Tee *et al.* 2009) approaches are used to resolve the output constraint problem. The logarithm-type state transformation function is widely applied to transform the constrained state into an unconstrained one. For instance, both constant symmetric and asymmetric cases were analysed for nonlinear output-constrained systems (Niu *et al.* 2017a), yet the lower restricted boundary is assumed to be negative, and the upper boundary is strictly positive. The time-varying asymmetric case was considered (Zheng and Li 2018) with both positive lower and upper boundaries. Moreover, a new nonlinear state-dependent transformation function with positive boundaries was proposed (Zhao and Song 2020) for time-varying asymmetric constraints. However, the above transformation functions cannot eliminate the limitation of the boundaries and solve both constrained and unconstrained cases simultaneously. Furthermore, the BLF method requires complex formulations in controller design (Qu *et al.* 2018), especially

for the time-varying asymmetric case. Therefore, a more general solution to the output constraint problem is desired to remove the limitations of the state transformation function and simplify the analysis of the BLF approach for nonlinear MAS.

More importantly, not many studies have been conducted on output constraints by state transformation technique for nonlinear MAS. Consequently, the UCD coexisting with the output constraint problem for leader-follower consensus control in nonlinear MAS is worth investigating. Motivated by the challenges and shortcomings in the controller design of nonlinear MAS, the primary contributions of this study can be summarized as follows:

- A new state transformation function is derived and implemented to transform a time-varying asymmetric constrained output into an equivalent unconstrained state. Compared with the state transformation functions (Ni and Shi 2021a, Niu *et al.* 2017a, Zheng and Li 2018, Zhao and Song 2020), the proposed function can not only deal with both time-varying symmetric and asymmetric cases but also remove the implicit conditions on boundaries. Furthermore, unlike the BLF methods (Qu *et al.* 2018) and (Wang *et al.* 2020b), the consensus control analysis and design are significantly simplified. In particular, the proposed function can address constrained and unconstrained cases uniformly.

- Two cases of UCD problems are analysed by introducing less restrictive assumptions to the control gain matrix. Two corresponding simulations are also carried out to verify the feasibility.

- A new framework of adaptive consensus controller is proposed to resolve the problems of output constraints and UCD for MIMO nonlinear MAS. Specifically, a general nonlinear MAS system model is considered which differs from the parametric strict-feedback model (Wang *et al.* 2020a). A sliding mode integral filter is also presented to estimate the derivative of virtual control law instead of calculating it tediously, which can circumvent the explosion of the complexity problem in backstepping control.

The remainder of this chapter is structured as follows. Section 5.2 presents problem formulation and preliminaries. In Section 5.3, the adaptive leader-follower consensus

controller is designed and the stability analysis is evaluated. Two examples are simulated in Section 5.4 to prove the validity of the proposed control scheme and Section 5.5 summarises this article.

5.2 Problem Formulation

We consider a group of N p-order nonlinear strict-feedback systems modelled as:

$$\begin{aligned} \dot{x}_{i,m} &= g_{i,m}(\bar{x}_{i,m})x_{i,m+1} + f_{i,m}(\bar{x}_{i,m}) + d_{i,m}(t), \\ \dot{x}_{i,p} &= g_{i,p}(\bar{x}_{i,p})u_i + f_{i,p}(\bar{x}_{i,p}) + d_{i,p}(t) \\ y_i &= x_{i,1} \end{aligned} \tag{5.1}$$

where $i = 1, \ldots, N$, $m = 1, \ldots, p-1$, $\bar{x}_{i,m} = [x_{i,1}^T, x_{i,2}^T, \cdots, x_{i,m}^T]^T$; $x_{i,q} \in \mathbb{R}^n$ with $q = 1, \ldots, m$, $\bar{x}_{i,p} = [x_{i,1}^T, x_{i,2}^T, \cdots, x_{i,p}^T]^T \in \mathbb{R}^{np}$ is the system state, $u_i \in \mathbb{R}^n$ is the control input and $y_i \in \mathbb{R}^n$ denotes the output. The functions $g_{i,m}(\bar{x}_{i,m}) \in \mathbb{R}^{n\times n}$ and $f_{i,q}(\bar{x}_{i,q}) \in \mathbb{R}^n$ are unknown smooth nonlinear functions, the control gain matrix $g_{i,p}(\bar{x}_{i,p}) \in \mathbb{R}^{n\times l}$ $(l \geq n)$ denotes a partially unknown smooth function. The time-varying function $d_{i,q}(t) \in \mathbb{R}^n$ represents bounded external disturbance for $q = 1, \ldots, p$. The state $x_{i,1k}$ represents each element of the system output $x_{i,1} = [x_{i,11}, x_{i,12}, \cdots, x_{i,1n}]^T \in \mathbb{R}^n$ and each entry of output state of ith agent is restricted to an open set $\mathcal{C}_{x_{i,1k}}$ defined as follows:

$$x_{i,1k} \in \mathcal{C}_{x_{i,1k}} := \{-k_{a_{i,1k}}(t) < x_{i,1k} < k_{b_{i,1k}}(t)\}. \tag{5.2}$$

where $x_{i,1k} \in \mathbb{R}$, $k_{a_{i,1k}}(t)$ and $k_{b_{i,1k}}(t)$ are time-varying asymmetric constraint functions on system output for $k = 1, \ldots, n$.

Remark 5.1. *Strict-feedback systems are dominated by the form of nonlinear functions $g_{i,m}(\bar{x}_{i,m})$ and $f_{i,m}(\bar{x}_{i,m})$ in the $\dot{x}_{i,m}$ equation that are only related to state $\bar{x}_{i,m} = [x_{i,1}, x_{i,2}, \cdots, x_{i,m}]^T$. They are also known as lower-triangular systems (Krstic* et al. *1995). Furthermore, the control gain matrix $g_{i,p}(\bar{x}_{i,p}) \in \mathbb{R}^{n\times n}$ is an asymmetric square matrix, which has a less restrictive assumption than the diagonal case.*

Our aim in this chapter is to design an adaptive leader-follower consensus scheme for system (5.1) such that

- All subsystem outputs are driven to approach a desired trajectory $y_r(t)$ without violating the predefined output boundaries (5.2).

- The leader-follower consensus tracking errors are guaranteed to move toward to an arbitrarily small neighborhood of zero under UCD in a finite time.

The following assumptions are needed for the development of our main results.

Assumption 5.1. *(Zhang* et al. *2012) The communication topology $\mathcal{G}$ is modelled by a directed graph that contains a spanning tree with a leader as the root.*

Remark 5.2. *From Assumption* 5.1*, we have* $\text{rank}(\bar{\mathcal{L}}) = N$ *and the Laplacian matrix* $\bar{\mathcal{L}}$ *is defined as* $\bar{\mathcal{L}} = \begin{bmatrix} 0 & 0_{1\times N} \\ -b & \mathcal{L}+\mathcal{B} \end{bmatrix}$ *where* $b = [b_1, \cdots, b_N]^T$*,* b_i *indicates the connectivity between the leader and followers,* $b_i = 1$ *if ith agent is able to access a leader; otherwise,* $b_i = 0$*. Then,* $\text{rank}(\mathcal{L}+\mathcal{B}) = N$*, thus,* $\mathcal{L}+\mathcal{B}$ *is an invertible matrix.*

Assumption 5.2. *The unknown control coefficient* $g_{i,m}(\bar{x}_{i,m}) \in \mathbb{R}^{n\times n}$ *is a square matrix yet unnecessary to be symmetric, and its sign is unknown. Moreover, the norm of matrices* $g_{i,m}(\bar{x}_{i,m})$ *and* $g_{i,p}(\bar{x}_{i,p})$ *are assumed to be bounded as* $\|g_{i,m}(\bar{x}_{i,m})\|^2 \leq \bar{g}_{i,m}$ *and* $\left\|g_{i,p}(\bar{x}_{i,p})\right\|^2 \leq \bar{g}_{i,p}$*, respectively.*

Remark 5.3. *Notice that Assumption* 5.2 *ensures system* (5.1) *is controllable. The majority of practical systems such as Euler-Lagrange systems and MAS (Zhao* et al. *2018, Sachan and Padhi 2019) satisfy this assumption.*

Assumption 5.3. *The output constraint functions* $k_{a_{i,1k}}(t)$ *and* $k_{b_{i,1k}}(t)$ *and their l-th* ($l = 0, \cdots, p$) *derivatives are bounded and continuous.*

Assumption 5.4. *(Zhao* et al. *2021) The dynamics of a leader* $y_r(t) = [y_{r1}(t), y_{r2}(t), \cdots, y_{rn}(t)]^T \in \Omega \subset \mathbb{R}^n$ *and its l-th derivative are continuous and bounded. It also satisfies the following conditions,* $y_{rn}(t) \in \mathcal{C}_{y_{rn}} := \{-k_{a_{i,1k}}(t) < -k_{a_{yrn}}(t) \leq y_{rn}(t) \leq k_{b_{yrn}}(t) < k_{b_{i,1k}}(t)\}$*, where* $k_{a_{yrn}}(t)$ *and* $k_{b_{yrn}}(t)$ *are time-varying functions.*

Assumption 5.5. *(Zhao* et al. *2021) For any time-varying functions* $k_{a_{i,1k}}(t)$ *and* $k_{b_{i,1k}}(t)$*, there exist functions* $k_{a_{yrn}}(t)$ *and* $k_{b_{yrn}}(t)$*, positive constants* ε_l ($l = 1, \cdots, 5$) *satisfying the following inequalities* $k_{a_{i,1k}}(t) + k_{b_{i,1k}}(t) \geq \varepsilon_1$*,* $k^2_{a_{i,1k}}(t) - \bar{k}_{a_{i,1k}} \geq \varepsilon_2$*,* $k^2_{b_{i,1k}}(t) - \bar{k}_{b_{i,1k}} \geq \varepsilon_3$*,* $k_{a_{i,1k}}(t) - k_{a_{yrn}}(t) \geq \varepsilon_4$*,* $k_{b_{i,1k}}(t) - k_{b_{yrn}}(t) \geq \varepsilon_5$*, where* $\bar{k}_{a_{i,1k}}$ *and* $\bar{k}_{b_{i,1k}}$ *are design constants.*

Remark 5.4. *The boundaries of output constraint functions can be constructed under Assumptions* 5.4*. Assumptions* 5.5 *ensures that the time-varying asymmetric output constraint functions are computable for each agent.*

Definition 5.1. *(Ge* et al. *2004) A continuous function $\mathcal{N}(\zeta)$ is defined as a Nussbaum-type function satisfying the following properties*

$$\lim_{s\to+\infty}\sup\frac{1}{s}\int_0^s \mathcal{N}(\zeta)d\zeta = +\infty$$
$$\lim_{s\to+\infty}\inf\frac{1}{s}\int_0^s \mathcal{N}(\zeta)d\zeta = -\infty$$

There exist various types of Nussbaum functions that are commonly applied to address the UCD problem such as $e^{\zeta^2}\cos(\zeta\pi/2)$, $\zeta^2\sin\zeta$, $\zeta^2\cos\zeta$, *etc.*

Before ending this section, we recall the following results that are needed to derive the main results in sequel.

Lemma 5.1. *(Xu and Ioannou 2003) There exists a symmetric matrix $\Psi_i \in \mathbb{R}^{n\times n}$, such that $|\gamma_i(x_i)| \geq \lambda_{\min}$ and $z^T(x_i)\Psi_i z(x_i) = \gamma_i(x_i)\|z(x_i)\|^2$ holds, where $\gamma_i(x_i) := z_e^T(x_i)\Psi_i z_e(x_i)$, $z_e := z/\|z\|$ is a unit vector and $\lambda_{\min}$ represents the smallest singular value of the matrix $(\Psi_i + \Psi_i^T)/2$.*

Lemma 5.2. *(Ge* et al. *2004) Consider smooth functions $\zeta(t)$ and $V(t) > 0$ for all $t \in [0, t_g)$. If the following inequality holds,*

$$V(t) \leq c_1 + e^{-c_2 t}\int_0^t (G(s)\mathcal{N}(\zeta)+1)\dot{\zeta}e^{c_2 s}ds$$

where c_1 and c_2 are positive constants, $\mathcal{N}(\zeta)$ is a Nussbaum function and $G(s)$ is a time-varying unknown parameter, then, $V(t)$, $\zeta(t)$ and $\int_0^t G(s)\mathcal{N}(\zeta)\dot{\zeta}e^{c_2 s}ds$ are bounded for all $t \in [0, t_g)$.

RBFNN are commonly employed to approximate unknown smooth functions due to their effective approximation performance and simple design process. An unknown continuous function $f(Z) : \mathbb{R}^l \to \mathbb{R}^n$ is defined on a compact set, i.e., $f(Z) \in \Omega$, which can be approximated by RBFNN as follows:

$$f(Z) = W^T\varphi(Z) + \sigma$$

where $Z \in \Omega \subset \mathbb{R}^l$ is a input vector, $W \in \mathbb{R}^{r\times n}$ denotes an optimal weight matrix, r represents the neuron nodes of RBFNN, $\varphi(Z) = [\varphi_1(Z), \cdots, \varphi_r(Z)]^T \in \mathbb{R}^r$ is a known radial basis function vector and $\sigma \in \mathbb{R}^n$ is an approximation error vector.

A general type of Gaussian function is selected as the entry of $\varphi(Z)$ such that $\varphi_i(Z) = \exp[-(Z-c_i)^T(Z-c_i)/w_i^2]$, $i = 1, \ldots, r$, where c_i and w_i are the center and width of

the Gaussian function, respectively. Moreover, considering the properties of RBFNN, the norm of RBFNN approximation error vector σ can be adjusted to a small arbitrary value by adding large enough neuron nodes.

Remark 5.5. *RBFNN approximation is only applicable within a compact set Ω. Consequently, the stability analysis of the closed-loop system can be performed as long as the system states stay within the compact set. i.e., $x_{i,m} \in \Omega \subset \mathbb{R}^n$, $\forall t \geq 0$, where the set Ω can be selected as large as desired.*

5.3 Main Results

This section is devoted to designing a leader-follower consensus controller with the problems of output constraints and UCD. Fig. 5.1 depicts the nonlinear MAS control diagram of the proposed adaptive leader-follower consensus control.

The control block diagram consists of five parts including leader signal y_r, state transformation block, controller block, i-th follower model and communication network. Specifically, the communication network is responsible for transmitting state information about the adjacent agents of i-th follower and the leader signal. The state transformation block aims to convert the constrained output to an unconstrained one, which is described in subsection A. Moreover, the actual controller u_i adopts the adaptive recursive design methodology, which comprises a number of steps. The detailed controller design procedure is shown in subsection B.

5.3.1 Time-varying Asymmetric Output Constraints

To prevent the output constraint violation from occurring for ith agent, we use a new state transformation method to solve this issue in nonlinear MAS as follows:

$$\chi_{i,1k} = \frac{k_{a_{i,1k}}(t)x_{i,1k} + \bar{k}_{a_{i,1k}}}{2\left(k_{a_{i,1k}}(t) + x_{i,1k}\right)} + \frac{k_{b_{i,1k}}(t)x_{i,1k} - \bar{k}_{b_{i,1k}}}{2\left(k_{b_{i,1k}}(t) - x_{i,1k}\right)} \tag{5.3}$$

where $\bar{k}_{a_{i,1k}}$ and $\bar{k}_{b_{i,1k}}$ are constants for ith agent satisfying the conditions in Assumption 5.5.

From (5.3) the unconstrained output state $\chi_{i,1k}$ tends to infinity as $x_{i,1k}$ reaches the limits of $\mathcal{C}_{x_{i,1k}}$, i.e., given the initial state $x_{i,1k}(0) \in \mathcal{C}_{x_{i,1k}}$ for ith agent, $\chi_{i,1k} \to \infty$ if

5.3.1 Time-varying Asymmetric Output Constraints

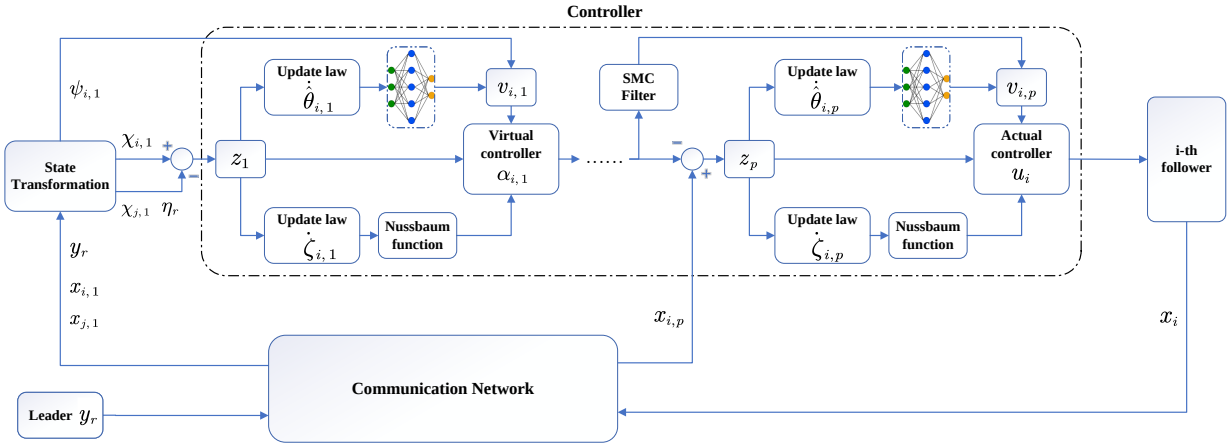

Figure 5.1. Block diagram of the proposed adaptive leader-follower consensus control system.

and only if $x_{i,1k} \to -k_{a_{i,1k}}(t)$ or $x_{i,1k} \to k_{b_{i,1k}}(t)$. Accordingly, the problem of output constraint for ith agent can be reformulated to the determination of the boundedness of unconstrained output state $\chi_{i,1k}$.

Then, the derivative of $\chi_{i,1k}$ is derived as

$$\dot{\chi}_{i,1k} = \psi_{i,1k}\dot{x}_{i,1k} + \omega_{i,1k} \tag{5.4}$$

where parameters $\psi_{i,1k}$ and $\omega_{i,1k}$ are defined as,

$$\psi_{i,1k} = \frac{k_{a_{i,1k}}^2(t) - \bar{k}_{a_{i,1k}}}{2\left(k_{a_{i,1k}}(t) + x_{i,1k}\right)^2} + \frac{k_{b_{i,1k}}^2(t) - \bar{k}_{b_{i,1k}}}{2\left(k_{b_{i,1k}}(t) - x_{i,1k}\right)^2}$$

$$\omega_{i,1k} = \frac{\left(x_{i,1k}^2 - \bar{k}_{a_{i,1k}}\right)\dot{k}_{a_{i,1k}}}{2\left(k_{a_{i,1k}}(t) + x_{i,1k}\right)^2} - \frac{\left(x_{i,1k}^2 - \bar{k}_{b_{i,1k}}\right)\dot{k}_{b_{i,1k}}}{2\left(k_{b_{i,1k}}(t) - x_{i,1k}\right)^2}$$

In order to facilitate the design of adaptive leader-follower consensus controller, then (5.4) can be rewritten as a matrix form

$$\dot{\chi}_{i,1} = \psi_{i,1}\dot{x}_{i,1} + \omega_{i,1} \tag{5.5}$$

where

$$\chi_{i,1} = [\chi_{i,11}, \chi_{i,12}, \cdots, \chi_{i,1k}]^T \in \mathbb{R}^n,$$
$$\omega_{i,1} = [\omega_{i,11}, \omega_{i,12}, \cdots, \omega_{i,1k}]^T \in \mathbb{R}^n,$$
$$\psi_{i,1} = \mathrm{diag}[\psi_{i,11}, \psi_{i,12}, \cdots, \psi_{i,1k}] \in \mathbb{R}^{n\times n}.$$

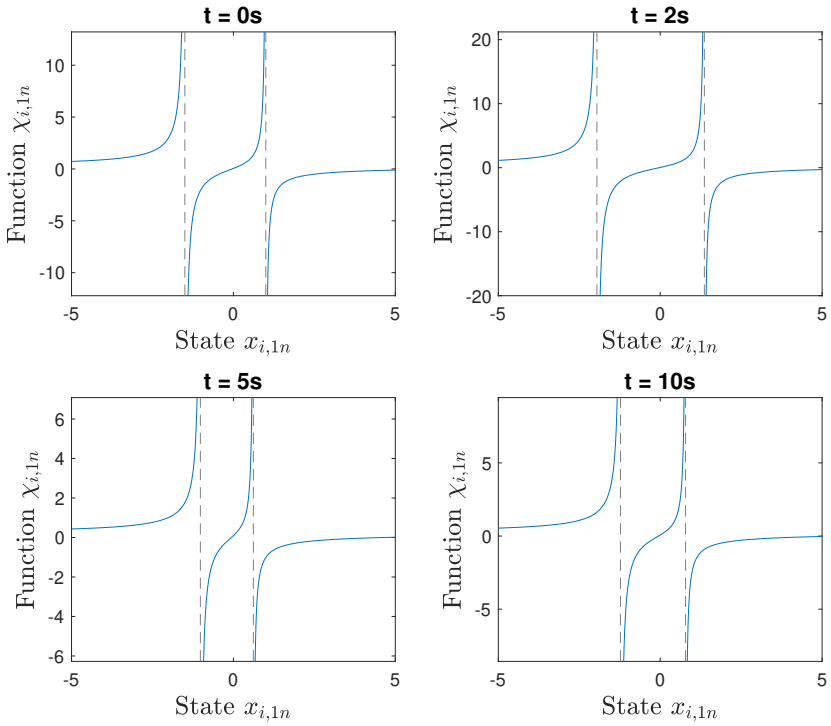

Figure 5.2. State transformation function $\chi_{i,1k}$ at distinct time points.

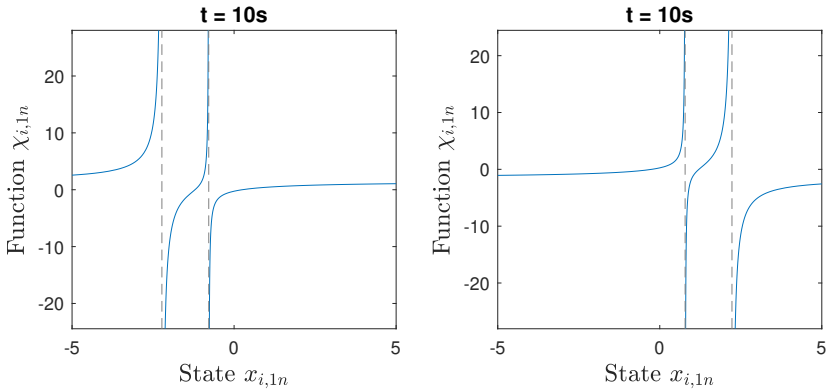

Figure 5.3. Two cases of state transformation function $\chi_{i,1k}$.

Remark 5.6. *The time-varying asymmetric state transformation function* (5.3) *is a new type of state transformation approach inspired by (Zhao* et al. *2021, Sun* et al. *2021) to address output constraint problem. Fig.* 5.2 *shows a state transformation function* $\chi_{i,1k}$ *at different time points with time-varying boundaries* $k_{a_{i,1k}} = 0.5\sin(t) + 1.5$, $k_{b_{i,1k}} = 0.4\sin(t) + 1$ *and* $\bar{k}_{a_{i,1k}} = \bar{k}_{b_{i,1k}} - 0.3$. *Fig.* 5.3 *indicates that the time-varying boundaries are not only both positive but also both negative, which is unlike the limitations on constraint boundaries (Zheng and Li 2018, Cao* et al. *2019). Furthermore, it differs from the classical BLF methods (Wang* et al. *2020b, Ni and Shi 2021b) in that the new approach relaxes the selection of initial conditions and significantly simplifies design procedure because of the design procedure depends on the unconstrained state* $\chi_{i,1}$ *rather than the constrained tracking error. Likewise, if the output is not constrained in a specific range, i.e.,* $K_i = k_{a_{i,1k}} = k_{b_{i,1k}} \to \infty$, *applying the L'Hôpital rule, we obtain* $\lim_{K_i\to\infty} \chi_{i,1k} = x_{1k}$, *which guarantees that this function can address constrained and unconstrained cases uniformly.*

5.3.2 Distributed Adaptive Leader-follower Consensus Controller Design

In this section, we will provide a systematic adaptive leader-follower consensus control design procedure for MIMO nonlinear MAS under output constraints and UCD. Adaptive neural network and backstepping control techniques are integrated to construct the leader-follower consensus controller.

Step 1: Introduce the following leader-follower consensus tracking error $z_{i,1}$ and error variable $z_{i,2}$

$$\begin{aligned} z_{i,1} &= \sum_{j=1}^{N} a_{ij}(\chi_{i,1} - \chi_{j,1}) + b_i(\chi_{i,1} - \eta_r), \quad i = 1, \ldots, N \\ z_{i,2} &= x_{i,2} - \alpha_{i,1} \end{aligned} \tag{5.6}$$

where $\alpha_{i,1}$ is a virtual control law to be designed later. The parameter η_r implies that the trajectory of the leader $y_r(t)$ is within the predefined constraint, consequently, each entry of η_r is defined within the constrained set $\mathcal{C}_{y_{rn}} \subset \mathcal{C}_{x_{i,1k}}$ as follows:

$$\eta_{rn} = \frac{k_{a_{i,1k}}(t)y_{rn} + \bar{k}_{a_{i,1k}}}{2\left(k_{a_{i,1k}}(t) + y_{rn}\right)} + \frac{k_{b_{i,1k}}(t)y_{rn} - \bar{k}_{b_{i,1k}}}{2\left(k_{b_{i,1k}}(t) - y_{rn}\right)} \tag{5.7}$$

with

$$\begin{aligned} y_r(t) &= [y_{r1}(t), y_{r2}(t), \cdots, y_{rn}(t)]^T \in \mathbb{R}^n \\ \eta_r(t) &= [\eta_{r1}(t), \eta_{r2}(t), \cdots, \eta_{rn}(t)]^T \in \mathbb{R}^n. \end{aligned}$$

Then, the dynamics of $z_{i,1}$ is calculated as

$$\begin{aligned}\dot{z}_{i,1} &= (d_i + b_i)\dot{\chi}_{i,1} - \sum_{j=1}^{N} a_{ij}\dot{\chi}_{j,1} - b_i\dot{\eta}_r \\ &= (d_i + b_i)\left(\psi_{i,1}g_{i,1}x_{i,2} + \psi_{i,1}f_{i,1} + \psi_{i,1}d_{i,1} + \omega_{i,1}\right) - \sum_{j=1}^{N} a_{ij}\dot{\chi}_{j,1} - b_i\dot{\eta}_r \\ &= h_i\left(\psi_{i,1}g_{i,1}x_{i,2} + \psi_{i,1}d_{i,1} + \Phi_{i,1}(Z_{i,1})\right)\end{aligned} \tag{5.8}$$

where $h_i = d_i + b_i$ and $\Phi_{i,1}(Z_{i,1}) = \psi_{i,1}f_{i,1} + \omega_{i,1} - \left(\sum_{j=1}^{N} a_{ij}\dot{\chi}_{j,1} + b_i\dot{\eta}_r\right)/h_i$. Since the function $\Phi_{i,1}(Z_{i,1})$ is not available for the closed-loop MAS, the RBFNN is used to approximate the unknown function $\Phi_{i,1}(Z_{i,1})$. It can be seen that the unknown function is a smooth function of inputs $x_{i,1}$, $\omega_{i,1}$ and η_r, and $Z_{i,1} = [x_{i,1}^T, \omega_{i,1}^T \eta_r^T]^T \in \Omega \subset \mathbb{R}^{3n}$. Thus, we have

$$\Phi_{i,1}(Z_{i,1}) = W_{i,1}^T \varphi_{i,1}(Z_{i,1}) + \sigma_{i,1} \tag{5.9}$$

The unknown approximation error vector $\sigma_{i,1}$ satisfies that $\|\sigma_{i,1}\|$ is bounded with $\|\sigma_{i,1}\| \leq \bar{\sigma}_{i,1}$, and $\bar{\sigma}_{i,1}$ is a positive constant. In order to simplify the control design process and reduce the computational complexity of RBFNN, we define $\theta_{i,1} = \|W_{i,1}\|^2$ as an intermediate variable of optimal weight matrix $W_{i,1}$, $\tilde{\theta}_{i,1} = \theta_{i,1} - \hat{\theta}_{i,1}$ and $\hat{\theta}_{i,1}$ is the estimate of parameter $\theta_{i,1}$.

Considering the following Lyapunov function candidate

$$V_{i,1} = \frac{1}{2h_i} z_{i,1}^T z_{i,1} + \frac{1}{2\lambda_{i,1}} \tilde{\theta}_{i,1}^2 \tag{5.10}$$

where $\lambda_{i,1}$ is a positive constant.

Taking the derivative of the Lyapunov function $V_{i,1}$ and consider the RBFNN approximation in (5.9), it yields

$$\begin{aligned}\dot{V}_{i,1} &= \frac{1}{h_i} z_{i,1}^T \dot{z}_{i,1} - \frac{1}{\lambda_{i,1}} \tilde{\theta}_{i,1}\dot{\hat{\theta}}_{i,1} \\ &= z_{i,1}^T\left(\psi_{i,1}g_{i,1}x_{i,2} + \psi_{i,1}d_{i,1}(t)\right) + z_{i,1}^T\Phi_{i,1}(Z_{i,1}) - \frac{1}{\lambda_{i,1}}\tilde{\theta}_{i,1}\dot{\hat{\theta}}_{i,1} \\ &= z_{i,1}^T\left(\psi_{i,1}g_{i,1}z_{i,2} + \psi_{i,1}g_{i,1}\alpha_{i,1} + \psi_{i,1}d_{i,1}(t)\right) \\ &\quad + z_{i,1}^T\left(W_{i,1}^T\varphi_{i,1}(Z_{i,1}) + \sigma_{i,1}\right) - \frac{1}{\lambda_{i,1}}\tilde{\theta}_{i,1}\dot{\hat{\theta}}_{i,1}\end{aligned} \tag{5.11}$$

By applying Young's inequality, we have

$$\begin{aligned} z_{i,1}^T \psi_{i,1} d_{i,1}(t) &\leq \frac{1}{2} \|z_{i,1}\|^2 \|\psi_{i,1}\|^2 + \frac{1}{2}\bar{d}_{i,1}^2 \\ z_{i,1}^T W_{i,1}^T \varphi_{i,1}(Z_{i,1}) &\leq \frac{1}{2} \|z_{i,1}\|^2 \theta_{i,1} \|\varphi_{i,1}(Z_{i,1})\|^2 + \frac{1}{2} \\ z_{i,1}^T \sigma_{i,1} &\leq \frac{1}{2} \|z_{i,1}\|^2 + \frac{1}{2}\bar{\sigma}_{i,1}^2 \end{aligned} \tag{5.12}$$

where the positive constant $\bar{d}_{i,1}$ is the upper bound of the external disturbance matrix $d_{i,1}(t)$ such that $\|d_{i,1}(t)\| \leq \bar{d}_{i,1}$.

The virtual control law $\alpha_{i,1}$ and the adaptation law of the parameter $\theta_{i,1}$ are designed as

$$\begin{aligned} \alpha_{i,1} &= \mathcal{N}(\zeta_{i,1}) v_{i,1} z_{i,1} \\ v_{i,1} &= \kappa_{i,1} + \frac{1}{2} \|\psi_{i,1}\|^2 + \frac{1}{2} + \frac{1}{2}\hat{\theta}_{i,1} \|\varphi_{i,1}(Z_{i,1})\|^2 \\ \dot{\zeta}_{i,1} &= v_{i,1} \|z_{i,1}\|^2 \\ \dot{\hat{\theta}}_{i,1} &= \frac{\lambda_{i,1}}{2} \|z_{i,1}\|^2 \|\varphi_{i,1}(Z_{i,1})\|^2 - \mu_{i,1}\hat{\theta}_{i,1} \end{aligned} \tag{5.13}$$

where $\kappa_{i,1}$ and $\mu_{i,1}$ are designed positive constants.

From the term $z_{i,1}^T \psi_{i,1} g_{i,1} \alpha_{i,1}$ and the definitions of $\psi_{i,1}$ and $g_{i,1}$, we obtain that the matrix $\psi_{i,1} g_{i,1}$ are unnecessarily symmetric. Since any real matrix can be expressed as the sum of a symmetric matrix and a skew symmetric matrix, the matrix $\psi_{i,1} g_{i,1}$ can be decomposed as $\psi_{i,1} g_{i,1} = G_{i,1} + G_{i,2}$, where $G_{i,1} = (\psi_{i,1} g_{i,1} + g_{i,1}^T \psi_{i,1})/2$ is a symmetric matrix and $G_{i,2} = (\psi_{i,1} g_{i,1} - g_{i,1}^T \psi_{i,1})/2$ is a skew symmetric matrix, respectively. According to Lemma 5.1 and the properties of skew symmetric matrix, we have

$$\begin{aligned} z_{i,1}^T \psi_{i,1} g_{i,1} z_{i,1} &= z_{i,1}^T (\psi_{i,1} g_{i,1} + g_{i,1}^T \psi_{i,1}) z_{i,1}/2 \\ &= \gamma_1(x_i) \|z_{i,1}\|^2 \end{aligned} \tag{5.14}$$

Then, substituting the virtual control law $\alpha_{i,1}$ into the term $z_{i,1}^T \psi_{i,1} g_{i,1} \alpha_{i,1}$, we derive

$$z_{i,1}^T \psi_{i,1} g_{i,1} \alpha_{i,1} = \gamma_1(t) \mathcal{N}(\zeta_{i,1}) \dot{\zeta}_{i,1} \tag{5.15}$$

Substituting (5.12), (5.13) and (5.15) into (5.11), we can obtain

$$\begin{aligned}\dot{V}_{i,1} \leq\ & z_{i,1}^T \psi_{i,1} g_{i,1} z_{i,2} + \left[\gamma_1(t)\mathcal{N}(\zeta_{i,1}) + 1\right]\dot{\zeta}_{i,1} - \dot{\zeta}_{i,1} + \frac{1}{2}\left\|z_{i,1}\right\|^2 \left\|\psi_{i,1}\right\|^2 + \frac{1}{2}\bar{d}_{i,1}^2 \\ & + \frac{1}{2}\left\|z_{i,1}\right\|^2 \theta_{i,1}\left\|\varphi_{i,1}(Z_{i,1})\right\|^2 + \frac{1}{2} + \frac{1}{2}\left\|z_{i,1}\right\|^2 + \frac{1}{2}\bar{\sigma}_{i,1}^2 - \frac{1}{\lambda_{i,1}}\tilde{\theta}_{i,1}\dot{\hat{\theta}}_{i,1} \\ \leq\ & -\kappa_{i,1}\left\|z_{i,1}\right\|^2 + z_{i,1}^T \psi_{i,1} g_{i,1} z_2 + \left[\gamma_1(t)\mathcal{N}(\zeta_{i,1}) + 1\right]\dot{\zeta}_{i,1} \\ & + \frac{\mu_{i,1}}{\lambda_{i,1}}\tilde{\theta}_{i,1}\hat{\theta}_{i,1} + \frac{1}{2} + \frac{1}{2}\bar{d}_{i,1}^2 + \frac{1}{2}\bar{\sigma}_{i,1}^2\end{aligned}$$

Considering the following inequality

$$\begin{aligned}\frac{\mu_{i,1}}{\lambda_{i,1}}\tilde{\theta}_{i,1}\hat{\theta}_1 &= \frac{\mu_{i,1}}{\lambda_{i,1}}\left(\tilde{\theta}_{i,1}\theta_{i,1} - \tilde{\theta}_{i,1}^2\right) \\ &\leq \frac{\mu_{i,1}}{2\lambda_1}\theta_{i,1}^2 - \frac{\mu_{i,1}}{2\lambda_{i,1}}\tilde{\theta}_{i,1}^2\end{aligned}$$

we have

$$\dot{V}_{i,1} \leq -\kappa_{i,1}\left\|z_{i,1}\right\|^2 + z_{i,1}^T \psi_{i,1} g_{i,1} z_{i,2} + \left[\gamma_1(t)\mathcal{N}(\zeta_{i,1}) + 1\right]\dot{\zeta}_{i,1} - \frac{b_{i,1}}{2\lambda_{i,1}}\tilde{\theta}_{i,1}^2 + C_{i,1}$$

where $C_{i,1} = \frac{1}{2} + \frac{\mu_{i,1}}{2\lambda_{i,1}}\theta_{i,1}^2 + \frac{1}{2}\bar{d}_{i,1}^2 + \frac{1}{2}\bar{\sigma}_{i,1}^2$.

Step 2: Consider the error variable $z_{i,2} = x_{i,2} - \alpha_{i,1}$, then, its derivative is expressed as follows:

$$\begin{aligned}\dot{z}_{i,2} &= \dot{x}_{i,2} - \dot{\alpha}_{i,1} \\ &= g_{i,2}x_{i,3} + f_{i,2} + d_{i,2}(t) - \dot{\alpha}_{i,1}\end{aligned}$$

Define the following Lyapunov function candidate

$$V_{i,2} = V_{i,1} + \frac{1}{2}z_{i,2}^T z_{i,2} + \frac{1}{2\lambda_{i,2}}\tilde{\theta}_{i,2}^2 \tag{5.16}$$

Its derivative yields

$$\begin{aligned}\dot{V}_{i,2} &= \dot{V}_{i,1} + z_{i,2}^T \dot{z}_{i,2} - \frac{1}{\lambda_{i,2}}\tilde{\theta}_{i,2}\dot{\hat{\theta}}_{i,2} \\ &= \dot{V}_{i,1} + z_{i,2}^T\left(g_{i,1}\psi_{i,1}z_{i,1} + g_{i,2}x_{i,3} + f_{i,2}\right) \\ &\quad + z_{i,2}^T\left(d_{i,2}(t) - \dot{\alpha}_{i,1} - g_{i,1}\psi_{i,1}z_{i,1}\right) - \frac{1}{\lambda_{i,2}}\tilde{\theta}_{i,2}\dot{\hat{\theta}}_{i,2}\end{aligned} \tag{5.17}$$

Since $\Phi_{i,2}(Z_{i,2}) = g_{i,1}\psi_{i,1}z_{i,1} + f_{i,2}$ is unknown for the closed-loop MAS, the RBFNN is used to approximate $\Phi_{i,2}(Z_{i,2})$. It can be seen that the unknown function is a smooth

function of inputs $\psi_{i,1}$, $x_{i,1}$ and $x_{i,2}$, and $Z_{i,2} = [\psi_{i,1}^T, \eta_r^T, x_{i,1}^T, x_{i,2}^T]^T \in \Omega \subset \mathbb{R}^{4nN}$. Thus, applying the RBFNN to approximate $\Phi_{i,2}(Z_{i,2})$, then (5.17) yields

$$\begin{aligned}\dot{V}_{i,2} = \dot{V}_{i,1} + z_{i,2}^T g_{i,2} z_{i,3} + z_{i,2}^T g_{i,2}\alpha_{i,2} + z_{i,2}^T d_{i,2}(t) \\ + z_{i,2}^T \left(W_{i,2}^T \varphi_{i,2}(Z_{i,2}) + \sigma_{i,2}\right) - z_{i,2}^T g_{i,1}\psi_{i,1} z_{i,1} - z_{i,2}^T \dot{\alpha}_{i,1} - \frac{1}{\lambda_{i,2}}\tilde{\theta}_{i,2}\dot{\hat{\theta}}_{i,2}\end{aligned} \tag{5.18}$$

By applying Young's inequality, we have

$$\begin{aligned} z_{i,2}^T d_{i,2}(t) &\leq \frac{1}{2}\|z_{i,2}\|^2 + \frac{1}{2}\bar{d}_{i,2}^2 \\ z_{i,2}^T W_{i,2}^T \varphi_{i,2}(Z_{i,2}) &\leq \frac{1}{2}\|z_{i,2}\|^2 \theta_{i,2}\|\varphi_{i,2}(Z_{i,2})\|^2 + \frac{1}{2} \\ z_{i,2}^T \sigma_{i,2} &\leq \frac{1}{2}\|z_{i,2}\|^2 + \frac{1}{2}\bar{\sigma}_{i,2}^2 \end{aligned}$$

To avoid recomputing the derivative of the virtual control law $\alpha_{i,1}$ in the following steps and reduce the computational burden for RBFNN, we can estimate $\dot{\alpha}_{i,1}$ by applying the SMC filter (Chen *et al.* 2017), then, we obtain

$$\begin{aligned} \dot{\xi}_{i,1} &= -\frac{\xi_{i,1} - \alpha_{i,1}}{\rho_{i,1}} - k_{i,1}\frac{\xi_{i,1} - \alpha_{i,1}}{\|\xi_{i,1} - \alpha_{i,1}\| + \beta_{i,1}} \\ \dot{\xi}_{i,2} &= -\frac{\xi_{i,2} - \dot{\xi}_{i,1}}{\rho_{i,2}} - k_{i,2}\frac{\xi_{i,2} - \dot{\xi}_{i,1}}{\|\xi_{i,2} - \dot{\xi}_{i,1}\| + \beta_{i,2}} \end{aligned} \tag{5.19}$$

where $\rho_{i,l}$, $k_{i,l}$ and $\beta_{i,l}$ are all positive design parameters with $l = 1, 2$. The parameter $\xi_{i,1}$ is the filtered value of a known function $\alpha_{i,}$. The parameter $\xi_{i,2}$ is the filtered value of $\dot{\xi}_{i,1}$ that is the approximated value of unknown function $\dot{\alpha}_{i,1}$, which can avoid the problem of 'explosion of complexity' in adaptive backstepping design procedure and reduce the computational burden of adaptive neural networks control. Furthermore, the filter error $\epsilon_{i,2}$ of the parameter $\xi_{i,2}$ is defined as $\epsilon_{i,2} = \xi_{i,2} - \dot{\alpha}_{i,1}$ and it is bounded with $\|\epsilon_{i,2}\| \leq \bar{\epsilon}_{i,2}$.

Applying Young's inequality again for the term $-z_{i,2}^T \dot{\alpha}_{i,1}$, we have

$$\begin{aligned} -z_{i,2}^T \xi_{i,2} &\leq \frac{1}{2}\|z_{i,2}\|^2\|\xi_{i,2}\|^2 + \frac{1}{2} \\ z_{i,2}^T \epsilon_{i,2} &\leq \frac{1}{2}\|z_{i,2}\|^2 + \frac{1}{2}\bar{\epsilon}_{i,2}^2 \end{aligned}$$

The virtual control law $\alpha_{i,2}$ and the adaptation law of the parameter $\theta_{i,2}$ are designed as

$$\begin{aligned}
\alpha_{i,2} &= \mathcal{N}(\zeta_{i,2}) v_{i,2} z_{i,2} \\
v_{i,2} &= \kappa_{i,2} + \frac{3}{2} + \frac{1}{2}\hat{\theta}_{i,2} \left\|\varphi_2(Z_{i,2})\right\|^2 + \frac{1}{2}\left\|\xi_{i,2}\right\|^2 \\
\dot{\zeta}_{i,2} &= v_{i,2} \left\|z_{i,2}\right\|^2 \\
\dot{\hat{\theta}}_{i,2} &= \frac{\lambda_{i,2}}{2} \left\|z_{i,2}\right\|^2 \left\|\varphi_{i,2}(Z_{i,2})\right\|^2 - \mu_{i,2}\hat{\theta}_{i,2}
\end{aligned}$$

Applying Lemma 5.1 and substituting the designed virtual control law $\alpha_{i,2}$ into the term $z_{i,2}^T g_{i,2}\alpha_{i,2}$, we obtain

$$z_{i,2}^T g_{i,2}\alpha_{i,2} = \gamma_2(t)\mathcal{N}(\zeta_{i,2})\dot{\zeta}_{i,2}$$

According to Young's inequality, one has

$$\begin{aligned}
\frac{\mu_{i,2}}{\lambda_{i,2}}\tilde{\theta}_{i,2}\hat{\theta}_{i,2} &= \frac{\mu_{i,2}}{\lambda_{i,2}}\left(\tilde{\theta}_{i,2}\theta_{i,2} - \tilde{\theta}_{i,2}^2\right) \\
&\leq \frac{\mu_{i,2}}{2\lambda_{i,2}}\theta_2^2 - \frac{\mu_{i,2}}{2\lambda_{i,2}}\tilde{\theta}_{i,2}^2
\end{aligned}$$

Then, (5.18) can be reformed as follows:

$$\begin{aligned}
\dot{V}_{i,2} \leq \dot{V}_{i,1} &- z_{i,2}^T g_{i,1}\psi_{i,1}z_{i,1} - \kappa_{i,2}\left\|z_{i,2}\right\|^2 + z_{i,2}^T g_{i,2}z_{i,3} \\
&+ \left[\gamma_2(t)\mathcal{N}(\zeta_{i,2}) + 1\right]\dot{\zeta}_{i,2} - \frac{\mu_{i,2}}{2\lambda_{i,2}}\tilde{\theta}_{i,2}^2 + C_{i,2}
\end{aligned}$$

where $C_{i,2} = 1 + \frac{\mu_{i,2}}{2\lambda_{i,2}}\theta_{i,2}^2 + \frac{1}{2}\bar{d}_{i,2}^2 + \frac{1}{2}\bar{\sigma}_{i,2}^2 + \frac{1}{2}\bar{\epsilon}_{i,2}^2$.

Step m $(3 \leq m \leq p-1)$: Introduce the error variable $z_{i,m} = x_{i,m} - \alpha_{i,m-1}$, then, its derivative is

$$\dot{z}_{i,m} = g_{i,m}x_{i,m+1} + f_{i,m} + d_{i,m}(t) - \dot{\alpha}_{i,m-1}$$

Consider the following Lyapunov function candidate

$$V_{i,m} = V_{i,m-1} + \frac{1}{2}z_{i,m}^T z_{i,m} + \frac{1}{2\lambda_{i,m}}\tilde{\theta}_{i,m}^2 \tag{5.20}$$

Taking the derivative of the Lyapunov function $V_{i,m}$, yields

$$\begin{aligned}
\dot{V}_{i,m} &= \dot{V}_{i,m-1} + z_{i,m}^T\dot{z}_{i,m} - \frac{1}{\lambda_{i,m}}\tilde{\theta}_{i,m}\dot{\hat{\theta}}_{i,m} \\
&= \dot{V}_{i,m-1} + z_{i,m}^T\left(g_{i,m-1}z_{i,m-1} + g_{i,m}x_{i,m+1} + f_{i,m}\right) \\
&\quad + z_{i,m}^T\left(d_{i,m}(t) - \dot{\alpha}_{i,m-1} - g_{i,m-1}z_{i,m-1}\right) - \frac{1}{\lambda_{i,m}}\tilde{\theta}_{i,m}\dot{\hat{\theta}}_{i,m}
\end{aligned} \tag{5.21}$$

Since $\Phi_{i,m}(Z_{i,m}) = g_{i,m-1}z_{i,m-1} + f_{i,m}$ is unknown for the closed-loop MAS, the RBFNN is used to approximate $\Phi_{i,m}(Z_{i,m})$. The unknown function is a smooth function of inputs $x_{i,1}, \cdots, x_{i,m}$, and $Z_{i,m} = [x_{i,1}^T, \cdots, x_{i,m}^T]^T \in \Omega \subset \mathbb{R}^{mnN}$. Thus, using the RBFNN to approximate the $\Phi_{i,m}(Z_{i,m})$, then (5.21) yields

$$\begin{aligned}\dot{V}_{i,m} = \dot{V}_{i,m-1} &+ z_{i,m}^T\left(g_{i,m}z_{i,m+1} + g_{i,m}\alpha_{i,m} + d_{i,m}(t)\right)\\ &+ z_{i,m}^T\left(W_{i,m}^T\varphi_{i,m}(Z_{i,m}) + \sigma_{i,m} - g_{i,m-1}z_{i,m-1}\right) - z_{i,m}^T\dot{\alpha}_{i,m-1} - \frac{1}{\lambda_{i,m}}\tilde{\theta}_{i,m}\dot{\hat{\theta}}_{i,m}\end{aligned}$$

By applying Young's inequality, we have

$$\begin{aligned}z_{i,m}^T d_{i,m}(t) &\le \frac{1}{2}\left\|z_{i,m}\right\|^2 + \frac{1}{2}\bar{d}_{i,m}^2\\ z_{i,m}^T W_{i,m}^T\varphi_{i,m}(Z_{i,m}) &\le \frac{1}{2}\left\|z_{i,m}\right\|^2\theta_{i,m}\left\|\varphi_{i,m}(Z_{i,m})\right\|^2 + \frac{1}{2}\\ z_{i,m}^T\sigma_{i,m} &\le \frac{1}{2}\left\|z_{i,m}\right\|^2 + \frac{1}{2}\bar{\sigma}_{i,m}^2\end{aligned}$$

In this step, applying the SMC filter again to avoid repeating the derivative of the virtual control law α_{m-1}, we obtain

$$\begin{aligned}\dot{\xi}_{i,m-1} &= -\frac{\xi_{i,m-1} - \alpha_{i,m-1}}{\rho_{i,m-1}} - \frac{k_{i,m-1}\left(\xi_{i,m-1} - \alpha_{i,m-1}\right)}{\left\|\xi_{i,m-1} - \alpha_{i,m-1}\right\| + \beta_{i,m-1}}\\ \dot{\xi}_{i,m} &= -\frac{\xi_{i,m} - \dot{\xi}_{i,m-1}}{\rho_{i,m}} - k_{i,m}\frac{\xi_{i,m} - \dot{\xi}_{i,m-1}}{\left\|\xi_{i,m} - \dot{\xi}_{i,m-1}\right\| + \beta_{i,m}}\end{aligned}$$

where $\dot{\alpha}_{i,m-1} = \xi_{i,m} - \epsilon_{i,m}$.

By applying Young's inequality again to the term $-z_{i,m}^T\dot{\alpha}_{i,m-1}$, we have

$$\begin{aligned}-z_{i,m}^T\xi_{i,m} &\le \frac{1}{2}\left\|z_{i,m}\right\|^2\left\|\xi_{i,m}\right\|^2 + \frac{1}{2}\\ z_{i,m}^T\epsilon_{i,m} &\le \frac{1}{2}\left\|z_{i,m}\right\|^2 + \frac{1}{2}\bar{\epsilon}_{i,m}^2\end{aligned}$$

The virtual control law $\alpha_{i,m}$ and the adaptation law of the parameter $\theta_{i,m}$ are designed as

$$\begin{aligned}\alpha_{i,m} &= \mathcal{N}(\zeta_{i,m})v_{i,m}z_{i,m}\\ v_{i,m} &= \kappa_{i,m} + \frac{3}{2} + \frac{1}{2}\hat{\theta}_{i,m}\left\|\varphi_{i,m}(Z_{i,m})\right\|^2 + \frac{1}{2}\left\|\xi_{i,m}\right\|^2\\ \dot{\zeta}_{i,m} &= v_{i,m}\left\|z_{i,m}\right\|^2\\ \dot{\hat{\theta}}_{i,m} &= \frac{\lambda_{i,m}}{2}\left\|z_{i,m}\right\|^2\left\|\varphi_{i,m}(Z_{i,m})\right\|^2 - \mu_{i,m}\hat{\theta}_{i,m}\end{aligned}$$

By applying Lemma 5.1 and substituting the designed virtual control law $\alpha_{i,m}$ into the term $z_{i,m}^T g_{i,m}\alpha_{i,m}$, we obtain

$$z_{i,m}^T g_{i,m}\alpha_{i,m} = \gamma_{i,m}(t)\mathcal{N}(\zeta_{i,m})\dot{\zeta}_{i,m}$$

According to Young's inequality, one has

$$\begin{aligned}\frac{\mu_{i,m}}{\lambda_{i,m}}\tilde{\theta}_{i,m}\hat{\theta}_{i,m} &= \frac{\mu_{i,m}}{\lambda_{i,m}}\left(\tilde{\theta}_{i,m}\theta_{i,m} - \tilde{\theta}_{i,m}^2\right)\\ &\leq \frac{\mu_{i,m}}{2\lambda_{i,m}}\theta_{i,m}^2 - \frac{\mu_{i,m}}{2\lambda_{i,m}}\tilde{\theta}_{i,m}^2\end{aligned}$$

Then, (5.22) can be organised as follows:

$$\begin{aligned}\dot{V}_{i,m} \leq \dot{V}_{i,m-1} &- z_{i,m}^T g_{i,m-1} z_{i,m-1} - \kappa_{i,m}\left\|z_{i,m}\right\|^2\\ &+ z_{i,m}^T g_{i,m} z_{i,m+1} + \left[\gamma_m(t)\mathcal{N}(\zeta_{i,m}) + 1\right]\dot{\zeta}_{i,m} - \frac{\mu_{i,m}}{2\lambda_{i,m}}\tilde{\theta}_{i,m}^2 + C_{i,m}\end{aligned}$$

where $C_{i,m} = 1 + \frac{\mu_{i,m}}{2\lambda_{i,m}}\theta_{i,m}^2 + \frac{1}{2}\bar{d}_{i,m}^2 + \frac{1}{2}\bar{\sigma}_{i,m}^2 + \frac{1}{2}\bar{\epsilon}_{i,m}^2$.

Step p: Introduce the error variable $z_{i,p} = x_{i,p} - \alpha_{i,p-1}$, then, its derivative is

$$\begin{aligned}\dot{z}_{i,p} &= \dot{x}_{i,p} - \dot{\alpha}_{i,p-1}\\ &= g_{i,p}u + f_{i,p} + d_{i,p}(t) - \dot{\alpha}_{i,p-1}\end{aligned}$$

Consider the following Lyapunov function candidate

$$V_{i,p} = V_{i,p-1} + \frac{1}{2}z_{i,p}^T z_{i,p} + \frac{1}{2\lambda_{i,p}}\tilde{\theta}_{i,p}^2 \tag{5.22}$$

Taking the derivative of the Lyapunov function $V_{i,m}$, yields

$$\begin{aligned}\dot{V}_{i,p} = \dot{V}_{i,p-1} &+ z_{i,p}^T\left(g_{i,p-1}z_{i,p-1} + g_{i,p}u + f_{i,p}\right)\\ &+ z_{i,p}^T\left(d_{i,p}(t) - \dot{\alpha}_{i,p-1} - g_{i,p-1}z_{i,p-1}\right) - \frac{1}{\lambda_{i,p}}\tilde{\theta}_{i,p}\dot{\hat{\theta}}_{i,p}\end{aligned} \tag{5.23}$$

Since $\Phi_{i,p}(Z_{i,p}) = g_{i,p-1}z_{i,p-1} + f_{i,p}$ is unknown for the closed-loop MAS, the RBFNN is used to approximate $\Phi_{i,p}(Z_{i,p})$. The unknown function is a smooth function of inputs $x_{i,1}, \cdots, x_p$, and $Z_{i,p} = [x_{i,1}^T, \cdots, x_{i,p}^T]^T \in \Omega \subset \mathbb{R}^{pnN}$. Thus, applying the RBFNN to approximate the $\Phi_{i,p}\left(Z_{i,p}\right)$, then (5.23) yields

$$\begin{aligned}\dot{V}_{i,p} = \dot{V}_{i,p-1} &- z_{i,p}^T g_{i,p-1} z_{i,p-1} + z_{i,p}^T g_{i,p} u_i\\ &+ z_{i,p}^T\left(W_{i,p}^T\varphi_{i,p}(Z_{i,p}) + \sigma_{i,p} + d_{i,p}(t)\right) - z_{i,p}^T\dot{\alpha}_{i,p-1} - \frac{1}{\lambda_{i,p}}\tilde{\theta}_{i,p}\dot{\hat{\theta}}_{i,p}\end{aligned}$$

By applying Young's inequality, we have

$$z_{i,p}^T d_{i,p}(t) \leq \frac{1}{2}\left\|z_{i,p}\right\|^2 + \frac{1}{2}\bar{d}_{i,p}^2$$
$$z_{i,p}^T W_{i,p}^T \varphi_{i,p}(Z_{i,p}) \leq \frac{1}{2}\left\|z_{i,p}\right\|^2 \theta_{i,p}\left\|\varphi_{i,p}(Z_{i,p})\right\|^2 + \frac{1}{2}$$
$$z_{i,p}^T \sigma_{i,p} \leq \frac{1}{2}\left\|z_{i,p}\right\|^2 + \frac{1}{2}\bar{\sigma}_{i,p}^2$$

At the final step, term $\dot{\alpha}_{i,m-1}$ can be estimated as

$$\dot{\xi}_{i,p-1} = -\frac{\xi_{i,p-1} - \alpha_{i,p-1}}{\rho_{i,p-1}} - \frac{k_{i,p-1}\left(\xi_{i,p-1} - \alpha_{i,p-1}\right)}{\left\|\xi_{i,p-1} - \alpha_{i,p-1}\right\| + \beta_{i,p-1}}$$
$$\dot{\xi}_{i,p} = -\frac{\xi_{i,p} - \dot{\xi}_{i,p-1}}{\rho_{i,p}} - k_{i,p}\frac{\xi_{i,p} - \dot{\xi}_{i,p-1}}{\left\|\xi_{i,p} - \dot{\xi}_{i,p-1}\right\| + \beta_{i,p}}$$

where $\dot{\alpha}_{i,p-1} = \xi_{i,p} - \epsilon_{i,p}$.

Applying Young's inequality again for the term $-z_{i,p}^T \dot{\alpha}_{i,p-1}$, we have

$$-z_{i,p}^T \xi_{i,p} \leq \frac{1}{2}\left\|z_{i,p}\right\|^2\left\|\xi_{i,p}\right\|^2 + \frac{1}{2}$$
$$z_{i,p}^T \epsilon_{i,p} \leq \frac{1}{2}\left\|z_{i,p}\right\|^2 + \frac{1}{2}\bar{\epsilon}_{i,p}^2$$

Since the control gain matrix $g_{i,p}(\bar{x}_{i,p}) \in \mathbb{R}^{n\times l}$ with $l \geq n$ is given, we consider two cases for actual controller design at the final step.

Adaptive Control for Square Systems ($l = n$)

First we consider the case that $g_{i,p}(\bar{x}_{i,p}) \in \mathbb{R}^{n\times n}$ is a square matrix and the following assumption is needed.

Assumption 5.6. *The unknown control gain matrix $g_{i,p}(\bar{x}_{i,p}) \in \mathbb{R}^{n\times n}$ is a square matrix yet unnecessarily symmetric, and its sign is unknown.*

Thus, the actual control law u_i and the adaptation law of the parameter $\theta_{i,p}$ are designed as

$$\begin{aligned} u_i &= \mathcal{N}(\zeta_{i,p}) v_{i,p} z_{i,p} \\ v_{i,p} &= \kappa_{i,p} + \frac{3}{2} + \frac{1}{2}\hat{\theta}_{i,p}\left\|\varphi_{i,p}(Z_{i,p})\right\|^2 + \frac{1}{2}\left\|\xi_{i,p}\right\|^2 \\ \dot{\zeta}_{i,p} &= v_{i,p}\left\|z_{i,p}\right\|^2 \\ \dot{\hat{\theta}}_{i,p} &= \frac{\lambda_{i,p}}{2}\left\|z_{i,p}\right\|^2\left\|\varphi_{i,p}(Z_p)\right\|^2 - \mu_{i,p}\hat{\theta}_{i,p} \end{aligned} \tag{5.24}$$

Moreover, according to Lemma 5.1 and Assumption 5.6, then, substituting the designed control law u_i into the term $z_{i,p}^T g_{i,p} u_i$, we obtain

$$z_{i,p}^T g_{i,p} u_i = \gamma_{p,1}(t)\mathcal{N}(\zeta_{i,p})\dot{\zeta}_{i,p}$$

According to Young's inequality, we have

$$\begin{aligned}\frac{\mu_{i,p}}{\lambda_{i,p}}\tilde{\theta}_{i,p}\hat{\theta}_{i,p} &= \frac{\mu_{i,p}}{\lambda_{i,p}}\left(\tilde{\theta}_{i,p}\theta_{i,p} - \tilde{\theta}_{i,p}^2\right) \\ &\leq \frac{\mu_{i,p}}{2\lambda_{i,p}}\theta_{i,p}^2 - \frac{\mu_{i,p}}{2\lambda_{i,p}}\tilde{\theta}_{i,p}^2\end{aligned}$$

Then, (5.22) can be rearranged as follows:

$$\begin{aligned}\dot{V}_{i,p} \leq \dot{V}_{i,p-1} - z_{i,p}^T g_{i,p-1} z_{i,p-1} - \kappa_{i,p}\left\|z_{i,p}\right\|^2 \\ + \left[\gamma_{p,1}(t)\mathcal{N}(\zeta_{i,p}) + 1\right]\dot{\zeta}_{i,p} - \frac{\mu_{i,p}}{2\lambda_{i,p}}\tilde{\theta}_{i,p}^2 + C_{i,p}\end{aligned}$$

where $C_{i,p} = 1 + \frac{\mu_{i,p}}{2\lambda_{i,p}}\theta_{i,p}^2 + \frac{1}{2}\bar{d}_{i,p}^2 + \frac{1}{2}\bar{\sigma}_{i,p}^2 + \frac{1}{2}\bar{\epsilon}_{i,p}^2$.

For the stability analysis, we choose the overall Lyapunov function V as

$$V = \sum_{i=1}^{N}\left(V_{i,p-1} + \frac{1}{2}z_{i,p}^T z_{i,p} + \frac{1}{2\lambda_{i,p}}\tilde{\theta}_{i,p}^2\right) \tag{5.25}$$

Differentiating (5.25) and substituting (5.10), (5.16) (5.20) and (5.22) into it, we have

$$\begin{aligned}\dot{V} \leq \sum_{i=1}^{N}\Bigg[-\sum_{k=1}^{p}\left(\kappa_{i,k}\left\|z_{i,k}\right\|^2 + \frac{\mu_{i,k}}{2\lambda_{i,k}}\tilde{\theta}_{i,k}^2\right) + \sum_{k=1}^{p}\left(\gamma_{p,1}(t)\mathcal{N}(\zeta_{i,p}) + 1\right)\dot{\zeta}_{i,p} \\ + \frac{1}{2}\sum_{k=1}^{p}\left(\bar{\sigma}_{i,k}^2 + \bar{d}_{i,k}^2 + \frac{\mu_{i,k}}{\lambda_{i,k}}\theta_{i,k}^2\right) + \frac{1}{2}\sum_{k=2}^{p}\left(\bar{\epsilon}_{i,k}^2 + \bar{\xi}_{i,k}^2\right) + p - \frac{1}{2}\Bigg] \\ \leq \sum_{i=1}^{N}\left[-\varrho_{i,1}V_{i,p} + \sum_{k=1}^{p}\left(\gamma_{p,1}(t)\mathcal{N}(\zeta_{i,p}) + 1\right)\dot{\zeta}_{i,p}\right] + C\end{aligned} \tag{5.26}$$

where $\varrho_{i,1} = \min\left(2\kappa_{i,1}, \ldots, 2\kappa_{i,p}, \mu_{i,1}, \ldots, \mu_{i,p}\right)$ and $C = \sum_{i=1}^{N}\left[\frac{1}{2}\sum_{k=1}^{p}\left(\bar{\sigma}_{i,k}^2 + \bar{d}_{i,k}^2 + \frac{b_{i,k}}{\lambda_{i,k}}\theta_{i,k}^2\right) + \frac{1}{2}\sum_{k=2}^{p}\left(\bar{\epsilon}_{i,k}^2 + \bar{\xi}_{i,k}^2\right) + p - \frac{1}{2}\right]$.

Adaptive Control for Nonsquare Systems ($l > n$)

After completing the square case, we now consider the case that $g_{i,p}(\bar{x}_{i,p}) \in \mathbb{R}^{n\times l}$ is a nonsquare matrix and the following assumption is needed.

Assumption 5.7. *(Song* et al. *2017) The unknown control gain matrix $g_{i,p}(\bar{x}_{i,p}) \in \mathbb{R}^{n\times l}$ is a partially unknown nonsquare matrix and can be decomposed as*

$$g_{i,p}(\cdot) = g_{i,p1}(\cdot)g_{i,p2}(\cdot) \tag{5.27}$$

where $g_{i,p1}(\cdot) \in \mathbb{R}^{n\times l}$ is a known matrix with full row rank and $g_{i,p2}(\cdot) \in \mathbb{R}^{l\times l}$ is an unknown and unnecessarily symmetric matrix.

Then, the actual control law u_i and the adaptation law of the parameter $\theta_{i,p}$ are designed as

$$\begin{aligned} u_i &= \mathcal{N}(\zeta_{i,p})\frac{g_{i,p1}^T}{\left\|g_{i,p1}\right\|}v_{i,p}z_{i,p} \\ v_{i,p} &= K_{i,p} + \frac{3}{2} + \frac{1}{2}\hat{\theta}_{i,p}\left\|\varphi_{i,p}(Z_{i,p})\right\|^2 + \frac{1}{2}\left\|\xi_{i,p}\right\|^2 \\ \dot{\zeta}_{i,p} &= v_{i,p}\left\|z_{i,p}\right\|^2 \\ \dot{\hat{\theta}}_{i,p} &= \frac{\lambda_{i,p}}{2}\left\|z_{i,p}\right\|^2\left\|\varphi_{i,p}(Z_p)\right\|^2 - \mu_{i,p}\hat{\theta}_{i,p} \end{aligned} \tag{5.28}$$

According to Lemma 5.1 and Assumption 5.7, then, decomposing matrix $g_{i,p2}(\cdot)$ into a symmetric matrix and a skew symmetric matrix, we have

$$\frac{z_{i,p}^T g_{i,p1}\left(g_{i,p2}^T + g_{i,p2}\right)g_{i,p1}^T z_{i,p}}{2\left\|g_{i,p1}\right\|} = \gamma_{p,2}(t)\left\|z_{i,p}\right\|^2 \tag{5.29}$$

Substituting the designed control law u_i into the term $z_{i,p}^T g_{i,p}u_i$ and considering (5.29), we derive

$$z_{i,p}^T g_{i,p}u_i = \gamma_{p,2}(t)\mathcal{N}(\zeta_{i,p})\dot{\zeta}_{i,p}$$

Similarly, the derivative of the total Lyapunov function yields

$$\dot{V}_{i,p} \le -\varrho_{i,2}V_{i,p} + \sum_{k=1}^{p}\left(\gamma_{p,2}(t)\mathcal{N}(\zeta_{i,p}) + 1\right)\dot{\zeta}_{i,p} + C_i \tag{5.30}$$

where $\varrho_{i,2} = \min\left(2\kappa_{i,1},\ldots,2\kappa_{i,p-1},2K_{i,p},\mu_{i,1},\ldots,\mu_{i,p}\right)$ and $C_i = \frac{1}{2}\sum_{k=1}^{p}\left(\bar{\sigma}_{i,k}^2 + \bar{d}_{i,k}^2 + \frac{b_{i,k}}{\lambda_{i,k}}\theta_{i,k}^2\right) + \frac{1}{2}\sum_{k=2}^{p}\left(\bar{\epsilon}_{i,k}^2 + \bar{\xi}_{i,k}^2\right) + p - \frac{1}{2}$. Based on the systemic adaptive neural network backstepping control design method, the main results is presented in the following theorems.

5.3.3 Stability Analysis

In this section, the boundedness of all the signals and the leader-follower consensus tracking performance are analysed in the following two theorems for case 1 and case 2, respectively.

Theorem 5.1. *Consider system* (5.1) *satisfying Assumptions 5.1-5.6 with output constraints* (5.2) *for any initial conditions* $x_{i,1k}(0) \in \mathcal{C}_{x_{i,1k}}$. *Then, all the signals in closed-loop system* (5.1) *with the controller and adaptive law* (5.24) *are bounded, and the consensus tracking errors are guaranteed to move toward to an arbitrarily small neighborhood of zero. Moreover, the output constraints property* (5.2) *will remain.*

Proof. Multiplying both sides of inequality (5.26) by $e^{\varrho t}$, then, integrating it over $[0, t]$, it yields

$$V(t) \leq \left(V(0) - \frac{C}{\varrho}\right) e^{-\varrho t} + \frac{C}{\varrho} + e^{-\varrho t} \int_0^t \sum_{i=1}^{N} \sum_{k=1}^{p} \left[\left(\gamma_{p,1}(s)\mathcal{N}(\zeta_{i,p}) + 1\right) \dot{\zeta}_{i,p}\right] e^{\varrho s} ds$$

where $\varrho = \min(\varrho_{i,1}) > 0$ with $i = 1, \ldots, N$.

Then, applying Lemma 5.2, the boundedness of $B = e^{-\varrho t} \int_0^t \sum_{i=1}^{N} \sum_{k=1}^{p} \left[\left(\gamma_{p,1}(s)\mathcal{N}(\zeta_{i,p}) + 1\right) \dot{\zeta}_{i,p}\right] e^{\varrho s} ds$, $V(t)$ and $\zeta_{i,p}(t)$ can be confirmed. Let $\bar{B}$ be the upper bound of B in $[0, \infty)$, then, we derive the following inequality

$$\frac{1}{2} \|z_1\|^2 \leq V(t) \leq e^{-\varrho t} V(0) + \frac{C}{\varrho} + \bar{B}$$

Thus, it yields

$$\|z_1\| \leq \left(2\left(e^{-\varrho t} V(0) + \frac{C}{\varrho} + \bar{B}\right)\right)^{\frac{1}{2}} \tag{5.31}$$

We have the actual consensus tracking error that is defined as $e_{i,1} = \sum_{j=1}^{N} a_{ij}(x_{i,1} - x_{j,1}) + b_i(x_{i,1} - y_r)$. From Remark 5.2, we get $e_1 = [(\mathcal{L} + \mathcal{B}) \otimes I_n](x_1 - I_N \otimes y_r)$. Since $z_1 = [(\mathcal{L} + \mathcal{B}) \otimes I_n](\chi_1 - I_N \otimes \eta_r)$ is derived from (5.6), we can rewritten $z_1 = \tau e_1$ with $\tau = \text{diag}[\tau_1, \tau_2, \cdots, \tau_k] \in \mathbb{R}^{n \times n}$, where

$$\tau_k = \frac{k_{a_{i,1k}}^2(t) - \bar{k}_{a_{i,1k}}}{2\left(k_{a_{i,1k}}(t) + x_{i,1k}\right)\left(k_{a_{i,1k}}(t) + y_{rk}\right)} + \frac{k_{b_{i,1k}}^2(t) - \bar{k}_{b_{i,1k}}}{2\left(k_{b_{i,1k}}(t) - x_{i,1k}\right)\left(k_{a_{i,1k}}(t) - y_{rk}\right)}$$

From the definitions of e_1 and z_1, we have $\|e_1\| \leq \|z_1\| / \|\tau\|$. Then, as time increases, all consensus tracking error $\|e_1\|$ converges to a compact set $\Phi = \{e_1 | \|e_1\| \leq$

$\left(2\left(e^{-\varrho t}V(0)+\frac{C}{\varrho}+\bar{B}\right)\right)^{\frac{1}{2}}/\|\tau\|\}$. According to the above analysis and $V_{i,p}$, the boundedness of $z_{i,p}$ and $\theta_{i,p}$ is ensured, then, it follows that $\hat{\theta}_{i,p}\in L_\infty$. According to the output constraints function (5.3) and the leader-follower consensus tracking error $z_{i,1}$ in (5.6), the constrained output $\chi_{i,1}$ is bounded. Therefore, the output $x_{i,1}$ is not off the predefined limit if its initial condition is within the open set $\mathcal{C}_{x_{i,1k}}$, and all the followers can track the reference leader within an arbitrarily small region Φ. Then, the boundedness of all the virtual controller $\alpha_{i,k}$ with $k=1,\cdots,p$ is guaranteed. Accordingly, the actual controller u_i is bounded. Consequently, all the signals in the closed-loop MAS are semi-globally ultimately uniformly bounded. This completes the proof. □

Theorem 5.2. *Consider system* (5.1) *satisfying Assumptions 5.1-5.5 and 5.7 with output constraints* (5.2) *for any initial conditions* $x_{i,1k}(0)\in\mathcal{C}_{x_{i,1k}}$. *Then, all the signals in closed-loop system* (5.1) *with the controller and adaptive law* (5.28) *are bounded, and the consensus tracking errors are guaranteed to move toward to an arbitrarily small neighborhood of zero. Moreover, the output constraints property* (5.2) *will remain.*

Proof. As the proof is similar to the one in Theorem 1, it is omitted. □

Remark 5.7. *Both square and nonsqaure cases of the control gain matrix are analysed with different assumptions that have less restrictive compared to the assumptions (Sachan and Padhi 2019). Furthermore, compared with (Ni and Shi 2021a) and (Wang* et al. *2020a), a new type of time-varying asymmetric output constraint function for leader-follower consensus of MIMO nonlinear MAS is applied in this chapter. A leaderless consensus controller was constructed with natural logarithm function-based state transformation method (Wang* et al. *2020a) to solve symmetric constant case of output constraints. The same method was used (Ni and Shi 2021a), the consensus tracking error was required to be restricted in a constant output constraint, which can reduce the selection range of initial value for each agent.*

5.4 Simulation Results

In this section, two cases of nonlinear MAS representing different conditions on control gain are presented to verify the effectiveness of the designed leader-follower consensus control scheme for system (5.1). The communication topology among agents is modelled by a directed graph displayed in Fig. 5.4.

Case 1: Square MIMO nonlinear MAS

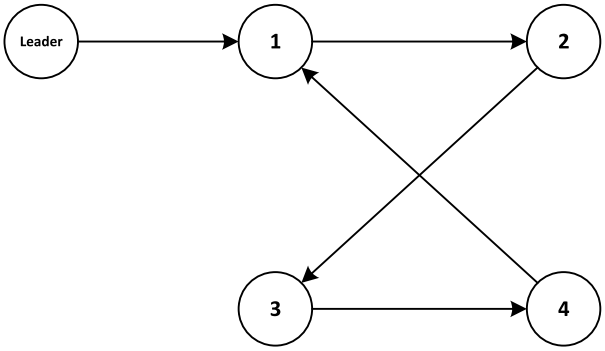

Figure 5.4. Communication topology of the MAS with a leader.

We consider the following nonlinear MAS:

$$\begin{aligned}\dot{x}_{i,1} &= x_{i,2}\\ \dot{x}_{i,2} &= g_{i,1}(x_{i,1}, x_{i,2})u_i + f_{i,1}(x_{i,1}, x_{i,2}) + d_{i,1}(t)\\ y_i &= x_{i,1}, \quad i = 1, \ldots, 4\end{aligned}$$

where $x_{i,1} = [x_{i,11}, x_{i,12}]^T$ and $x_{i,2} = [x_{i,21}, x_{i,22}]^T$ are the system states, u_i is the control input, $g_{i,1}$ is a diagonal matrix representing the control coefficient matrix $g_{i,1} = \text{diag}[1 + x_{i,11}^2, 1 + x_{i,12}^2]$, $f_{i,1} = [x_{i,11}x_{i,21} + x_{i,21}^2, x_{i,21}x_{i,22}]^T$ and the external disturbance $d_{i,1}(t)$ is given as $d_{i,1}(t) = [0.2\cos 0.4t, 0.1\sin 0.3t\,]$.

Each agent has the identical output constraint that is given as

$$x_{i,1k} \in \mathcal{C}_{x_{i,1k}} := \{-k_{a_{i,1k}}(t) < x_{i,1k} < k_{b_{i,1k}}(t)\}. \tag{5.32}$$

where $k_{a_{i,1k}}(t) = [0.2\sin(0.2t) + 0.7,\ -0.2\sin(0.3t) + 0.4]^T$ and $k_{b_{i,1k}}(t) = [0.2\cos(0.2t) + 1,\ 0.2\cos(0.2t) + 0.8]^T$ with $i = 1, \ldots, 4$, and $n = 1, 2$.

In this numerical simulation, the trajectory of a leader is given as $y_{rn} = [0.3 + 0.2\sin(0.2t),\ 0.2 + 0.2\sin(0.4t)]^T$, the parameters $\bar{k}_{a_{i,1k}}$ and $\bar{k}_{a_{i,1k}}$ in (5.3) are $\bar{k}_{a_{i,1k}} = [-0.2,\ -0.2]^T$ and $\bar{k}_{a_{i,1k}} = [-0.2,\ -0.2]^T$, the initial conditions of system states $x_{i,1}$ and $x_{i,2}$ are randomly selected from the range $(-0.2,\ 0.6)$ which lies in the output constraints (5.32) and the initial condition of parameter ζ_i is chosen as $\zeta_i(0) = 3.1\pi$, and the Nussbaum function is $\zeta_i^2 \sin \zeta_i$. Moreover, the system design parameters are chosen as $\kappa_{i,1} = \kappa_{i,2} = 6$, $\lambda_{i,1} = \lambda_{i,2} = 1$ and $\mu_{i,1} = \mu_{i,2} = 0.1$, the parameters of SMC filter (5.19) are selected as $\rho_{i,1} = \rho_{i,2} = 1$, $k_{i,1} = 20$, $k_{i,2} = 30$, $\beta_{i,1} = 1$ and $\beta_{i,2} = 10$, the RBFNN $W_i^T\varphi(Z_i)$ contains $r = 61$ neuron nodes that evenly distributed in $[-3,\ 3]$ with width $w_i = 0.1$ and its activation function is selected as Gaussian function.

This simulation results are displayed in Figs. 5.5-5.9 which show all agents can follow the trajectories of a leader, and each entry of the output $x_{i,1}$ is restricted within the time-varying output constraints all the time. Therefore, the proposed leader-follower consensus controller is effective to address the output constraints and UCD.

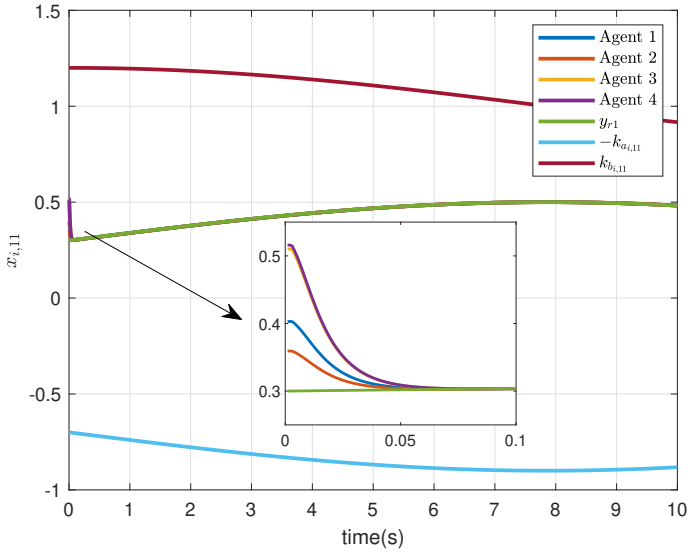

Figure 5.5. Constrained states $x_{i,11}$ of each agent under controller u_i.

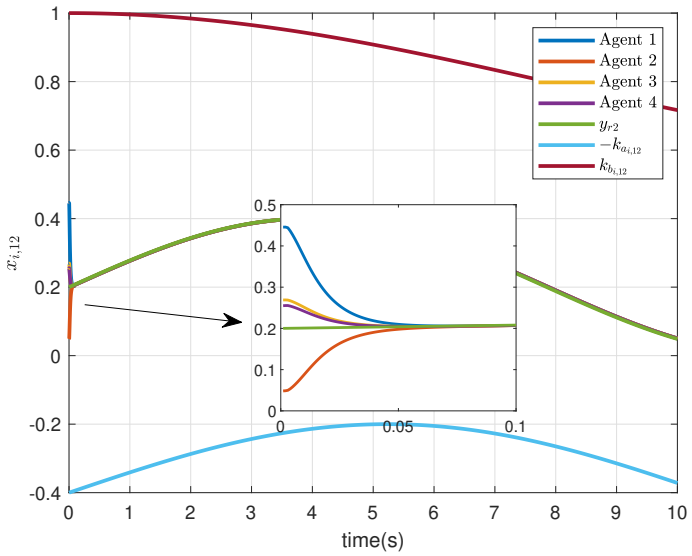

Figure 5.6. Constrained states $x_{i,12}$ of each agent under controller u_i.

Case 2: Nonsquare MIMO nonlinear MAS

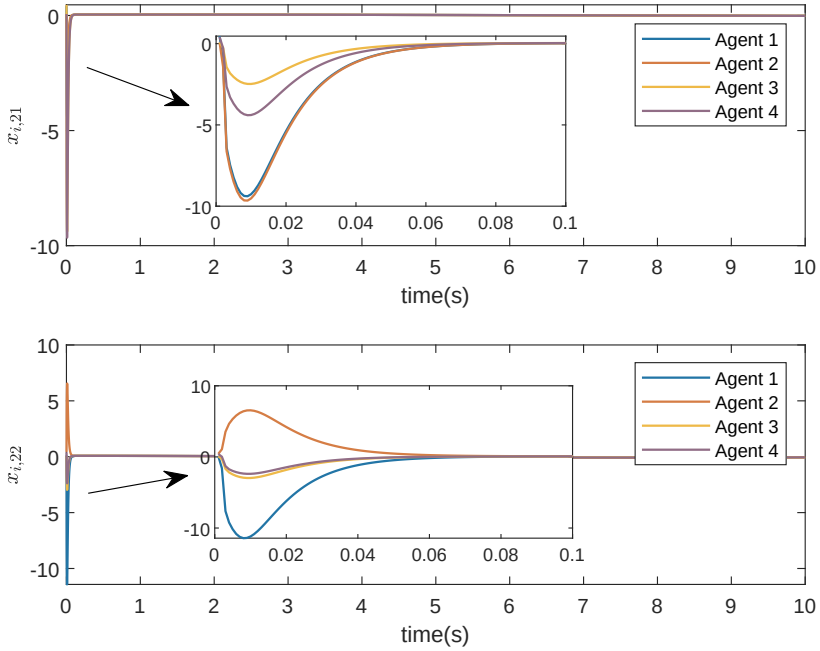

Figure 5.7. Profiles of state $x_{i,2}$ under controller u_i.

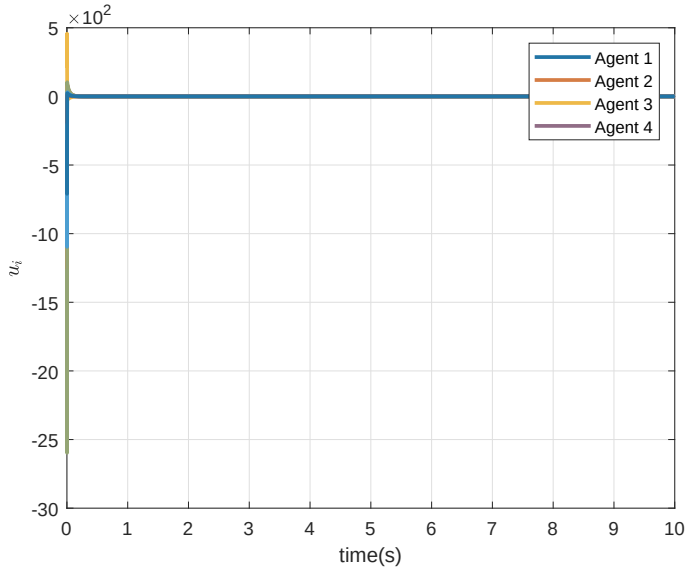

Figure 5.8. Control input u_i.

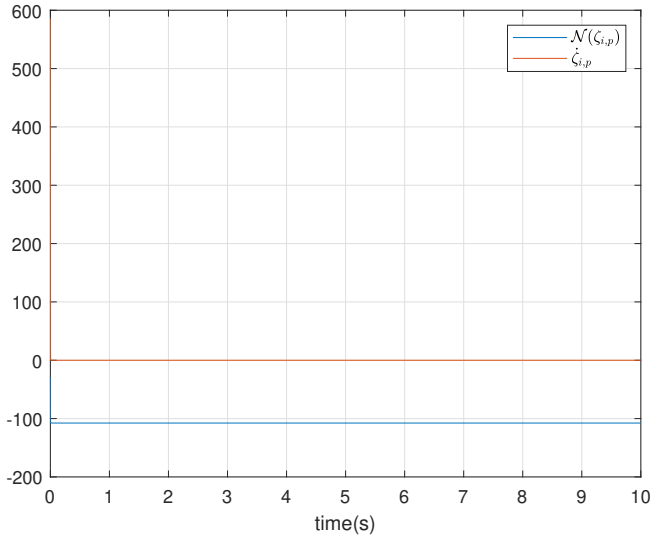

Figure 5.9. Adaptive parameter $\zeta_{i,p}$ and gain $\mathcal{N}(\zeta_{i,p})$.

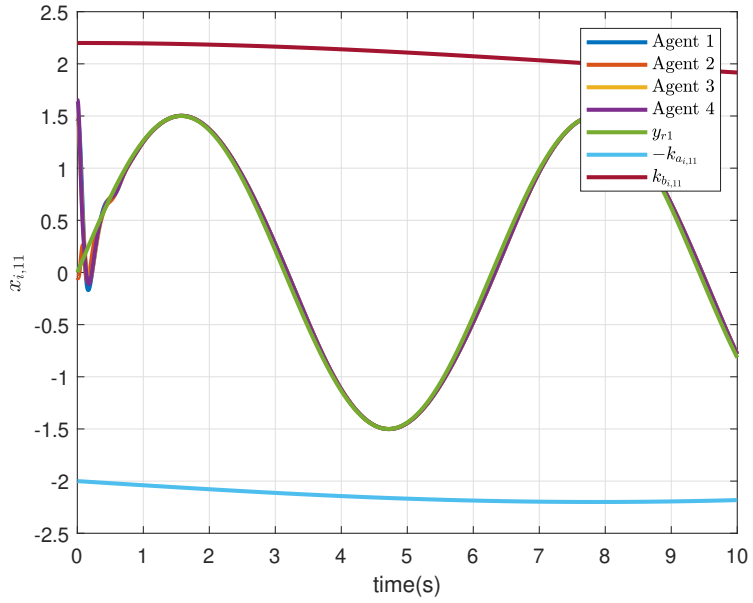

Figure 5.10. Constrained states $x_{i,11}$ of each agent under controller u_i.

We consider a nonsquare MIMO nonlinear MAS as follows.

$$\begin{aligned}
\dot{x}_{i,1} &= x_{i,2} \\
\dot{x}_{i,2} &= g_{i,1}(x_{i,1}, x_{i,2})u_i + f_{i,1}(x_{i,1}, x_{i,2}) + d_{i,1}(t) \\
y_i &= x_{i,1}, \quad i = 1, \ldots, 4
\end{aligned}$$

where $x_{i,1} = [x_{i,11},\ x_{i,12}]^T$ and $x_{i,2} = [x_{i,21},\ x_{i,22}]^T$ are the system states, $u_i \in \mathbb{R}^3$ is the control input, $g_{i,1} = [2 + 0.2\sin t,\ 1,\ 0; 0,\ 2 + 0.2\sin t,\ 1] \in \mathbb{R}^{2\times 3}$ represents the control

coefficient matrix, $f_{i,1} = [0.2x_{i,11}^2 + 0.2x_{i,12} + \sin x_{i,21},\ (\exp(x_{i,22}) - 1)/(\exp(x_{i,22}) + 1) + \cos x_{i,11}]^T$ and the external disturbance $d_{i,1}(t)$ is given as $d_{i,1}(t) = [1.2\cos t,\ \sin t]$.

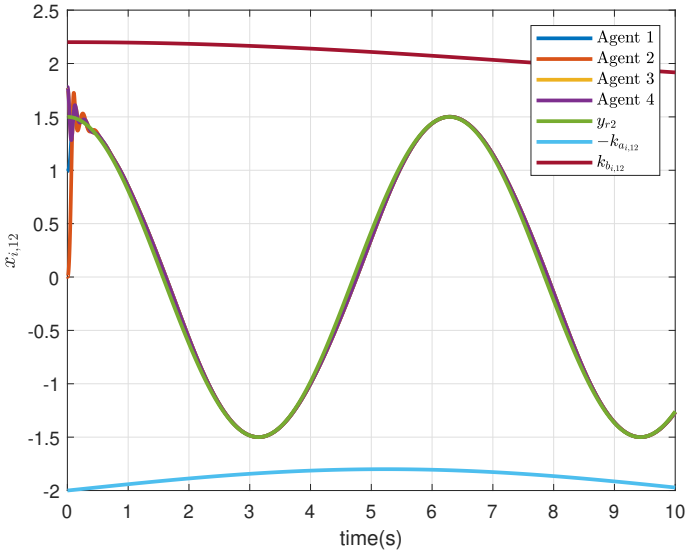

Figure 5.11. Constrained states $x_{i,12}$ of each agent under controller u_i.

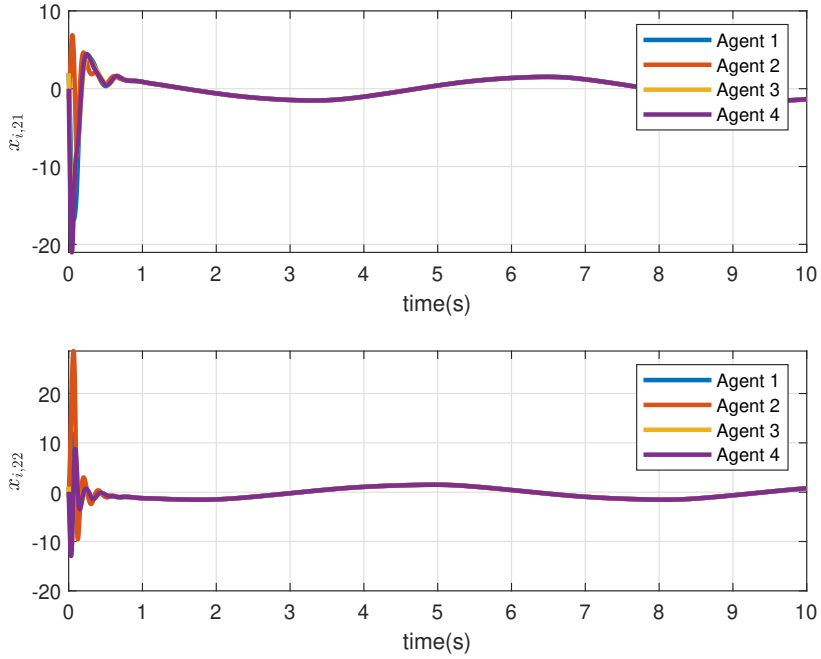

Figure 5.12. Profiles of state $x_{i,2}$ under controller u_i.

In this simulation, the reference signal y_{rn} is given as $y_{rn} = [1.5\sin(t),\ 1.5\sin(t)]^T$, the time-varying output constraint functions of each agent are defined as $k_{a_{i,1k}}(t) = [0.2\sin(0.2t) + 2,\ -0.2\sin(0.3t) + 2]^T$ and $k_{b_{i,1k}}(t) = [0.2\sin(0.t) + 2,\ 0.2\sin(0.2t) + 2]^T$ and the parameters $\bar{k}_{a_{i,1k}}$ and $\bar{k}_{a_{i,1k}}$ in (5.3) are selected as $\bar{k}_{a_{i,1k}} = \bar{k}_{a_{i,1k}} = [-0.2,\ -0.2]^T$.

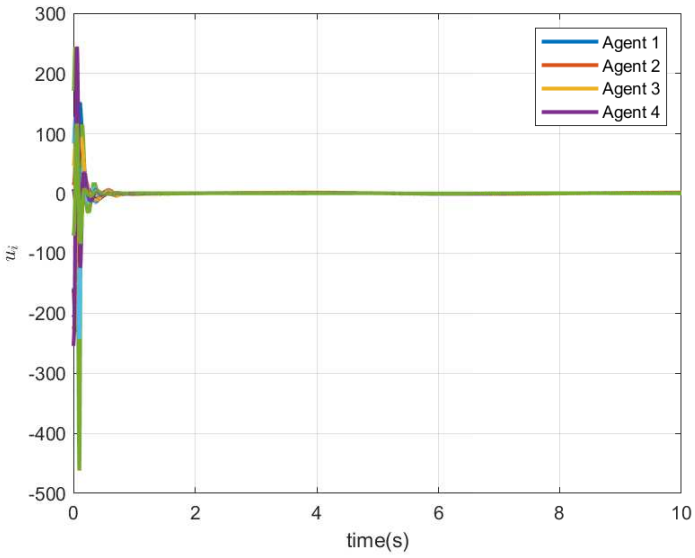

Figure 5.13. Control input u_i.

The initial conditions of each helicopter states $x_{i,1}$ and $x_{i,2}$ are randomly selected from the range $(-1.6, 2)$ which also lies in the output constraints (5.32), the system parameters are designed as $\kappa_{i,1} = 10$, $\kappa_{i,2} = 8$, $\lambda_{i,1} = \lambda_{i,2} = 1$ and $\mu_{i,1} = \mu_{i,2} = 0.1$. The RBFNN $W_i^T \varphi(Z_i)$ contains $r = 121$ neuron nodes that evenly distributed in $[-6, 6]$ with width $w_i = 0.1$. Figs. 5.10 - 5.12 show the leader-follower consensus tracking performance is achieved. From Fig. 5.10 and 5.11, each agent follows the trajectories of the leader without violating the time-varying output constraints. Hence, the proposed controller (5.24) is capable of driving all agents to achieve the leader-follower consensus under UCD without violating the time-varying output constraints.

5.5 Chapter Summary

In this chapter, the adaptive leader-follower consensus control problem with time-varying output constraints and UCD has been investigated for MIMO nonlinear MAS. Both square and nonsquare nonlinear MAS are consider for the UCD problem with less restrictive condition on control gain. Furthermore, the asymmetric time-varying output constraints have been considered and the limitations on the boundaries of the constraints have been removed by using a new state transformation technique. The proposed systematic leader-follower consensus control method has been developed for a class of strict-feedback nonlinear MAS. Two different cases modelling control gain of nonlinear MAS have been simulated to test the designed controller. Further

work will be conducted for general MAS with full-state constraints so that each state of an agent can be constrained in a specific range for some safety requirements.

Chapter 6

Safe Consensus Control of Collision-free Multi-agent Systems

6.1 Introduction

MAS emerges as a promising research topic in system and control engineering fields due to its flexibility, scalability and robustness compared to a single-agent system. Its research ideas have the potential to improve intelligence and autonomy in practical applications, for example, lights-out factories and autonomous farms. The consensus control problem appears as a fundamental problem in MAS and bridges the networked dynamical systems and graph theory, which has attracted considerable interest from researchers (Lunze 2019, Huang *et al.* 2020, Shi and Yan 2021, Sun *et al.* 2022c). The consensus control problem can be categorized into leaderless consensus and leader-follower consensus. The leader-follower consensus control problem aims to drive all followers to approach the prescribed trajectory of a leader, which is studied in this chapter.

The obstacle avoidance problem is considered impossible to be ignored when the leader-follower consensus control theory is turned into practice. As both the inter-robot collision and static obstacles are necessary to be considered for a multi-robot system, an obstacle avoidance algorithm is required to ensure that the system is able to safely complete complex tasks. The obstacle avoidance problem generally is converted into equivalent state or input constraints that are enforced by different methods (Hoffmann and Tomlin 2008, Zhu and Alonso-Mora 2020, Zhang *et al.* 2021).

Recently, the control barrier function (CBF) is a popular tool to solve constrained control problems to achieve safety guarantees via optimization-based controllers

(Ames *et al.* 2017). It is widely applied in safety-critical control areas due to its real-time desired performance and robustness (Choi *et al.* 2020, Taylor *et al.* 2020). The core point of the CBF technique is to impose inequality constraints on the derivative of a suitable CBF to develop a controller that renders a given stable set. Thus, CBF is able to address the obstacle avoidance problem for MAS. For instance, the centralized and decentralized control barrier certificates have been designed to develop an obstacle avoidance algorithm for swarm behaviour (Borrmann *et al.* 2015). The same safety barrier certificates have been extended to a heterogeneous multi-robot system for achieving collision-free behaviour (Wang *et al.* 2016a). A more conservative collision avoidance strategy has been synthesised with centralized control barrier certificates to form relaxed safety barrier certificates for a multi-robot system (Wang *et al.* 2017b). Nevertheless, the constrained consensus control problem with CBF has not been investigated yet, which motivates us to develop a safe consensus control framework for MAS.

The contribution is twofold. First, this chapter develops a real-time optimization-based safe consensus controller that allows a LQR-based consensus controller to unify with safety constraints expressed as a distributed zeroing barrier function (ZBF). Second, the practical validation of the ZBF-based consensus control framework is built on a multi-robot platform setup including two mobile robots, a motion capture camera system and two static obstacles for safe consensus tracking.

The remainder of this chapter is organized as follows. Section 6.2 is problem formulation. A safe leader-follower consensus framework is designed in Section 6.3. Experimental results on a practical multi-robot system are shown in Section 6.4.

6.2 Problem Formulation

Consider $\mathcal{M} = \{i \mid i = 1, 2, \cdots, N\}$ be a group of N identical networked agents, the dynamics of i-th agent is described as

$$\begin{aligned} \dot{x}_i(t) &= Ax_i(t) + Bu_i(t) \\ y_i(t) &= Cx_i(t) \end{aligned} \tag{6.1}$$

where $x_i = [p_i^T, v_i^T]^T \in \mathbb{R}^4$ represent positions and velocities of agents, $u_i(t) \in \mathbb{R}^2$ are the acceleration signals and $y_i(t)$ is the system output. In real-world applications, there exists limits on velocity and acceleration, i.e., $\|v_i\|_\infty \leq \beta_i$ and $\|u_i\|_\infty \leq \alpha_i$.

The dynamics of the leader is given by

$$\begin{aligned} \dot{x}_r(t) &= Ax_r(t) \\ y_r(t) &= Cx_r(t) \end{aligned} \tag{6.2}$$

Definition 6.1. *The leader-follower consensus tracking problem is to design a local control protocol u_i for all agents, such that all agents can reach consensus on the state trajectory of the leader, i.e.,* $\lim_{t\to\infty}(x_i(t) - x_r(t)) = 0, \forall i \in \mathcal{M}$.

Definition 6.2. *The MAS in* (6.1) *is said to be safe if global state $x(t)$ stays in a safe set $\mathcal{C}$ of system* (6.1) *for all time, i.e., $x \in \mathcal{C}$, $\forall t \geq 0$, where the global state $x(t) = [x_1(t)^T, x_2(t)^T, \cdots, x_N(t)^T]^T \in \mathbb{R}^{4N}$ and the safe set $\mathcal{C}$ is defined in the following section.*

The control design objectives of this chapter are twofold and described as follows

1. Distributed leader-follower consensus tracking can be achieved.
2. Safety between moving agents and static obstacles and between agent and its related neighbour can be guaranteed.

6.3 Safe Consensus Control Framework

In this section, a novel safe consensus control framework is designed by synthesizing the LQR and CBF techniques. As illustrated in Figure 6.1, the proposed QP-based safe consensus controller u_i^* includes a nominal LQR-based consensus controller $\hat{u}_i$ and a distributed ZBF h_{ij}.

6.3.1 Nominal LQR-based Consensus Controller Design

We consider a distributed leader-follower consensus algorithm for each robot as

$$u_i = -cK \sum_{j\in N} a_{ij}(x_i - x_j) + b_i(x_i - x_r) \tag{6.3}$$

with scalar coupling gain c and feedback control design gain matrix $K \in \mathbb{R}^{2\times 4}$ to be designed.

6.3.1 Nominal LQR-based Consensus Controller Design

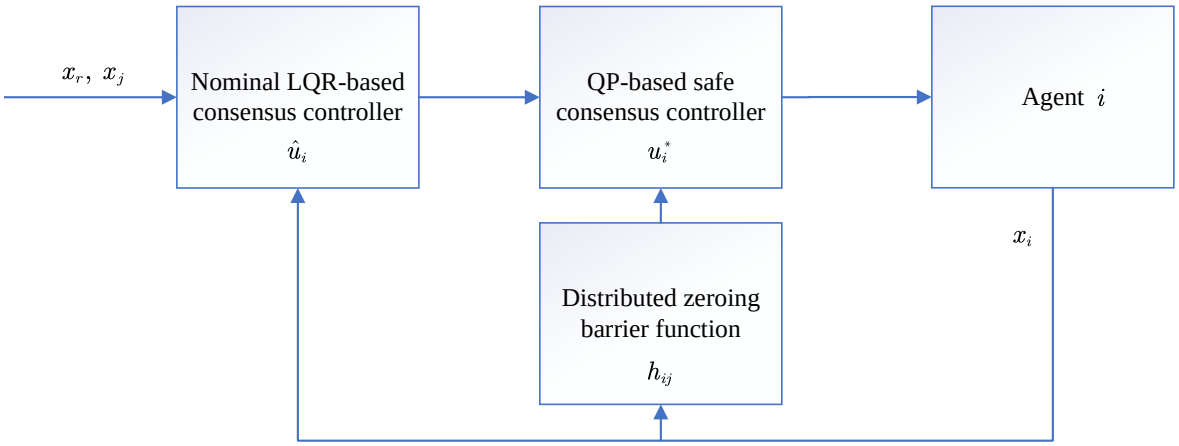

Figure 6.1. Block diagram of the proposed safe consensus control system.

Since LQR is an optimal regulator that derives the feedback control gain matrix K and minimizes the performance index $J = \int_0^\infty (x^T Q x + u^T R u) dt$ where the design matrices $Q = Q^T$ and $R = R^T$ are positive definite with appropriate dimensions, P is the unique positive definite solution of the control algebraic Riccati equation

$$A^T P + PA + Q - PBR^{-1}B^T P = 0 \tag{6.4}$$

In order to develop the nominal LQR consensus controller, the matrix form of the overall closed-loop system dynamics can be written by considering (6.1) and (6.3) as

$$\dot{x} = A_c x + B_c \bar{x}_r \tag{6.5}$$

where the global state $x = [x_1^T, x_2^T, \cdots, x_N^T]^T \in \mathbb{R}^{4N}$, $\bar{x}_r = 1_N \otimes x_r \in \mathbb{R}^{4N}$ and matrices A_c and B_c are defined as

$$\begin{aligned} A_c &= I_N \otimes A - c(\mathcal{L} + \mathcal{B}) \otimes BK, \\ B_c &= c(\mathcal{L} + \mathcal{B}) \otimes BK \end{aligned} \tag{6.6}$$

The following lemma is introduced to determine the feedback control gain matrix K.

Lemma 6.1. *(Fax and Murray 2004) Let $\lambda_i = a_i + jb_i$ with $i \in \mathcal{M}$ be the eigenvalues of $\mathcal{L} + \mathcal{B}$ where a_i, $b_i \in \mathbb{R}$ and j is the imaginary unit, thus the global consensus error dynamics $\dot{e}$ is asymptotically stable if and only if all the matrices $A - c\lambda_i BK$ are Hurwitz, where the global consensus error dynamics is given as $\dot{e} = \dot{x} - \dot{\bar{x}}_r = A_c e$.*

Consider the global system in (6.5) and the proposed consensus controller (6.3), the feedback control gain matrix K can be derived by solving the Riccati equation from the following corollary.

Corollary 6.1. *(Zhang* et al. *2011) Let design matrices $Q = Q^T \in \mathbb{R}^{4\times4}$ and $R = R^T \in \mathbb{R}^{2\times2}$ be positive definite. Design the state feedback control gain K as*

$$K = R^{-1}B^TP \tag{6.7}$$

where P is the unique positive definite solution of the control algebraic Riccati equation

$$(A - c\lambda_i BK)^T P + P(A - c\lambda_i BK) + Q + (2ca_i - 1)K^T RK = 0 \tag{6.8}$$

With the MATLAB function $lqr(\cdot)$ to compute the control matrix K to derive the nominal LQR consensus controller u_i, then we can apply the ZBF strategy to ensure that the proposed control framework guarantees collision-free behaviour in MAS.

6.3.2 Distributed Zeroing Barrier Function for Collision Avoidance

Consider an affine control system

$$\dot{x} = f(x) + g(x)u \tag{6.9}$$

where $x \in \mathcal{D} \in \mathbb{R}^n$ and control input $u \in U \subset \mathbb{R}^m$, f and g are locally Lipschitz continuous.

Definition 6.3 (Forward invariant set)**.** *For any initial condition $x_0 \in \mathcal{D}$ there exists a maximum interval of existence $I(x_0) = [0, \tau)$ such that $x(t)$ is the unique solution to (6.9) on $I(x_0)$. A set $\mathcal{C}$ is forward invariant if for every initial condition $x(0) = x_0 \in \mathcal{C}$ and every trajectory $x(t) \in \mathcal{C}$ for all $t \in I(x_0)$.*

A set $\mathcal{C}$ is defined as the superlevel set of a continuously differentiable function $h : \mathcal{D} \subset \mathbb{R}^n \to \mathbb{R}$, yielding

$$\mathcal{C} = \{x \in \mathcal{D} \subset \mathbb{R}^n : h(x) \geq 0\} \tag{6.10}$$

Thus, system (6.9) is safe with respect to the set $\mathcal{C}$ if the set $\mathcal{C}$ is forward invariant (Ames *et al.* 2019).

Definition 6.4. *(Ames* et al. *2014) A continuous function $\kappa : (-b, a) \to (-\infty, \infty)$ is said to belong to extended class $\mathcal{K}$ function for some $a, b > 0$ if it is strictly increasing and $\kappa(0) = 0$.*

Notice that, function $\kappa(t) = t^m$ is one selection of extended class $\mathcal{K}$ function for any positive odd integer m. In this chapter, we choose $\kappa(t) = t^3$ as the extended class $\mathcal{K}$ function.

Definition 6.5. *(Xu* et al. *2015) For the dynamical system* (6.9)*, a continuously differentiable function* $h : \mathbb{R}^n \to \mathbb{R}$ *is a ZBF for the safe set* $\mathcal{C}$*, if there exist an extended class* $\mathcal{K}$ *function* κ *and a set* $\mathcal{D}$ *with* $\mathcal{C} \subseteq \mathcal{D} \subseteq \mathbb{R}^n$ *such that, for all* $x \in \mathcal{D}$

$$\sup_{u \in U} \{L_f h(x) + L_g h(x) u + \kappa(h(x)) \geq 0\} \tag{6.11}$$

where L_f *and* L_g *indicate the elements of the Lie derivative formalism* $\frac{dh(x)}{dx} = \frac{\partial h(x)}{\partial x}\dot{x} = \frac{\partial h(x)}{\partial x}(f(x) + g(x)u) = L_f h(x) + L_g h(x) u.$

Next, we need to define a proper safety constraint h and the appropriate safe set $\mathcal{C}$, which guarantees the collision-free behaviour is achieved.

The existing safety constraint for MAS is derived from a classic collision avoidance algorithm (Ogren and Leonard 2005) by applying the maximum braking force $(\alpha_i + \alpha_j)$ until relative velocity $\Delta\bar{v}$ reaches to zero while keeping a safety distance D_s all time, which mathematically describes as follows

$$\left\|\Delta p_{ij}\right\| + \int_{t_0}^{t_0+T_b} \Delta\bar{v}(t_0 + t)dt \geq D_s\,, \quad \forall i \neq j \tag{6.12}$$

where $\Delta\bar{v}(t_0 + t) = \Delta\bar{v}(t_0) + (\alpha_i + \alpha_j)t$, which means that

$$\left\|\Delta p_{ij}\right\| - \frac{(\Delta\bar{v})^2}{2(\alpha_i + \alpha_j)} \geq D_s\,, \quad \forall i \neq j \tag{6.13}$$

As the safety constraint needs to be enforced when agents are approaching to each other, i.e., when $\Delta\bar{v} \leq 0$, which gives,

$$-\frac{\Delta p_{ij}^T}{\left\|\Delta p_{ij}\right\|}\Delta v_{ij} \leq \sqrt{2(\alpha_i + \alpha_j)\left(\left\|\Delta p_{ij}\right\| - D_s\right)}\,, \quad \forall i \neq j \tag{6.14}$$

Inspired by (Borrmann *et al.* 2015, Wang *et al.* 2016a) and the classic collision avoidance algorithm (Ogren and Leonard 2005), we introduce the following distributed safety constraint h_{ij} as a ZBF

$$h_{ij}(p, v) = \sqrt{2(\alpha_i + \alpha_j)\left(\left\|\Delta p_{ij}\right\| - D_s\right)} + \frac{\Delta p_{ij}^T}{\left\|\Delta p_{ij}\right\|}\Delta v_{ij} \tag{6.15}$$

where D_s is a safety distance, $\Delta p_{ij} = p_i - p_j$ and $\Delta\bar{v} = \left\|\Delta\dot{p}_{ij}\right\| = \frac{\Delta p_{ij}^T}{\left\|\Delta p_{ij}\right\|}\Delta v_{ij}$ with $\Delta v_{ij} = v_i - v_j$ represent relative position and velocity between two agents, respectively.

Hence, the safe set $\mathcal{C}$ is defined as

$$\mathcal{C}_{ij} = \{(p_i, v_i) \in \mathbb{R}^4 | \, h_{ij}(p, v) \geq 0\} \quad \forall i \neq j, \tag{6.16}$$

$$\mathcal{C} = \prod_{i \in \mathcal{M}} \left\{ \bigcap_{\substack{i \in \mathcal{M} \\ i \neq j}} \mathcal{C}_{ij} \right\}, \tag{6.17}$$

where h_{ij} is a ZBF for set $\mathcal{C}_{ij}$ and $\prod_{i \in \mathcal{M}}$ is the Cartesian product over the states of all agents.

By selecting the extended class $\mathcal{K}$ function $\kappa(h(x)) = \gamma h(x)^3$ with $\gamma > 0$, we have

$$L_f h(x) + L_g h(x) u + \gamma h^3(x) \geq 0 \tag{6.18}$$

Integrating (6.15) and (6.18), the safety barrier function can be reorganized as

$$-\Delta p_{ij}^T \Delta u_{ij} \leq \gamma h_{ij}^3 \left\| \Delta p_{ij} \right\| - \frac{(\Delta v_{ij}^T \Delta p_{ij})^2}{\left\| \Delta p_{ij} \right\|^2} + \left\| \Delta v_{ij} \right\|^2 + \frac{(\alpha_i + \alpha_j) \Delta v_{ij}^T \Delta p_{ij}}{\sqrt{2(\alpha_i + \alpha_j) \left(\left\| \Delta p_{ij} \right\| - D_s \right)}}, \forall i \neq j \tag{6.19}$$

The above inequality can be reformulated as a linear constraint in u_i and u_j, which can be represented as $A_{ij} u \leq b_{ij}$, with

$$A_{ij} = [0, \cdots, \underbrace{-\Delta p_{ij}^T}_{\text{agent i}}, \cdots, \underbrace{\Delta p_{ij}^T}_{\text{agent j}}, \cdots, 0] \tag{6.20}$$

and b_{ij} is defined as

$$b_{ij} = \gamma h_{ij}^3 \left\| \Delta p_{ij} \right\| - \frac{(\Delta v_{ij}^T \Delta p_{ij})^2}{\left\| \Delta p_{ij} \right\|^2} + \left\| \Delta v_{ij} \right\|^2 + \frac{(\alpha_i + \alpha_j) \Delta v_{ij}^T \Delta p_{ij}}{\sqrt{2(\alpha_i + \alpha_j) \left(\left\| \Delta p_{ij} \right\| - D_s \right)}} \tag{6.21}$$

More specifically, the safety barrier function between agent i and agent j is distributed to each agent as

$$\begin{aligned} -\Delta p_{ij}^T u_i &\leq \frac{\alpha_i}{\alpha_i + \alpha_j} b_{ij} \\ \Delta p_{ij}^T u_j &\leq \frac{\alpha_j}{\alpha_i + \alpha_j} b_{ij} \end{aligned} \tag{6.22}$$

The following corollary proves other obstacles that do not belong to the set $\mathcal{M}$ and the neighbouring agents satisfy the distributed safety constraint h_{ij} in (6.15) with agent i.

Corollary 6.2. *(Wang* et al. *2017b) Agent $i \in \mathcal{M}$ only needs to form ZBF with its neighbour $\mathcal{N}_i$ to achieve collision-free behaviour. The neighbour set of agent i is defined as*

$$\mathcal{N}_i = \{j \in \mathcal{M} \mid ||\Delta p_{ij}|| \leq D_{\mathcal{N}_i}\} \tag{6.23}$$

where $D_{\mathcal{N}_i} = D_s + \frac{1}{2(\alpha_i+\alpha_{\min})}\left(\sqrt[3]{\frac{2(\alpha_i+\alpha_{\min})}{\gamma}} + \beta_i + \beta_{\max}\right)$ *with* $\alpha_{\min} = \min_{j\in\mathcal{M}}\{\alpha_j\}$ *and* $\alpha_{\max} = \max_{j\in\mathcal{M}}\{\alpha_j\}$ *are the lower and upper bounds of all agents' acceleration limits, and* $\beta_{\max} = \max_{j\in\mathcal{M}}\{\beta_j\}$ *is the upper bound of all agents' velocity limits.*

Therefore, each agent i runs its own QP-based LQR consensus controller as follows

$$\begin{aligned} u_i^* = \arg\min_{u_i\in\mathbb{R}^2} \ & \mathrm{J}(u_i) = \|u_i - \hat{u}_i\| \\ \text{s.t.} \quad & \bar{A}_{ij}u_i \leq \bar{b}_{ij}, \quad \forall j \in \mathcal{N}_i \\ & \|u_i\|_\infty \leq \alpha_i \end{aligned} \tag{6.24}$$

where $\bar{A}_{ij} = -\Delta p_{ij}^T$, $\bar{b}_{ij} = \frac{\alpha_i}{\alpha_i+\alpha_j} b_{ij}$ and $\hat{u}_i$ is the nominal LQR consensus controller.

Theorem 6.1. *Consider a MAS* (6.1)*, if the nominal LQR consensus controller u_i in* (6.3) *satisfies the distributed safety barrier function h_{ij} in* (6.15) *for all agents with initial conditions $(p(0), v(0)) \in \mathcal{C}$, then the MAS is guaranteed to be safe.*

Proof. If the distributed safety barrier function in (6.15) is enforced for all agents, then the set $\mathcal{C}_{ij}$ in (6.16) is forward invariant $\forall i \in \mathcal{M}$ and $j \in \mathcal{N}_i$. According to Corollary 1, (p_i, v_i) always stays in $\mathcal{C}_{ij}$ even $j \neq \mathcal{N}_i$. Therefore, set $\mathcal{C}$ in (6.17) is forward invariant and this completes the proof. □

6.4 Experimental Results on Multi-robot System

In this section, a multi-robot system is built to verify the effectiveness of the proposed safe consensus control framework. The system consists of two mobile robots named Qbot from Quanser, two static obstacles and an OptiTrack motion capture system as shown in Figure 6.2. The OptiTrack motion capture system uses cameras to detect reflective markers attached to the object that is tracked, in our case a mobile robot as shown in Figure 6.3. Each robot perceives its own position and velocity information from the tracked markers in a global reference frame.

Figure 6.2. A multi-robot system.

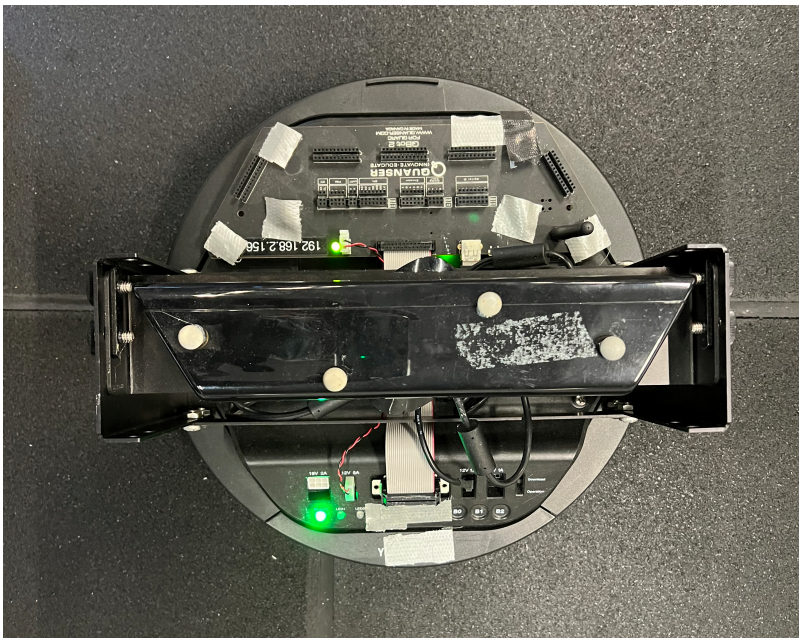

Figure 6.3. A single mobile robot attached with reflective markers.

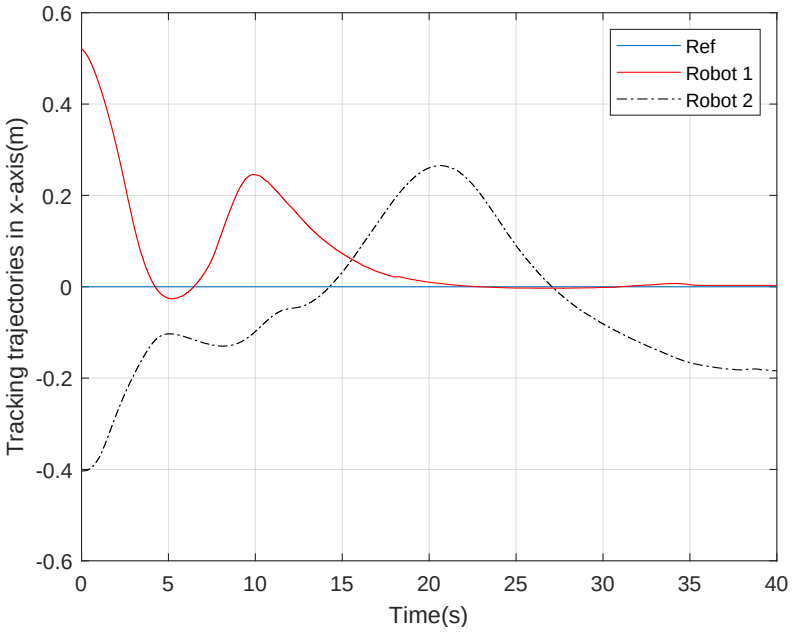

Figure 6.4. Tracking trajectories in x-axis.

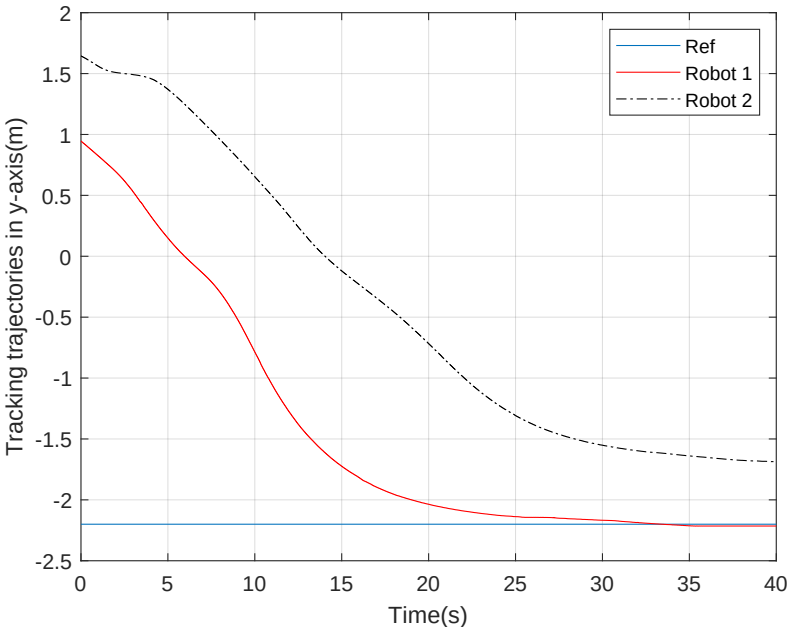

Figure 6.5. Tracking trajectories in y-axis.

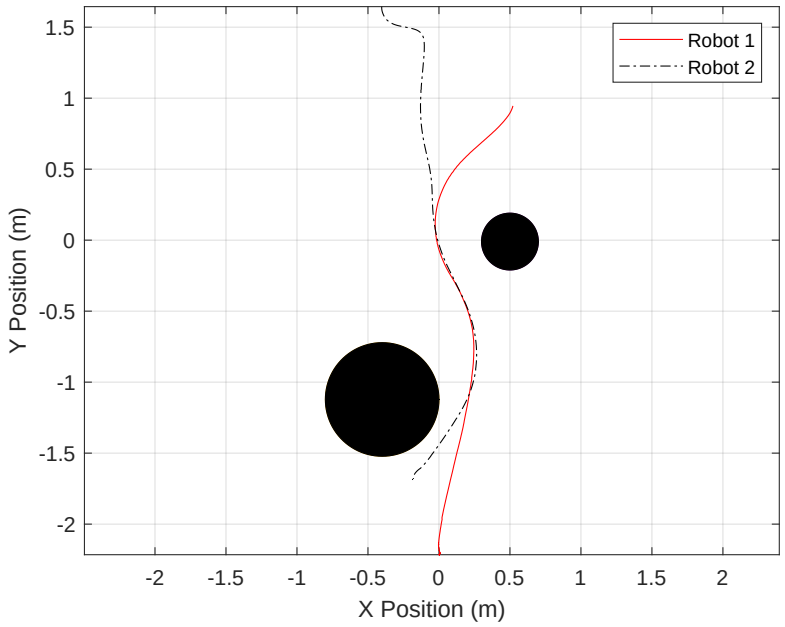

Figure 6.6. Safe tracking trajectories of all robots.

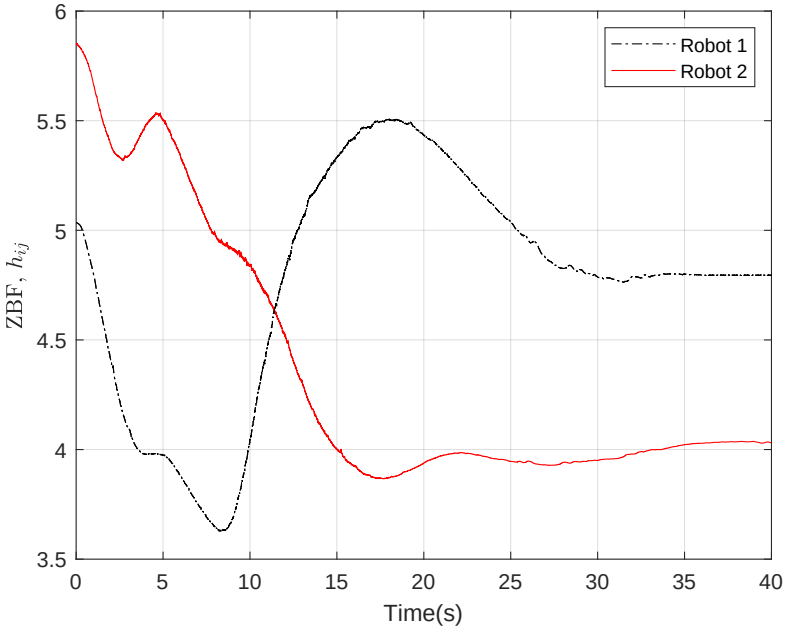

Figure 6.7. The proposed controller keeps the system safe (the ZBF h_{ij} of each robot is positive for all time).

For this experiment, our control problem is to control two mobile robots to track a desired setpoint while avoiding collision with each other and static obstacles. The initial conditions of robots are given as $x_1 = [0.52, 0.95, 0, 0]^T$ and $x_2 = [-0.40, 1.64, 0, 0]^T$, the limits of velocity and acceleration are $\beta_1 = \beta_2 = 0.5\text{m/s}$ and $\alpha_1 = \alpha_2 = 1\text{m/s}^2$. The safety distance $D_s = 0.1\text{m}$, the design parameter γ in (6.18) is given as 0.1.

The nominal LQR-based consensus controller gain K is derived by considering the following matrices

$$Q = \begin{bmatrix} 0.05 & 0 & 0 & 0 \\ 0 & 0.05 & 0 & 0 \\ 0 & 0 & 1 & 0 \\ 0 & 0 & 0 & 1 \end{bmatrix} \tag{6.25}$$

$$R = \begin{bmatrix} 1 & 0 \\ 0 & 1 \end{bmatrix} \tag{6.26}$$

and applying the MATLAB function $lqr(\cdot)$ to obtain

$$K = \begin{bmatrix} 0.2236 & 0 & 1.2030 & 0 \\ 0 & 0.2236 & 0 & 1.2030 \end{bmatrix}. \tag{6.27}$$

We consider the distributed safe CBF in (6.15) as a ZBF, then, the QP-based controller in (6.24) is formed by synthesizing LQR and ZBF methods to guarantee safety between robots and static obstacles. As illustrated in Figures 6.4 and 6.5, the two mobile robots can track the desired set point and reach a consensus. From Figures 6.6 and 6.7, we obtain that the mobile robots can avoid colliding with each other while achieving collision-free behaviour with the two static obstacles.

6.5 Chapter Summary

In this chapter, a new safe consensus control framework has been developed by designing a QP-based consensus controller. The LQR-based consensus controller has been adopted as a nominal controller and a distributed ZBF has been introduced to ensure the safety of MAS. Furthermore, a multi-robot system has been built to test the effectiveness of the safe consensus controller.

Chapter 7

Conclusions and Future Work

7.1 Conclusions

This section concludes the thesis by summarizing the main results presented in chapters 2–6.

7.1.1 Summary

Chapter 2 studies the discrete-time scaled consensus problem subject to time-varying state delay and external disturbance by integrating the SMC approach with an event-triggered scheme. A new sliding surface function is designed to drive the state trajectories to reach a predesigned sliding surface. Besides, for implementing the event-triggered control mechanism, Zeno behaviour analysis is inevitable because infinite events are triggered in a finite time interval, therefore, in this work, it is unnecessary to be considered since the triggering instants are generated in a discrete manner. Furthermore, a synthesis SMC controller with the event-triggered control technique is developed to force the trajectories onto the predefined sliding surface. Finally, a sufficient condition is obtained to guarantee the robust scaled consensus with a predefined H_∞ performance adopting the LMIs-based method.

Chapter 3 explores the event-triggered leaderless consensus tracking problem with unknown backlash-like hysteresis for MAS. Most consensus schemes require the global information of a predetermined leader or exosystem, which decreases the degree of autonomy in MAS. On the contrary, leaderless consensus can be reached without a predefined global exosystem. Moreover, an auxiliary system represented by local information interactions is introduced to overcome the barrier brought by the asymmetric

semi-definite positive Laplacian matrix. Likewise, an event-triggered strategy based on a dynamic threshold is proposed to achieve a considerable reduction in controller updates. The designed event-triggered adaptive leaderless consensus control protocol is applicable to improve the leaderless consensus tracking performance of the nonlinear MAS by compensating for the impact of the unknown backlash-like hysteresis. Moreover, the controller can ensure the leaderless consensus tracking error asymptotically converges to zero. An example is given to show the effectiveness of the new control design method.

In chapter 4, we propose a distributed fault-tolerant consensus control scheme for nonlinear MAS under output constraint by synthesizing the adaptive backstepping and neural network methods. More specifically, we introduce a new state transformation function for each agent to directly map the constrained output into a constraint-free one, which averts the limitations of the BLF method and is able to cope with constrained and unconstrained cases uniformly. Since the conventional adaptive approximation-based control techniques require one adaptive law at each design step, a single parameter estimator is introduced to mitigate the computation of the controller. Furthermore, a more general fault model is used to represent four operating modes of an actuator for each agent. The adaptive compensation technique is applied to tackle the actuator fault problem for nonlinear MAS. Consequently, an effective fault-tolerant consensus control framework is proposed to improve the consensus control performance and reliability of the nonlinear MAS.

In chapter 5, a new state transformation function is derived and implemented to transform a time-varying asymmetric constrained output into an equivalent unconstrained state. The proposed function can not only deal with both time-varying symmetric and asymmetric cases but also remove the implicit conditions on boundaries. Furthermore, the proposed function can address constrained and unconstrained cases uniformly. Two cases of UCD problems are analysed by introducing less restrictive assumptions to the control gain matrix. Two corresponding simulations are also carried out to verify the feasibility. A new framework of adaptive consensus controller is proposed to resolve the problems of output constraints and UCD for MIMO nonlinear MAS. Specifically, a sliding mode integral filter is presented to estimate the derivative of virtual control law instead of calculating it tediously, which can circumvent the explosion of the complexity problem in backstepping control.

Chapter 6 develops a real-time optimization-based safe consensus controller that allows a LQR-based consensus controller to unify with safety constraints expressed as a distributed ZBF. Moreover, the practical validation of the ZBF-based consensus control framework is built on a multi-robot platform setup including two mobile robots, a motion capture camera system and two static obstacles for safe consensus tracking.

7.2 Future Work

This thesis only studied distributed consensus control problems with communication, output and input constraints, there are still some potential future research directions including constrained consensus control for heterogeneous MAS, distributed optimization and learning-based control for MAS.

7.2.1 Constrained Consensus Control for Heterogeneous Multi-agent Systems

In this thesis, all agents are assumed to be identical, which is homogeneous MAS. However, agents with different dynamics form a heterogeneous MAS that is commonly encountered in real-world applications. Whether the theoretical results of constrained consensus control for homogeneous MAS can be extended to heterogeneous MAS is a problem worth investigating. Furthermore, the development of practical heterogeneous MAS including UAV and mobile robots with physical constraints is an interesting research topic.

7.2.2 Distributed Control Barrier Functions for Nonlinear Multi-agent Systems

In chapter 6, the safe consensus control strategy incorporates obstacle avoidance as an input constraint named ZBF to be considered while solving the optimal control problem, which forms a distributed optimization-based scheme. Thus, constraints on state, output and input can be easily incorporated into this framework. Nevertheless, nonlinear MAS and MAS with uncertainties have not been intensively studied under such a framework. Moreover, the core idea of this framework is to propose a suitable CBF.

How to transform communication constraints into a proper CBF is still an unsolved problem.

7.2.3 Learning-based Control for Constrained Multi-agent Systems

The constrained MAS performs complex tasks that require long-duration autonomy in dynamic social environments is the ultimate goal of autonomous MAS. Recently, learning-based control methods are emerging as potential solutions for autonomous MAS. It is also a powerful tool to increase the autonomy of MAS. As the changing environmental conditions and various constraints bring more challenges, learning-based solving algorithms could be favourable to achieve the desired performance for MAS.

Bibliography

AMES-A. D., COOGAN-S., EGERSTEDT-M., NOTOMISTA-G., SREENATH-K., AND TABUADA-P. (2019). Control barrier functions: Theory and applications, *2019 18th European Control Conference (ECC)*, IEEE, pp. 3420–3431.

AMES-A. D., GRIZZLE-J. W., AND TABUADA-P. (2014). Control barrier function based quadratic programs with application to adaptive cruise control, *53rd IEEE Conference on Decision and Control*, IEEE, pp. 6271–6278.

AMES-A. D., XU-X., GRIZZLE-J. W., AND TABUADA-P. (2017). Control barrier function based quadratic programs for safety critical systems, *IEEE Transactions on Automatic Control*, **62**(8), pp. 3861–3876.

BEHERA-A. K., AND BANDYOPADHYAY-B. (2015). Self-triggering-based sliding-mode control for linear systems, *IET Control Theory Applications*, **9**(17), pp. 2541–2547.

BLACKMORE-L., ONO-M., AND WILLIAMS-B. C. (2011). Chance-constrained optimal path planning with obstacles, *IEEE Transactions on Robotics*, **27**(6), pp. 1080–1094.

BORRMANN-U., WANG-L., AMES-A. D., AND EGERSTEDT-M. (2015). Control barrier certificates for safe swarm behavior, *IFAC-PapersOnLine*, **48**(27), pp. 68–73.

CAO-W., ZHANG-J., AND REN-W. (2015). Leader–follower consensus of linear multi-agent systems with unknown external disturbances, *Systems & Control Letters*, **82**, pp. 64–70.

CAO-Y., SONG-Y., AND WEN-C. (2019). Practical tracking control of perturbed uncertain nonaffine systems with full state constraints, *Automatica*, **110**, p. 108608.

CAO-Y., YU-W., REN-W., AND CHEN-G. (2012). An overview of recent progress in the study of distributed multi-agent coordination, *IEEE Transactions on Industrial Informatics*, **9**(1), pp. 427–438.

CHEN-H., SHI-P., AND LIM-C. C. (2019). Cluster synchronization for neutral stochastic delay networks via intermittent adaptive control, *IEEE Transactions on Neural Networks and Learning Systems*, **30**(11), pp. 3246–3259.

CHEN-K., WANG-J., ZHANG-Y., AND LIU-Z. (2016). Adaptive consensus of nonlinear multi-agent systems with unknown backlash-like hysteresis, *Neurocomputing*, **175**, pp. 698–703.

CHEN-M., JIANG-B., WU-Q., AND JIANG-C. (2013a). Robust control of near-space vehicles with input backlash-like hysteresis, *Proceedings of the Institution of Mechanical Engineers, Part I: Journal of Systems and Control Engineering*, **227**(8), pp. 635–644.

CHEN-M., SHAO-S., AND JIANG-B. (2017). Adaptive neural control of uncertain nonlinear systems using disturbance observer, *IEEE Transactions on Cybernetics*, **47**(10), pp. 3110–3123.

CHEN-S., LIM-C. C., SHI-P., AND LU-Z. (2020). Asymptotic consensus of dynamical points in a strict max-convex space and its applications, *SIAM Journal on Control and Optimization*, **58**(4), pp. 1984–2005.

CHEN-W., LI-X., REN-W., AND WEN-C. (2013b). Adaptive consensus of multi-agent systems with unknown identical control directions based on a novel Nussbaum-type function, *IEEE Transactions on Automatic Control*, **59**(7), pp. 1887–1892.

CHEN-Y., PENG-H., AND GRIZZLE-J. (2018). Obstacle avoidance for low-speed autonomous vehicles with barrier function, *IEEE Transactions on Control Systems Technology*, **26**(1), pp. 194–206.

CHOI-J., CASTANEDA-F., TOMLIN-C. J., AND SREENATH-K. (2020). Reinforcement learning for safety-critical control under model uncertainty, using control lyapunov functions and control barrier functions, *arXiv preprint arXiv:2004.07584*.

CHOI-J. J., LEE-D., SREENATH-K., TOMLIN-C. J., AND HERBERT-S. L. (2021). Robust control barrier–value functions for safety-critical control, *2021 60th IEEE Conference on Decision and Control (CDC)*, IEEE, pp. 6814–6821.

DAI-L., CAO-Q., XIA-Y., AND GAO-Y. (2017). Distributed mpc for formation of multi-agent systems with collision avoidance and obstacle avoidance, *Journal of the Franklin Institute*, **354**(4), pp. 2068–2085.

DENG-C., CHE-W., AND SHI-P. (2020). Cooperative fault-tolerant output regulation for multiagent systems by distributed learning control approach, *IEEE Transactions on Neural Networks and Learning Systems*, **31**(11), pp. 4831–4841.

DIMAROGONAS-D. V., FRAZZOLI-E., AND JOHANSSON-K. H. (2011). Distributed event-triggered control for multi-agent systems, *IEEE Transactions on Automatic Control*, **57**(5), pp. 1291–1297.

DONG-X., ZHOU-Y., REN-Z., AND ZHONG-Y. (2016). Time-varying formation control for unmanned aerial vehicles with switching interaction topologies, *Control Engineering Practice*, **46**, pp. 26–36.

FANG-M., SHI-P., AND DONG-S. (2021). Sliding mode control for markov jump systems with delays via asynchronous approach, *IEEE Transactions on Systems, Man, and Cybernetics: Systems*, **51**(5), pp. 2916–2925.

FAX-J. A., AND MURRAY-R. M. (2004). Information flow and cooperative control of vehicle formations, *IEEE Transactions on Automatic Control*, **49**(9), pp. 1465–1476.

FERRAGUTI-F., BERTULETTI-M., LANDI-C. T., BONFÈ-M., FANTUZZI-C., AND SECCHI-C. (2020). A control barrier function approach for maximizing performance while fulfilling to iso/ts 15066 regulations, *IEEE Robotics and Automation Letters*, **5**(4), pp. 5921–5928.

FU-J., WEN-G., YU-X., AND WU-Z.-G. (2022). Distributed formation navigation of constrained second-order multiagent systems with collision avoidance and connectivity maintenance, *IEEE Transactions on Cybernetics*, **52**(4), pp. 2149–2162.

GE-S. S., HONG-F., AND LEE-T. H. (2004). Adaptive neural control of nonlinear time-delay systems with unknown virtual control coefficients, *IEEE Transactions on Systems, Man, and Cybernetics, Part B (Cybernetics)*, **34**(1), pp. 499–516.

GODSIL-C., AND ROYLE-G. F. (2013). *Algebraic Graph Theory*, Springer Science & Business Media.

HE-W., XUE-C., YU-X., LI-Z., AND YANG-C. (2020). Admittance-based controller design for physical human–robot interaction in the constrained task space, *IEEE Transactions on Automation Science and Engineering*, **17**(4), pp. 1937–1949.

HOFFMANN-G. M., AND TOMLIN-C. J. (2008). Decentralized cooperative collision avoidance for acceleration constrained vehicles, *2008 47th IEEE Conference on Decision and Control*, IEEE, pp. 4357–4363.

HSU-S.-C., XU-X., AND AMES-A. D. (2015). Control barrier function based quadratic programs with application to bipedal robotic walking, *2015 American Control Conference (ACC)*, IEEE, pp. 4542–4548.

HUANG-J., SONG-Y.-D., WANG-W., WEN-C., AND LI-G. (2017). Smooth control design for adaptive leader-following consensus control of a class of high-order nonlinear systems with time-varying reference, *Automatica*, **83**, pp. 361–367.

HUANG-J., SONG-Y., WANG-W., WEN-C., AND LI-G. (2018a). Fully distributed adaptive consensus control of a class of high-order nonlinear systems with a directed topology and unknown control directions, *IEEE Transactions on Cybernetics*, **48**(8), pp. 2349–2356.

HUANG-J., WANG-W., WEN-C., AND ZHOU-J. (2018b). Adaptive control of a class of strict-feedback time-varying nonlinear systems with unknown control coefficients, *Automatica*, **93**, pp. 98–105.

HUANG-J., WANG-W., WEN-C., ZHOU-J., AND LI-G. (2020). Distributed adaptive leader–follower and leaderless consensus control of a class of strict-feedback nonlinear systems: A unified approach, *Automatica*, **118**, p. 109021.

JIN-X., WANG-S., QIN-J., ZHENG-W. X., AND KANG-Y. (2018). Adaptive fault-tolerant consensus for a class of uncertain nonlinear second-order multi-agent systems with circuit implementation, *IEEE Transactions on Circuits and Systems I: Regular Papers*, **65**(7), pp. 2243–2255.

KHALIL-H. K. (2002). *Nonlinear Systems*, Prentice Hall.

KIA-S. S., VAN SCOY-B., CORTES-J., FREEMAN-R. A., LYNCH-K. M., AND MARTINEZ-S. (2019). Tutorial on dynamic average consensus: The problem, its applications, and the algorithms, *IEEE Control Systems Magazine*, **39**(3), pp. 40–72.

KOLATHAYA-S., AND AMES-A. D. (2018). Input-to-state safety with control barrier functions, *IEEE Control Systems Letters*, **3**(1), pp. 108–113.

KRSTIC-M., KOKOTOVIC-P. V., AND KANELLAKOPOULOS-I. (1995). *Nonlinear and Adaptive Control Design*, New York: Wiley.

LI-H., XIA-S., MU-R., AND ZHANG-X. (2021). On designing a distributed event-triggered output feedback consensus protocol for nonlinear multiagent systems, *International Journal of Robust and Nonlinear Control*, **31**(15), pp. 7173–7185.

LI-K., HUA-C. C., YOU-X., AND GUAN-X. P. (2020). Output feedback-based consensus control for nonlinear time delay multiagent systems, *Automatica*, **111**, p. 108669.

LI-M., AND CHEN-Y. (2019). Robust adaptive sliding mode control for switched networked control systems with disturbance and faults, *IEEE Transactions on Industrial Informatics*, **15**(1), pp. 193–204.

LIU-X., SU-X., SHI-P., AND SHEN-C. (2019). Observer-based sliding mode control for uncertain fuzzy systems via event-triggered strategy, *IEEE Transactions on Fuzzy Systems*, **27**(11), pp. 2190–2201.

LIU-Y., AND JIA-Y. (2012). H_∞ consensus control for multi-agent systems with linear coupling dynamics and communication delays, *International Journal of Systems Science*, **43**(1), pp. 50–62.

LIU-Y., AND JIA-Y. (2019). Event-triggered consensus control for uncertain multi-agent systems with external disturbance, *International Journal of Systems Science*, **50**(1), pp. 130–140.

LIU-Y., AND TONG-S. (2016). Barrier lyapunov functions-based adaptive control for a class of nonlinear pure-feedback systems with full state constraints, *Automatica*, **64**, pp. 70–75.

LI-X., AND WANG-J. (2020). Active fault-tolerant consensus control of Lipschitz nonlinear multiagent systems, *International Journal of Robust and Nonlinear Control*, **30**(13), pp. 5233–5252.

LI-Y.-X., YANG-G.-H., AND TONG-S. (2018). Fuzzy adaptive distributed event-triggered consensus control of uncertain nonlinear multiagent systems, *IEEE Transactions on Systems, Man, and Cybernetics: Systems*, **49**(9), pp. 1777–1786.

LI-Z., WEN-G., DUAN-Z., AND REN-W. (2014). Designing fully distributed consensus protocols for linear multi-agent systems with directed graphs, *IEEE Transactions on Automatic Control*, **60**(4), pp. 1152–1157.

LI-Z., XIA-Y., AND SUN-F. (2013). Adaptive fuzzy control for multilateral cooperative teleoperation of multiple robotic manipulators under random network-induced delays, *IEEE Transactions on Fuzzy Systems*, **22**(2), pp. 437–450.

LUNZE-J. (2019). *Networked Control of Multi-agent Systems: Consensus and Synchronisation, Communication Structure Design, Self-organisation in Networked Systems, Event-triggered Control*, Bookmundo.

MAMMARELLA-M., COMBA-L., BIGLIA-A., DABBENE-F., AND GAY-P. (2021). Cooperation of unmanned systems for agricultural applications: A theoretical framework, *Biosystems Engineering*.

MENG-D., AND JIA-Y. (2016). Scaled consensus problems on switching networks, *IEEE Transactions on Automatic Control*, **61**(6), pp. 1664–1669.

MYLVAGANAM-T., SASSANO-M., AND ASTOLFI-A. (2017). A differential game approach to multi-agent collision avoidance, *IEEE Transactions on Automatic Control*, **62**(8), pp. 4229–4235.

NGUYEN-Q., AND SREENATH-K. (2021). Robust safety-critical control for dynamic robotics, *IEEE Transactions on Automatic Control*, **67**(3), pp. 1073–1088.

NI-J., AND SHI-P. (2021a). Adaptive neural network fixed-time leader–follower consensus for multiagent systems with constraints and disturbances, *IEEE Transactions on Cybernetics*, **51**(4), pp. 1835–1848.

NI-J., AND SHI-P. (2021b). Global predefined time and accuracy adaptive neural network control for uncertain strict-feedback systems with output constraint and dead zone, *IEEE Transactions on Systems, Man, and Cybernetics: Systems*, **51**(12), pp. 7903–7918.

NIU-B., LIU-Y., ZONG-G., HAN-Z., AND FU-J. (2017a). Command filter-based adaptive neural tracking controller design for uncertain switched nonlinear output-constrained systems, *IEEE Transactions on Cybernetics*, **47**(10), pp. 3160–3171.

NIU-X., LIU-Y., AND MAN-Y. (2017b). Consensus via time-varying feedback for uncertain nonlinear multi-agent systems with rather coarse input disturbances, *Systems & Control Letters*, **105**, pp. 70–77.

OGREN-P., AND LEONARD-N. E. (2005). A convergent dynamic window approach to obstacle avoidance, *IEEE Transactions on Robotics*, **21**(2), pp. 188–195.

PATEL-R. B., AND GOULART-P. J. (2011). Trajectory generation for aircraft avoidance maneuvers using online optimization, *Journal of guidance, control, and dynamics*, **34**(1), pp. 218–230.

PREISS-J. A., HONIG-W., SUKHATME-G. S., AND AYANIAN-N. (2017). Crazyswarm: A large nano-quadcopter swarm, *2017 IEEE International Conference on Robotics and Automation (ICRA)*, IEEE, pp. 3299–3304.

QU-F., TONG-S., AND LI-Y. (2018). Observer-based adaptive fuzzy output constrained control for uncertain nonlinear multi-agent systems, *Information Sciences*, **467**, pp. 446–463.

RAKOTONDRABE-M. (2010). Bouc–wen modeling and inverse multiplicative structure to compensate hysteresis nonlinearity in piezoelectric actuators, *IEEE Transactions on Automation Science and Engineering*, **8**(2), pp. 428–431.

REN-B., SAN-P. P., GE-S. S., AND LEE-T. H. (2009). Adaptive dynamic surface control for a class of strict-feedback nonlinear systems with unknown backlash-like hysteresis, *2009 American control conference*, IEEE, pp. 4482–4487.

REN-W., AND BEARD-R. W. (2004). Decentralized scheme for spacecraft formation flying via the virtual structure approach, *Journal of Guidance, Control, and Dynamics*, **27**(1), pp. 73–82.

REN-W., AND BEARD-R. W. (2008). *Distributed Consensus in Multi-vehicle Cooperative Control*, London: Springer.

REN-W., BEARD-R. W., AND ATKINS-E. M. (2007). Information consensus in multivehicle cooperative control, *IEEE Control Systems Magazine*, **27**(2), pp. 71–82.

REZAEE-H., AND ABDOLLAHI-F. (2020). Secure consensus control of multiagent cyber-physical systems with uncertain nonlinear models, *IEEE Systems Journal*, **14**(3), pp. 3539–3546.

ROSOLIA-U., DE BRUYNE-S., AND ALLEYNE-A. G. (2016). Autonomous vehicle control: A nonconvex approach for obstacle avoidance, *IEEE Transactions on Control Systems Technology*, **25**(2), pp. 469–484.

ROY-S. (2015). Scaled consensus, *Automatica*, **51**, pp. 259–262.

SACHAN-K., AND PADHI-R. (2019). Output-constrained robust adaptive control for uncertain nonlinear MIMO systems with unknown control directions, *IEEE Control Systems Letters*, **3**(4), pp. 823–828.

SHEN-D., AND XU-J. (2018). Distributed learning consensus for heterogenous high-order nonlinear multi-agent systems with output constraints, *Automatica*, **97**, pp. 64–72.

SHEN-Q., AND SHI-P. (2015). Distributed command filtered backstepping consensus tracking control of nonlinear multiple-agent systems in strict-feedback form, *Automatica*, **53**, pp. 120–124.

SHI-P., AND SHEN-Q. (2015). Cooperative control of multi-agent systems with unknown state-dependent controlling effects, *IEEE Transactions on Automation Science and Engineering*, **12**(3), pp. 827–834.

SHI-P., AND SHEN-Q. (2017). Observer-based leader-following consensus of uncertain nonlinear multi-agent systems, *International Journal of Robust and Nonlinear Control*, **27**(17), pp. 3794–3811.

SHI-P., AND YAN-B. (2021). A survey on intelligent control for multiagent systems, *IEEE Transactions on Systems, Man, and Cybernetics: Systems*, **51**(1), pp. 161–175.

SHI-P., AND YU-J. (2021). Dissipativity-based consensus for fuzzy multi-agent systems under switching directed topologies, *IEEE Transactions on Fuzzy Systems*, **29**(5), pp. 1143–1151.

SHTESSEL-Y., EDWARDS-C., FRIDMAN-L., AND LEVANT-A. (2014). *Sliding mode control and observation*, Springer.

SONG-Y., HUANG-X., AND WEN-C. (2017). Robust adaptive fault-tolerant PID control of MIMO nonlinear systems with unknown control direction, *IEEE Transactions on Industrial Electronics*, **64**(6), pp. 4876–4884.

SU-C.-Y., STEPANENKO-Y., SVOBODA-J., AND LEUNG-T.-P. (2000). Robust adaptive control of a class of nonlinear systems with unknown backlash-like hysteresis, *IEEE Transactions on Automatic Control*, **45**(12), pp. 2427–2432.

SUN-Y., SHI-P., AND LIM-C. C. (2021). Event-triggered adaptive leaderless consensus control for nonlinear multi-agent systems with unknown backlash-like hysteresis, *International Journal of Robust and Nonlinear Control*, **31**(15), pp. 7409–7424.

SUN-Y., SHI-P., AND LIM-C. C. (2022a). Adaptive consensus control for output-constrained nonlinear multi-agent systems with actuator faults, *Journal of the Franklin Institute*, **359**(9), pp. 4216–4232.

SUN-Y., SHI-P., AND LIM-C. C. (2022b). Event-triggered sliding mode scaled consensus control for multi-agent systems, *Journal of the Franklin Institute*, **359**(2), pp. 981–998.

SUN-Y., YAN-B., SHI-P., AND LIM-C. C. (2022c). Consensus for multi-agent systems under output constraints and unknown control directions, *IEEE Systems Journal*. Doi: 10.1109/JSYST.2022.3192573.

TAYLOR-A. J., AND AMES-A. D. (2020). Adaptive safety with control barrier functions, *2020 American Control Conference (ACC)*, IEEE, pp. 1399–1405.

TAYLOR-A., SINGLETARY-A., YUE-Y., AND AMES-A. (2020). Learning for safety-critical control with control barrier functions, *Learning for Dynamics and Control*, PMLR, pp. 708–717.

TEE-K. P., GE-S. S., AND TAY-E. H. (2009). Barrier Lyapunov functions for the control of output-constrained nonlinear systems, *Automatica*, **45**(4), pp. 918–927.

WANG-G., WANG-C., AND CAI-X. (2020a). Consensus control of output-constrained multiagent systems with unknown control directions under a directed graph, *International Journal of Robust and Nonlinear Control*, **30**(5), pp. 1802–1818.

WANG-L., AMES-A., AND EGERSTEDT-M. (2016a). Safety barrier certificates for heterogeneous multi-robot systems, *2016 American Control Conference (ACC)*, IEEE, pp. 5213–5218.

WANG-L., AMES-A. D., AND EGERSTEDT-M. (2017a). Safe certificate-based maneuvers for teams of quadrotors using differential flatness, *2017 IEEE International Conference on Robotics and Automation (ICRA)*, IEEE, pp. 3293–3298.

WANG-L., AMES-A. D., AND EGERSTEDT-M. (2017b). Safety barrier certificates for collisions-free multirobot systems, *IEEE Transactions on Robotics*, **33**(3), pp. 661–674.

WANG-L., DONG-J., AND XI-C. (2020b). Event-triggered adaptive consensus for fuzzy output-constrained multi-agent systems with observers, *Journal of the Franklin Institute*, **357**(1), pp. 82–105.

WANG-Q. (2017). Scaled consensus of multi-agent systems with output saturation, *Journal of the Franklin Institute*, **354**(14), pp. 6190–6199.

WANG-W., LONG-J., WEN-C., AND HUANG-J. (2020c). Recent advances in distributed adaptive consensus control of uncertain nonlinear multi-agent systems, *Journal of Control and Decision*, **7**(1), pp. 44–63.

WANG-W., WEN-C., AND HUANG-J. (2017c). Distributed adaptive asymptotically consensus tracking control of nonlinear multi-agent systems with unknown parameters and uncertain disturbances, *Automatica*, **77**, pp. 133–142.

WANG-W., WEN-C., HUANG-J., AND ZHOU-J. (2020d). Adaptive consensus of uncertain nonlinear systems with event triggered communication and intermittent actuator faults, *Automatica*, **111**, p. 108667.

WANG-X., LI-S., YU-X., AND YANG-J. (2016b). Distributed active anti-disturbance consensus for leader-follower higher-order multi-agent systems with mismatched disturbances, *IEEE Transactions on Automatic Control*, **62**(11), pp. 5795–5801.

WEN-G., DUAN-Z., REN-W., AND CHEN-G. (2014). Distributed consensus of multi-agent systems with general linear node dynamics and intermittent communications, *International Journal of Robust and Nonlinear Control*, **24**(16), pp. 2438–2457.

WOOLDRIDGE-M. (2009). *An introduction to multiagent systems*, John wiley & sons.

XIAO-W., AND BELTA-C. (2019). Control barrier functions for systems with high relative degree, *2019 IEEE 58th Conference on Decision and Control (CDC)*, IEEE, pp. 474–479.

XIAO-W., CAO-L., DONG-G., BAI-W., AND ZHOU-Q. (2020). Adaptive consensus control for stochastic nonlinear multiagent systems with full state constraints, *International Journal of Robust and Nonlinear Control*, **30**(4), pp. 1487–1511.

XIE-K., CHEN-C., LEWIS-F. L., AND XIE-S. (2018). Adaptive compensation for nonlinear time-varying multiagent systems with actuator failures and unknown control directions, *IEEE Transactions on Cybernetics*, **49**(5), pp. 1780–1790.

XING-L., WEN-C., GUO-F., LIU-Z., AND SU-H. (2016). Event-based consensus for linear multiagent systems without continuous communication, *IEEE Transactions on Cybernetics*, **47**(8), pp. 2132–2142.

XING-L., WEN-C., LIU-Z., SU-H., AND CAI-J. (2018). Event-triggered output feedback control for a class of uncertain nonlinear systems, *IEEE Transactions on Automatic Control*, **64**(1), pp. 290–297.

XING-M., AND DENG-F. (2018). Scaled consensus for multi-agent systems with communication time delays, *Transactions of the Institute of Measurement and Control*, **40**(8), pp. 2651–2659.

XU-H., AND IOANNOU-P. A. (2003). Robust adaptive control for a class of MIMO nonlinear systems with guaranteed error bounds, *IEEE Transactions on Automatic Control*, **48**(5), pp. 728–742.

XU-X., TABUADA-P., GRIZZLE-J. W., AND AMES-A. D. (2015). Robustness of control barrier functions for safety critical control, *IFAC-PapersOnLine*, **48**(27), pp. 54–61.

YAN-B., SHI-P., LIM-C. C., WU-C., AND SHI-Z. (2018). Optimally distributed formation control with obstacle avoidance for mixed-order multi-agent systems under switching topologies, *IET Control Theory & Applications*, **12**(13), pp. 1853–1863.

YAN-B., WU-C., AND SHI-P. (2019). Formation consensus for discrete-time heterogeneous multi-agent systems with link failures and actuator/sensor faults, *Journal of the Franklin Institute*, **356**(12), pp. 6547–6570.

YE-D., CHEN-M., AND YANG-H. (2019). Distributed adaptive event-triggered fault-tolerant consensus of multiagent systems with general linear dynamics, *IEEE Transactions on Cybernetics*, **49**(3), pp. 757–767.

YOO-S. J. (2018). Connectivity-preserving consensus tracking of uncertain nonlinear strict-feedback multiagent systems: An error transformation approach, *IEEE Transactions on Neural Networks and Learning Systems*, **29**(9), pp. 4542–4548.

YU-P., FISCHIONE-C., AND DIMAROGONAS-D. V. (2018). Distributed event-triggered communication and control of linear multiagent systems under tactile communication, *IEEE Transactions on Automatic Control*, **63**(11), pp. 3979–3985.

ZENG-J., ZHANG-B., AND SREENATH-K. (2021). Safety-critical model predictive control with discrete-time control barrier function, *2021 American Control Conference (ACC)*, IEEE, pp. 3882–3889.

ZHANG-G., QIN-J., ZHENG-W. X., AND KANG-Y. (2018a). Fault-tolerant coordination control for second-order multi-agent systems with partial actuator effectiveness, *Information Sciences*, **423**, pp. 115–127.

ZHANG-H., AND LEWIS-F. L. (2012). Adaptive cooperative tracking control of higher-order nonlinear systems with unknown dynamics, *Automatica*, **48**(7), pp. 1432–1439.

ZHANG-H., LEWIS-F. L., AND DAS-A. (2011). Optimal design for synchronization of cooperative systems: state feedback, observer and output feedback, *IEEE Transactions on Automatic Control*, **56**(8), pp. 1948–1952.

ZHANG-H., LEWIS-F. L., AND QU-Z. (2012). Lyapunov, adaptive, and optimal design techniques for cooperative systems on directed communication graphs, *IEEE Transactions on Industrial Electronics*, **59**(7), pp. 3026–3041.

ZHANG-H.-T., ZHAI-C., AND CHEN-Z. (2010). A general alignment repulsion algorithm for flocking of multi-agent systems, *IEEE Transactions on Automatic Control*, **56**(2), pp. 430–435.

ZHANG-X., LINIGER-A., AND BORRELLI-F. (2021). Optimization-based collision avoidance, *IEEE Transactions on Control Systems Technology*, **29**(3), pp. 972–983.

ZHANG-Y., LIANG-H., MA-H., ZHOU-Q., AND YU-Z. (2018b). Distributed adaptive consensus tracking control for nonlinear multi-agent systems with state constraints, *Applied Mathematics and Computation*, **326**, pp. 16–32.

ZHAO-K., AND SONG-Y. (2019). Removing the feasibility conditions imposed on tracking control designs for state-constrained strict-feedback systems, *IEEE Transactions on Automatic Control*, **64**(3), pp. 1265–1272.

ZHAO-K., AND SONG-Y. (2020). Neuroadaptive robotic control under time-varying asymmetric motion constraints: A feasibility-condition-free approach, *IEEE Transactions on Cybernetics*, **50**(1), pp. 15–24.

ZHAO-K., SONG-Y., CHEN-C. P., AND CHEN-L. (2020). Control of nonlinear systems under dynamic constraints: A unified barrier function-based approach, *Automatica*, **119**, p. 109102.

ZHAO-K., SONG-Y., MA-T., AND HE-L. (2018). Prescribed performance control of uncertain Euler–Lagrange systems subject to full-state constraints, *IEEE Transactions on Neural Networks and Learning Systems*, **29**(8), pp. 3478–3489.

ZHAO-K., SONG-Y., MENG-W., CHEN-C. P., AND CHEN-L. (2021). Low-cost approximation-based adaptive tracking control of output-constrained nonlinear systems, *IEEE Transactions on Neural Networks and Learning Systems*, **32**(11), pp. 4890–4900.

ZHAO-L., JIA-Y., YU-J., AND DU-J. (2017). H_∞ sliding mode based scaled consensus control for linear multi-agent systems with disturbances, *Applied Mathematics and Computation*, **292**, pp. 375–389.

ZHENG-S., AND LI-W. (2018). Adaptive control for switched nonlinear systems with coupled input nonlinearities and state constraints, *Information Sciences*, **462**, pp. 331–356.

ZHENG-T., XI-J., YUAN-M., AND LIU-G. (2019). Guaranteed-performance consensus design for lipschitz nonlinear multiagent systems with jointly connected topologies, *International Journal of Robust and Nonlinear Control*, **29**(11), pp. 3627–3649.

ZHOU-J., AND WEN-C. (2008). *Adaptive backstepping control of uncertain systems: Nonsmooth nonlinearities, interactions or time-variations*, Springer.

ZHOU-J., WEN-C., AND LI-T. (2012). Adaptive output feedback control of uncertain nonlinear systems with hysteresis nonlinearity, *IEEE Transactions on Automatic Control*, **57**(10), pp. 2627–2633.

ZHU-H., AND ALONSO-MORA-J. (2020). Chance-constrained collision avoidance for MAVs in dynamic environments, *IEEE Robotics and Automation Letters*, **4**(2), pp. 776–783.